THE UNIVERSITY of TULSA

COLLEGE OF ENGINEERING AND NATURAL SCIENCES

PETROLEUM ENGINEERING

TULSA UNIVERSITY SEVERE SLUGGING JOINT INDUSTRY PROJECT (TUSSP)

DATE: October 7, 2002

FROM: Cem Sarica, Principal Investigator

TO: Severe Slugging Joint Industry Project Participants

This is a copy Dr. Jarl Ø. Tengesdal's thesis titled "Investigation of self-lifting concept for severe slugging elimination in deep-water pipeline/riser systems". This serves as the final report of the Joint Industry Project titled "Severe Slugging Elimination in Ultra-Deep Water Tiebacks and Risers".

The Pennsylvania State University

The Graduate School

Energy and Geo-Environmental Engineering

INVESTIGATION OF SELF-LIFTING CONCEPT FOR SEVERE SLUGGING

ELIMINATION IN DEEP-WATER PIPELINE/RISER SYSTEMS

A Thesis in

Petroleum and Natural Gas Engineering

by

Jarl Øystein Tengesdal

Submitted in Partial Fulfillment
of the Requirements
for the Degree of

Doctor of Philosophy

August 2002

ABSTRACT

Recently, exploitation of offshore petroleum reservoirs has moved to ever increasing water depths. Production from fields in water deeper than 1800 m is now a reality. The use of long deep-water risers that conduct production from multiple wellheads on the sea floor to the surface predisposes the system to severe slugging in the riser for a wide range of flow rates and seabed topography. Considering the length of the deep-water risers, the problem is expected to be more severe than in production systems installed in shallower waters. Severe slugging could occur at high pressure, with the magnitude of the pressure fluctuations so large as to cause a shorter natural flow period with subsequent consequences such as premature field abandonment, loss of recoverable reserves and earlier-than-planned deployment of boosting devices.

In this study, a novel idea to lessen or eliminate severe slugging in pipeline-riser systems has been investigated. This idea was first proposed by Barbuto[2], and later developed independently by Sarica and Tengesdal[28]. The principle of the technique is to transfer the pipeline gas to the riser at a point above the riser-base. The transfer process will reduce both the hydrostatic head in the riser and the pressure in the pipeline, consequently lessening or eliminating the severe slugging by maintaining the steady-state two-phase flow in the riser.

An experimental study has been conducted using a 7.62 cm. inner diameter riser (14.63 m high) and pipeline (19.81 m long) system. A broad range of data was collected from the facility both in the severe slugging and stable regions. It was found that

currently available severe slugging models do not predict the severe slugging region accurately for larger diameter pipes. Data acquired with the external gas bypass have proven the proposed elimination technique.

The transient model of Sarica and Shoham[27] was modified so that it could be used to model the bypass option in addition to predicting the severe slugging cycle and region. In addition, a steady state model was developed that will be used as a design tool in order to determine the optimum placement of the take-off and injection points. Both models were found to perform well when compared to the gathered experimental data.

TABLE OF CONTENTS

LIST OF FIGURES

LIST OF TABLES

NOMENCLATURE

ROMAN

A	=	area, m^2
b_i	=	elemental systematic uncertainty, source i
B_R	=	systematic uncertainty of the result
C_0	=	distribution coefficient, dimensionless
d	=	diameter, m
df	=	degrees of freedom
dx	=	ordinary derivative in space
dt	=	ordinary derivative in time
f	=	friction factor, dimensionless
g	=	gravitational constant, m/s^2
h	=	height of riser, m
H	=	holdup, dimensionless
ℓ	=	pipeline length, m
m	=	mass, kg
M	=	molecular weight of gas, lb/lb-mole
N	=	number of data points
Q	=	flow rate, m^3/s
p	=	pressure, Pa
R	=	Universal Gas Constant, Pam^3/K

S	=	perimeter, m
$S_{x(bar)}$	=	estimate of sample standard deviation of the average data set of N
$S_{x,i}$	=	sample standard deviation, source i
T	=	temperature, K
t_{95}	=	student "t" of 95% confidence interval
U_{ASME}	=	overall uncertainty (American Society of Mechanical Engineering)
v	=	velocity, m/s
W	=	mass flow rate, kg/s
x	=	liquid penetration length, m
x_i	=	the generic data point of measurement
x (bar)	=	sample average
y	=	injection point in riser, m
Z	=	gas deviation factor, dimensionless
z	=	vertical coordinate, m
z_n	=	liquid height in the riser, m

GREEK

ρ	=	density, kg/m^3
Δ	=	differential
θ	=	angle, degrees
α	=	gas void fraction, dimensionless
α'	=	void fraction of the gas penetrated region in the riser
τ	=	shear stress, N·m^2

∂	=	partial derivative
μ	=	population mean

SUBSCRIPTS

B	=	bubble
d	=	drift
g	=	gas
i	=	initial
in	=	inlet
L	=	liquid
o	=	oil
p	=	pipe
r	=	riser
sc	=	standard conditions
sep	=	separator
Sg	=	superficial gas
SL	=	superficial liquid
w	=	wall

ABBREVIATIONS

API	=	American Petroleum Institute
ASME	=	American Society of Mechanical Engineers

ASTM	=	testing standard
BHRG	=	group of engineering companies
BP	=	British Petroleum
BV08	=	ball valve number 8
BV09	=	ball valve number 9
BV10	=	ball valve number 10
BV11	=	ball valve number 11
BV12	=	ball valve number 12
BV13	=	ball valve number 13
BV14	=	ball valve number 14
CMF	=	gas micro motion meter
cSt	=	centistokes
df	=	degrees of freedom
DPT	=	differential pressure transducer
DS	=	liquid micro motion meter
GOR	=	gas oil ratio
ID	=	inner diameter
MMSCF/D	=	million standard cubic feet per day
MRBL	=	multiphase riser base lift
OLGA	=	transient multiphase simulator
PeTra	=	transient multiphase simulator
PLAC	=	transient multiphase simulator
PT	=	pressure transducer

RBGL   =   riser base gas lift

SINTEF   =   research institute in Norway

TACITE   =   transient multiphase simulator

TRAC   =   transient multiphase simulator

TT   =   temperature transducer

UK   =   United Kingdom

ACKNOWLEDGEMENTS

Thanks to all my classmates and friends at Penn State who made the stay in State College a memorable one. I wish to thank all my friends in Tulsa new and old for making my stay there a very pleasant one.

Chapter 1 INTRODUCTION

Most of the new discoveries of oil and gas reserves are expected to occur offshore. Since the early 1960's, discovery and exploitation of offshore hydrocarbon reservoirs have been steadily increasing. With the current trends of technological advancements in exploration, drilling, production and transportation, the deep waters (with depths greater than 1000 meters), are seen as the new frontiers. Production from deep-waters poses a host of new challenges ranging from reservoir management to flow assurance. Some of the challenges such as wax deposition; hydrate formation, multiphase pumping, and phase separation have been studied since late 1980's. Although, it has been identified as early as 1973, severe slugging phenomenon has not received much attention until late 1990's for the deep-water developments.

Severe slugging can occur in gas-liquids multiphase flow systems where a pipeline segment with a downward inclination angle is followed by another segment/riser with an upward inclination angle (See Fig. 1-1). Severe slugging is normally described as occurring in four phases: slug formation, slug production, blowout, and liquid fallback (See Figures 1-2 - 1-5). During the slug formation phase the riser entrance is blocked by falling liquid from the riser. The gas is prevented entering from the riser resulting in a buildup in pipeline pressure until the liquid level in the riser reaches the surface. When the liquid level reaches the surface, liquid begins to be produced into the separator until the trapped gas arrives at the riser base; consequently the maximum pipeline pressure is attained at this point. This is called the slug production phase. As the gas penetrates into

the riser, it will eventually push the liquid in the riser with a violent chaotic blowout. During the blowout phase the pipeline pressure will decline sharply leading to the fallback of the remaining liquids and accumulation at the riser base.
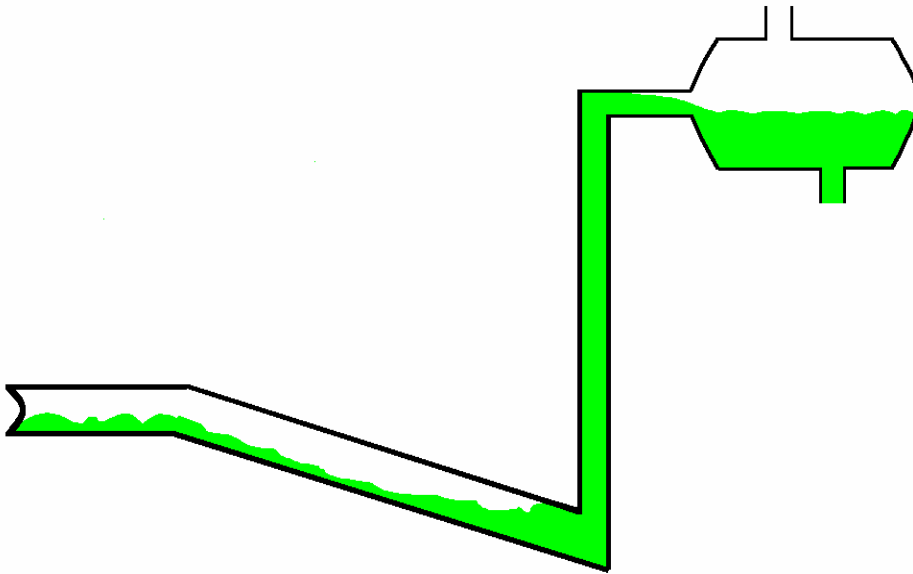
Figure 1–1: A typical pipeline-riser system
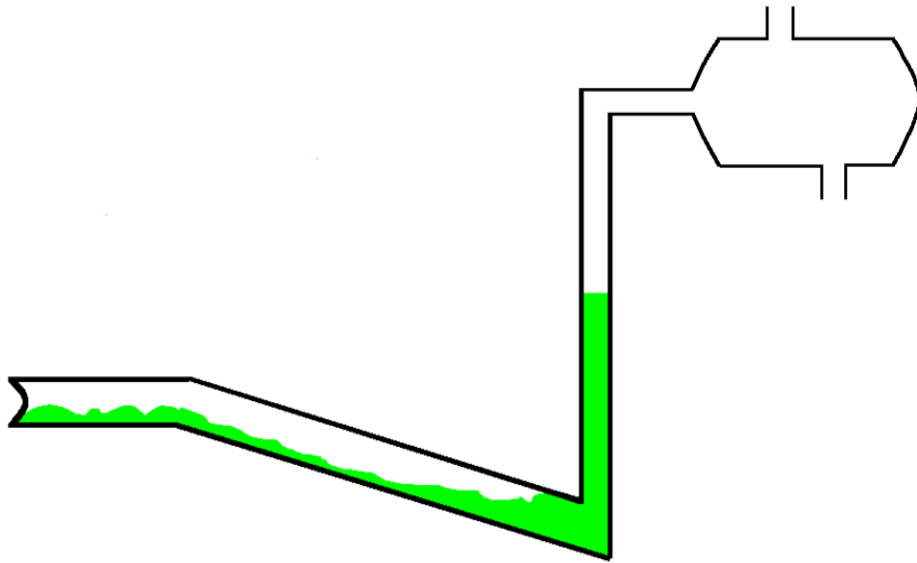
Figure 1–2: Slug formation
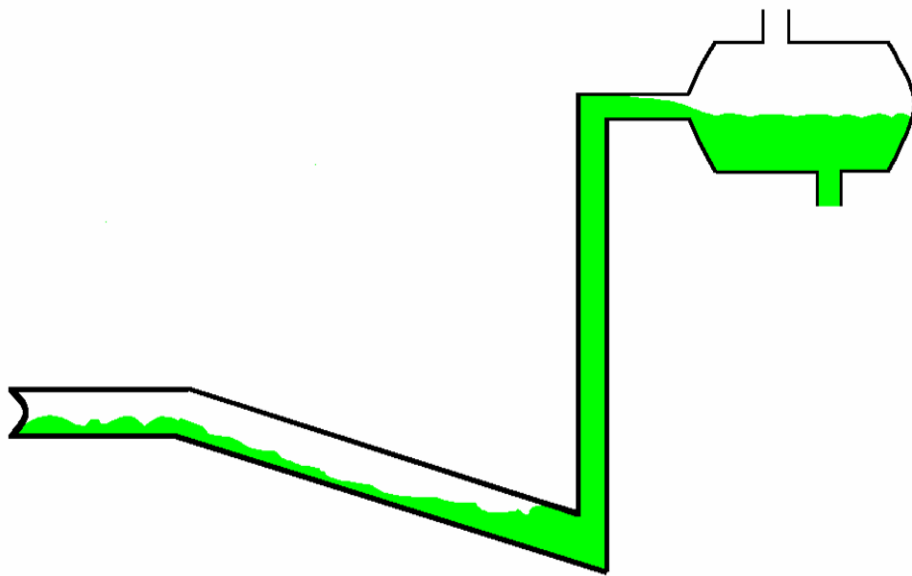
Figure 1–3: Slug production
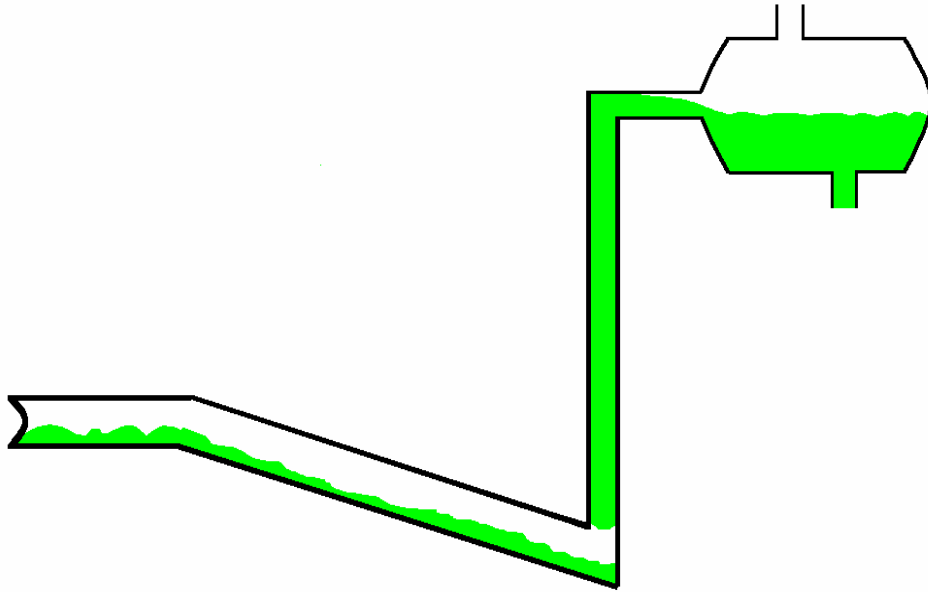
Figure 1–4: Blowout
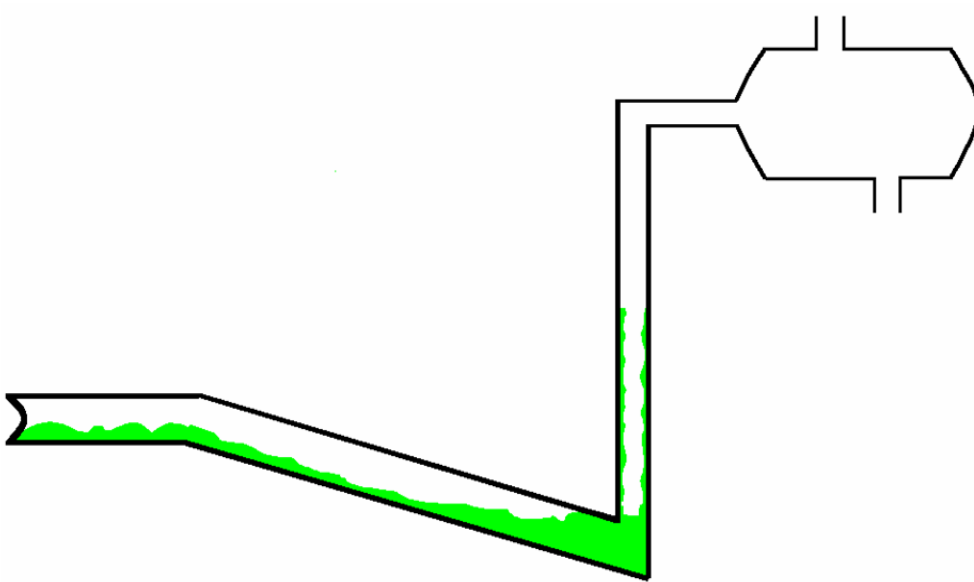
Figure 1–5: Liquid fallback

Severe slugging will cause periods of no liquid and gas production in the separator followed by very high liquid and gas flow rates. This phenomenon is very undesirable due to large pressure and flow rate fluctuations. Currently, there are three main elimination methods that have been proposed: Back-Pressure increase, Gas Lift, and Choking. The Back-Pressure increase method eliminates the severe slugging by significantly increasing the system pressure resulting in production capacity reduction. In gas lifting, external gas is injected either into the riser or pipeline at the riser bottom to reduce the hydrostatic head in the riser or increase the gas flow rate in the pipeline. Both hydrostatic head reduction and gas flow rate increases will facilitate continuous removal of liquids from the riser resulting in elimination of severe slugging. Gas-Lift requires large amounts of gas and compressors on platforms to accomplish the elimination. The operational costs of gas lift can be very significant. Choking increases the back-pressure proportional to the velocity increase in the riser. If the movement of the gas in the riser is stabilized before reaching the choke, steady flow will occur after a short flow period. The stabilization requires very careful choking to ensure minimum back-pressure. Although there are several other methods proposed to eliminate severe slugging, their working principles are very similar to the three methods described above. These will be further discussed in the literature review section.

The applicability of the current practices in prediction and elimination of severe slugging to deep-water developments is very much in question. Severe slugging conditions might occur at considerably high reservoir pressures, and the magnitude of the pressure fluctuations can be significantly high eventually causing premature abandonment of the wells and reducing the ultimate recovery of the field. Considering

the length of the deep-water risers, and the expansion capacity of gas due to very large hydrostatic pressures, the severe slugging phenomenon is expected to have a greater impact in deep-water systems compared to the production systems installed in shallower depths. Therefore, the design of downstream facilities at the platform becomes very crucial considering the safety of the operation and the limited available space on the platform. Moreover, the cost of a deep-water production riser system is expected to be very high, and the remediation efforts of any reliability failures can be cost prohibitive. Cost figures as high as $30 to $50 million for typical systems of 1150 to 1650 ft water depths have been reported in the literature[12].

It is clear that the elimination of severe slugging for deep waters is an unresolved issue although there are some attempts to address the issue. Different techniques can be suitable for different type of problems and production systems.

The objective of this study is to present a novel severe slugging elimination technique suitable for deep-water developments. The idea is to connect the riser to the downward inclined segment of the pipeline with a small diameter conduit (See Figure 1-6). The by-pass pipe will transfer the gas from the downward inclined segment to the riser. The gas will reduce the hydrostatic head in the riser. Consequently, the severe slugging will be lessened or eliminated. This can be considered as self-gas lifting (i.e., no additional gas injection is required from the platform).
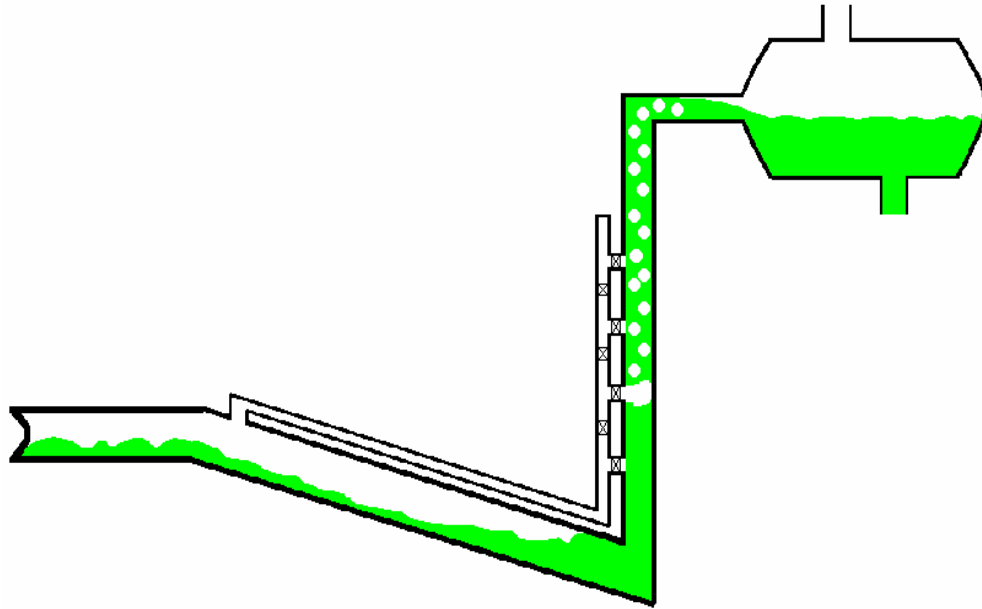
Figure 1–6: Proposed elimination method

An extensive experimental program was performed to acquire high quality severe slug flow data. The objectives of the experimental program were to better understand the physics of severe slugging in a deep-water pipeline-riser system and investigate the characteristics of the new elimination technique for a wide range of angles, take-off and injection points, and different flow rates.

In the modeling part of the study, two modeling approaches were investigated, one transient model for severe slugging identification and elimination, and a steady state model that can be used as a design tool for the proposed elimination technique.

The thesis' organization is as follows: After the introduction is presented in Chapter 1, Chapter 2 presents the literature review. The review discusses the work that has been performed in the area of severe slugging since it was identified as being a separate problem other than normal slugging. The first part discusses the occurrence and

the prediction tools available, as well as, the different transient models that are available that can model severe slugging. Chapter 2 concludes with the available state of the art methods to eliminate severe slugging and discusses their applicability in today's petroleum industry. Chapter 3 focuses on the proof of concept study that was performed to validate the approach, and consists of both an experimental and modeling part. Chapter 4 is dedicated to the experimental work conducted using a large and versatile test facility. In Chapter 4, the facility is described in detail for fluid handling system, instrumentation, and experimental procedure. Also, an analysis of a typical test run is shown. A section in Chapter 4 is dedicated to the uncertainty analysis performed that addresses the instrumentation errors, as well as, the velocity propagation errors. In this chapter, the experimental data are presented and analyzed. Chapter 5 is devoted to the mathematical formulation of the proposed models. The first part of this chapter focuses on the transient model for severe slugging prediction and elimination. In this part, model predictions for severe slugging identification, predictions and elimination are compared to the results generated by the transient model. The last part of this chapter is dedicated to the steady state model used to design the bypass system. The last part of Chapter 5 presents the steady state model predictions together with the experimental data. Chapter 6 presents the summary, conclusions and suggestions for future research.

Chapter 2 BACKGROUND

2.1 Severe Slugging Occurrence and Prediction

Yocum[43] was the first to report the symptoms of severe slugging phenomena although he did not provide a description of the severe slugging. He noticed that flow capacity could be reduced by 50% due to back-pressure fluctuations caused by severe slugging. He proposed a prediction model based on the available hydrodynamic slugging models.

Schmidt[30,31] realized that what Yocum[43] reported was significantly different than the hydrodynamic slugging, and he characterized the phenomena as "Severe Slugging". Jupraset[19] and Schmidt[29] proposed flow pattern maps for severe slugging based on Duns and Ros dimensionless gas and liquid velocity numbers. Schmidt et al.[32] developed a hydrodynamic model to predict the dynamic slug characteristics of severe slugging. The model assumed constant inlet liquid and gas mass flow rates, constant separator pressure, and liquid slugs free of entrained bubbles, and required empirical correlations for the liquid holdup in the pipeline and the liquid fall back in the riser. No verification for the model was presented. The authors provided three separate severe slugging transition criteria:

1) Stratified – non-stratified flow transition; i.e., they postulate that the flow in the pipeline segment before the riser has to be stratified for severe slugging to occur.

2) The stability of the flow in the riser, i.e., if the pressure drop in the riser decreases as the gas flow rate is increased for a given liquid flow rate, then the flow is said to be unstable and susceptible to severe slugging.

3) The criterion in assigning the boundary between severe slugging and transition to severe slugging is a direct solution of their hydrodynamic model for the lowest gas flow rate corresponding to a liquid flow rate that will produce riser generated slugs shorter than the riser length.

Bøe[5] proposed the following mathematical criterion based on the forces that are acting on a liquid slug blocking the entrance into the riser for the occurrence of the severe slugging, namely the gas pressure that is building up in the pipeline and the hydrostatic head of the liquid in the riser.

$$\frac{w_g}{w_L} \frac{RT/M}{\ell_p \alpha g} = 1 \qquad (1)$$

Pots et al.[26] carried out a detailed investigation of severe slugging that included small-scale tests, field tests and hydrodynamic modeling. They proposed a similar criterion to Bøe[5] criterion to predict the severe slugging region. They claimed that stratified flow in the pipeline was not necessarily a pre-condition for severe slugging occurrence. Instead, the separation of the phases and the momentum carried by the liquid were claimed to be the key factors.

Taitel[35] investigated the conditions for stable riser flow. A simple force balance on the gas phase and the liquid column was applied, where the system is stable when the expansion force from the gas increases slower than the hydrostatic force of the liquid column in the riser. The stability criterion is given below:

$$\frac{p_{Sep}}{p_o} > \frac{\Phi([\alpha/\alpha']\ell_p - h)}{p_o/(\rho_L g)} \qquad (2)$$

Taitel's[35] stability and Bøe's[5] criteria were proposed by Taitel[35] to be used together to predict the severe slugging region. Taitel[35] claimed Bøe[5] criterion alone over predicted the severe slugging region based on Schmidt's[29] experimental data.

Experiments conducted by Vierkandt[40] showed slugging even above the stability line predicted from Taitel's[35] criterion. This observation led Taitel et al.[37] to refine the definition of severe slugging and propose three different severe slugging types namely, "cyclic with fallback", "cyclic without fallback", and "unstable oscillations". "cyclic with fallback" exhibits a fallback of liquid and accumulation of gas at the top of the riser. It encompasses what is known as violent blowouts. The Taitel[35] stability line seems to distinguish between the classical violent severe slugging and not so violent severe slugging. The relevance of this distinction is questionable. "cyclic without fallback" exhibits no fallback while liquid blockage can occur at the riser base and liquid or gas liquid production into the separator is not halted. "unstable oscillations" are characterized with their much shorter slug lengths compared to severe slugs and continuous gas flow in the riser (no liquid blockage at the riser base). A new model predicting the change of void fraction in the riser and the movement of liquid into the pipeline has been developed. The distinction between "cyclic with fall back" and "cyclic without fallback" was made based on the liquid velocity at the riser top. The comparison of the experimental results of the study with the Bøe[5] predictions indicated that for all practical purposes Bøe[5] criterion gave quite reasonable results to distinguish between severe and non-severe slugging.

Based on field-testing from the Upper Zakuim pipeline riser system, Farghaly[10] presented a field study of severe slugging. Severe slugging occurred at low liquid and gas rates in undulating, nearly horizontal pipelines of various diameters, lengths and riser heights. Severe slugging caused several problems and instability in the entire field. In some cases the average production rate was reduced to less than 50% of its desired capacity.

Fabre et al.[9] proposed a model based on method of characteristics to simulate the transient flow in the riser under the conditions of continuous gas penetration into the riser, and presented experimental data obtained from 2 in. inner diameter pipeline-riser system. The transient model is a Lagrangian drift-flux model. No friction and mass transfer between phases are allowed, and isothermal flow conditions and ideal gas assumptions are made. Later, Sarica and Shoham[27] adapted their model, and modified it for the discontinuities of the two-phase and single-phase interface in the riser.

Barbuto and Caetano[3] presented a single severe slugging data point obtained from Fargo-1 platform, Campos Basin. They also showed that Taitel's[35] stability criterion along with the stratified non-stratified flow transition boundary was able to predict the observed severe slugging.

Tin[38] and Tin and Sarshar[39] presented their experimental and modeling study for "S" shaped risers. Experimental results indicated that the trapped gas in the downward inclined section before the last upward inclined section of the riser had significant impact on the severe slugging behavior. The extent and variation of this effect was not analyzed. The acquired data are considered to be reliable for "S" shaped risers and have been used by other investigators such as Kashou[21] in a later simulator verification study.

Corteville et al.[7] experimentally studied severe slugging in a "U" shaped flow line that resembles a transport line between two platforms. The facility consisted of a 3 in. inner diameter pipe composed of a 50 ft long downcomer, a 492 ft long horizontal flexible pipe and 50 ft long riser. At very low flow rates, the severe slugging phenomenon is claimed to be very similar to that observed in pipeline-riser systems. There was no report of slug lengths greater than riser height indicating that severity of the slugging is less than that in the pipeline-riser systems. It was reported that the gas flow in the riser was continuous supporting the understanding that slugging was not so severe. On the other hand, this observation cannot be generalized for "U" shaped systems since the topography of the line might present downward inclinations right before the riser implying the possibility of the larger terrain slugs.

Montgomery and Yeung[24] conducted an experimental study on 2" inner diameter 225 ft long S-shaped pipeline-riser system. They concluded that largest liquid volumes were produced for the type of severe slugging where no liquid accumulates in the pipeline.

Philbin & Black[25], and Hall & Butcher[11] presented the use of PLAC, a general-purpose transient multiphase flow simulator. PLAC is a two-fluid model originated from TRAC, a dynamic nuclear reactor core. PLAC numerically solves a system of equations consisting of continuity and momentum conservation equations for each phase and one mixture energy conservation equation. Philbin and Black[25] gave a comparison of PLAC results with one of the BP severe slugging experiments at Sunbury. Also provided in the paper were the results of a simulation study performed for Amerada Hess in their Hudson field development.

Bendiksen et al.[4] presented one of the most widely used general-purpose transient multiphase flow simulators, OLGA. OLGA is a two-fluid model that numerically solves a system of equations consisting of separate continuity equations for gas, liquid bulk and liquid droplets, two momentum equations for the liquid film, and gas and liquid droplets, and one energy conservation equation. OLGA has its own flow pattern prediction model. OLGA has been verified with the severe slugging data from SINTEF laboratory and Schmidt's[29] data. Kashou[21] verified that OLGA could simulate severe slugging in S-shaped or catenary risers by comparing simulation results with the data taken at the BHRG facilities (1991). Xu[45] presented the capabilities of OLGA in predicting different multiphase flows including severe slugging. Song and Kouba[33] have used OLGA to simulate the severe slugging for water depths up to 15,000 ft for both conventional and "S" shaped risers. They have concluded that severe slugging is extremely likely to occur especially at the later stage of the field life when flow rates become too low. It is pointed out that increasing water cuts for a constant GOR can enhance the severe slugging due to its higher density. They have also emphasized that the gas and liquid velocities will be higher than erosion velocities.

Larsen et al.[22] presented another transient model, PeTra, designed for tracking slugs and pigs. The simulator is a one-dimensional, three-phase model utilizing separate mass, momentum equations for each phase. It is based on a Lagrangian approach, providing information about the movement of slug front and tail. This can be considered as an advantage over the other general-purpose transient multiphase flow simulators. PeTra has been successfully tested against the SINTEF severe slugging data. PeTra's

current version excludes the energy balance leaving out the temperature-related issues that might be an important factor in production from deep-waters.

Henriot et al.[13] have showed that TACITE a compositional general-purpose transient multiphase flow simulator can simulate the severe slugging and the effects of different elimination techniques including gas lifting and riser base pressure control. TACITE is a drift flux simulator with the capability of component tracking. Based on TACITE runs, the authors claimed that the fluid properties or the characterization of the fluids might have an impact on the severity and cycle times of the severe slugging. This might be very important for deep-water developments because of large pressure and temperature differences between the riser base and the platform.

2.2 Severe Slugging Elimination

Yocum[43] identified different severe slugging elimination techniques that are still considered at the present time. These are the reduction of the line diameter; the splitting of the flow into dual or multiple streams; the gas injection into the riser; the use of mixing devices at the riser base, choking, and back-pressure increase. Yocum[43] observed that increased back-pressure could eliminate severe slugging but would severely reduce the flow capacity. He claimed that choking would also cause severe reductions in the flow capacity.

Contrary to Yocum's[43] claim, Schmidt[30] and Schmidt et al.[31] noted that the severe slugging in a pipeline-riser system could be eliminated or minimized by choking at the riser top, causing little or no change in either flow rates or pipeline pressure. Schmidt also indicated that elimination of severe slugging could be obtained by gas injection, but

dismissed it as not being economically feasible due to the cost of a compressor to compress the gas for injection and piping required to transport the gas to the base of the riser. Taitel[35] provided a theoretical explanation for the success of choking in stabilizing the flow as reported by Schmidt[30,31,32]. Fargalhy[10] presented field examples showing that choking can eliminate severe slugging. Pots et al.[26] investigated the use of gas injection as an elimination method of severe slugging. They concluded that the severity of the cycle was considerably lower for riser injection of about 50% inlet gas flow. It was observed that even with injection rates 300% higher than the inlet gas flow rate, the severe slugging did not disappear. Hill[14,15] described riser-base gas injection tests performed in the S.E. Forties field to eliminate severe slugging. The gas injection was shown to reduce the extent of the severe slugging. The condition for eliminating severe slugging was to bring the flow pattern in the riser to annular flow preventing liquid accumulation at the riser base. Therefore, large volumes of injection gas were needed to completely stabilize the flow.

Jansen[17] investigated different elimination techniques such as back-pressure increase, choking, gas lifting, and choking and gas lifting combination. He proposed the stability, and the quasi-equilibrium models for the analysis of the above elimination techniques. He experimentally made the following observations:

1) Very high back-pressures were required to eliminate the severe slugging.

2) Careful choking was needed to stabilize the flow with minimal back-pressure increase.

3) Large amounts of injected gas were needed to stabilize the flow with gas-lifting method.

4) Choking and gas-lifting combination was the best elimination method reducing the degree of choking and the amount of injected gas needed to stabilize the flow. The stability criteria for choking and gas lifting were developed by modifying the original Taitel et al.[37] model.

Kaasa[20] proposed a second riser, connecting the pipeline to the platform to eliminate severe slugging. Downward sloping pipeline acts like a slug catcher since the prevailing flow pattern is mostly stratified flow at low flow rates. The second riser is placed at such a point on the pipeline that all of the gas is diverted to it, and the original riser transports all of the liquid. The second riser is equipped with a pressure control valve to control the pressure fluctuations. There are two disadvantages of this method: The original riser will be almost full of liquid imposing a considerable back-pressure to the system that can result in significant reduction in production capacity: and, a second riser may not be economically viable.

McGuinness and Cooke[23] presented a field case in St. Joseph field, Sabah, Malaysia. The severe slugging problem was observed when a new satellite field was brought on stream due to increased pipeline volume available for the gas to expand and compress. The severe slugging resulted in higher back-pressure and reduced the production capacity of the system. Their solution to the problem was the separation of the fluids at the satellite platform and transporting the liquid and gas in separate flow lines to the main production platform. A minimum back-pressure was accomplished by utilization of a surge vessel operating at atmospheric pressure for liquid stream rather than a low-pressure separator.

Wyllie and Brackenridge[41] proposed a retrofit solution to reduce severe slugging effects. Their solution requires a small diameter pipe insert into the riser, thereby; creating an annulus that can be used for gas injection. This might be considered a good retrofit solution when there is no provision for severe slugging on the existing riser. On the other hand, conceptually, it is a restriction to the flow that might pose problems for operations such as pigging. Wyllie[42] filed an UK Patent Application for a very similar device. The modified device is retrievable but still requires a workover operation for the retrieval. It is claimed to allow the passage of variable diameter pigs. No details are given on how to size and design such a device.

Barbuto[2] proposed a different approach to eliminate severe slugging. The pipeline and riser were connected to each other to transmit the pipeline gas to the riser at a predetermined position. This point was said to be at 1/3 of the total riser height. Different control schemes on the by-pass line were discussed. The main theme was to keep the pipeline pressure under control. Although Barbuto[2] provided neither an explanation nor a justification (i.e. field trials, experimental data, and theoretical proof) for the method of elimination, the idea was a novel one.

Hollenberg et al.[16] proposed a topside flow control system to eliminate severe slugging. The principle of the system is to control the mixture flow rate constant throughout the operation with a control valve. The authors realized that it was not possible to implement the control valve because of difficulties in measuring the two-phase mixture velocity, which is the parameter of interest for the control. They solved the problem by replacing the control valve with a control separator, which was a small separator allowing separation of phases and therefore the measurements of the separate

phase flow rates. They conducted laboratory experiments (2" inner diameter, 328-ft long pipeline and a 54 ft high riser). Their control system was shown to work for all of the cases investigated. The riser base pressures were tripled indicating a tremendous back-pressure applied to the upstream.

Courbot[6] proposed an automatic control scheme to prevent severe slugging in Dunbar 16" Multiphase Pipeline. The control parameter, the riser base pressure was kept constant by a control valve upstream of the separator. The field experience proved that the control scheme was a success although considerable increases in the riser base pressure were observed. Other elimination techniques were considered. The only other viable alternative, gas lifting, was found to be expensive due to high capital expenditures. Controlling separator pressure or separator fluid level was found ineffective as a result of simulation studies performed with OLGA.

Hassanein and Fairhurst[12] presented the challenges in mechanical and hydraulic aspects of riser design for deep-water developments (6,000 ft and deeper). They have concluded that the ideal design scenarios of mechanical and hydraulic designs are opposites, and an optimum solution needs to be found. For the deep-water hydraulic design, the authors pointed out that flow rate variations would be larger due to bigger hydrodynamic slugs owing to larger flow line diameters. Besides, the longer flowlines combined with the risers may increase the possibility of severe slugging. The larger system volume can lead to more severe surges during transient operations. Severe slugging, if allowed, is expected to create very large flow rate variations. They suggested the riser base gas lift (RBGL) or the use of foams. No additional information was provided on the utilization of above techniques.

Johal et al.[18] pointed out that RBGL may cause additional problems due to Joule-Thompson cooling of the injected gas. Gas acts like a heat sink and lowers the temperature of the fluids making the flow conditions more susceptible for the wax and hydrate problems. Therefore, operators need either to heat the gas before injecting or use chemicals to prevent the formation of wax and hydrates. Johal et al.[18] proposed an alternative riser-base gas lift, which is called Multiphase Riser-Base Lift (MRBL), for deep-water developments. MRBL is based on the idea of diverting a nearby multiphase flow stream to the multiphase–riser system. This would help lessen the severe slugging problem without exposing the system to other potential problems. The author claimed that using MRBL would save up to $8,000,000 in capital expenditures alone compared to a conventional RBGL. Obviously, this method requires the availability and usability of other multiphase lines.

Song and Kouba[34] proposed subsea separation of gas and liquid as a method of severe slugging elimination. After separation, gas and liquid would be separately transported to the platform. A liquid pump would be used to overcome the hydrostatic head therefore preventing the capacity reduction due to back-pressure.

Almeida and Gonçalves[1] proposed the use of a venturi valve at the riser base inlet to eliminate severe slugging. The venturi device accelerates the fluids in the flowline near riser base. The absence of stratified flow in this region prevents the liquid accumulation at the riser base and consequently lessens the presence of severe slugging. The method has been verified using a small test facility, where the proposed method was compared to choking for severe slugging elimination.

2.3 Applicability of Current Elimination
Techniques

The following is a brief discussion on the applicability of the existing elimination methods to deep-water systems.

Back-pressure Increase. This is not a viable option even for shallow water systems since production capacity reduction is experienced due to back-pressures imposed. The reduction in production capacity is expected to be worse for deep-water production systems.

Riser Base Gas Lift (RBGL). It is one of the most used methods for the current applications. For deep waters, increased frictional pressure loss and Joule-Thompson cooling are potential problems resulting from high injection gas flow rates. The other shortcomings are the necessity of injection gas and gas injection system.

Choking. Although choking is a proven technique to reduce or eliminate severe slugging, careful choking is needed to have the least back-pressure increase in order to avoid production reduction. Only one reported successful field application (Fargalhy[10]) could be found in the literature. For deep water systems, the back pressure increase could even be more important due to potential production loses.

Gas-Lift and Choking Combination. Although it is suggested to be a viable method by Jansen et al.[17], no field application was reported for current pipeline-riser systems. It might alleviate some of the cooling and excessive frictional pressure loss problems by requiring less injection gas. It will require injection gas and the necessary gas lift installation.

Riser Base Pressure Control with a Surface Control Valve. This technique was successfully applied in a Dunbar 16" pipeline-riser system[6]. In principle, this technique

is very similar to choking. The field data indicated significant overall system pressure increase. It may pose potential production reduction problems for deep-water productions.

Flow Rate Control. The principle of this approach is to keep the mixture flow rate constant throughout the operation with a control valve[16]. Experimental studies showed that back-pressure was tripled when the stable flow was achieved. For deep waters, this system will inherently have the problems of significant reduction in production capacity due to increased riser base pressure and the longer travel times of information from riser base to the top side causing delays in the responses of the control system.

Smaller Diameter Pipe Insertion. It is a retrofit gas lift method. The same concerns for the gas lifting are expected to be equally valid in this technique. This technique may not be suitable, since it is an intrusive solution. For deep waters frequent pigging is considered to be one of the flow wax management techniques

Multiphase Riser Base Lift (MRBL). This method requires nearby high capacity multiphase lines that some part of their production could be diverted to a pipeline-riser system to either eliminate severe slugging or startup the production after a shutdown period. It is proposed as a better alternative to RBGL since the lift fluids will not cause cooling, and no injection gas and related apparatus will be required. This method requires the availability and usability of other multiphase lines. Therefore, it is a system specific solution, and could be feasible for limited cases.

Subsea Separation. This is a viable solution that does not impose back-pressure on the system. But it requires two separate flow lines and a liquid pump to pump the liquids to the surface.

Foaming. Hassanein and Fairhurst[12] originally mentioned this method without providing any details. This method requires foaming agents and a way to form the foam.

Venturi Device. Almeida and Gonçalves[1] experimentally showed this method to be viable. Careful selection of proper throat diameter of the venturi device is needed to ensure that the flow is moved outside the severe slugging envelope. Additional pressure losses through the device and its intrusive nature may render it unsuitable for certain production systems.

Although, several severe slugging elimination techniques are reported in the literature, none of them has been tested and verified for the elimination of severe slugging in deep waters. Drastic differences in capital expenditures and operational expenditures among the different techniques have been reported.

Some of the promising concepts such as self-lifting and foaming are still conceptual and they need to be further studied. In this study, the self-lifting concept has been thoroughly investigated

Chapter 3 PROOF OF CONCEPT STUDY

An experimental and theoretical proof of concept study was performed to evaluate the proposed elimination technique. Both the experimental data and the model predictions show that the proposed elimination concept is feasible. In the following sections a summary of the experimental and modeling studies is presented.

3.1 Experimental Study

A small-scale test facility was constructed to study the occurrence and elimination of severe slugging. A schematic of the facility is shown in Figure 3-1.
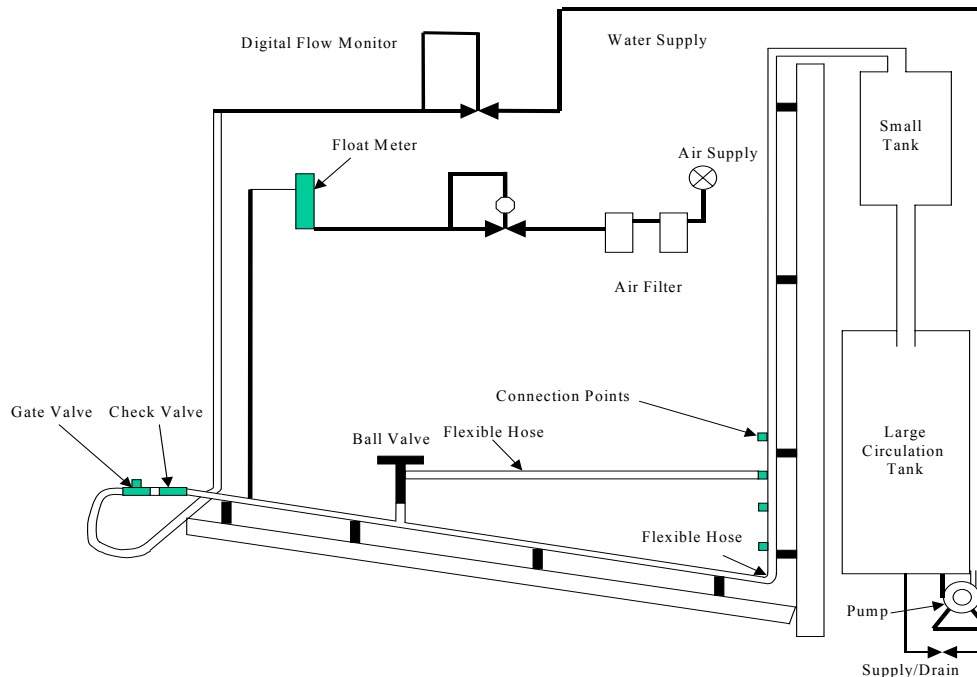
Figure 3–1: Small-scale experimental facility

The facility consisted of a 2.82 m long pipeline connected to a 1.88 m high riser (See Fig. 3-1). The volume for gas to expand or compress after the metering section was converted to additional pipe length resulting in an effective pipeline length of 7.57 m. The pipeline and the riser were both made out of clear PVC pipe, 1.905 cm in diameter, and mounted on a metal frame. The pipeline is connected to the riser by a flexible transparent hose, and could be inclined from about - 5° to +5° from the horizontal. In this study, pipeline inclination angle was kept at a representative inclination angle of -3°.

An external bypass ran from the pipeline to the riser at a pipeline distance of 2.66 m from the riser base, and consisted of a clear hose with diameter of 1.27 cm. The connection points on the riser were at distances of 22.86 cm, 30.48 cm, 38.10 cm and 45.72 cm above the riser base.

3.1.1 Fluid Handling System

Water was used as the liquid phase, supplied from the city water system. A closed system was used, with a large tank acting as the reservoir. A liquid pump was used for the flow of water through the system and back to the reservoir. A check valve and a gate valve were placed at the pipeline inlet, to avoid liquid back flow and ensure a stable inlet liquid flow rate when the system is experiencing severe slugging.

Air was used as the gas phase and was supplied by a central air supply with an inlet pressure of 100 psig. The air is passed through a filter to eliminate any impurities. The air flowmeter was complemented with a variable supply valve to provide a stable gas flow rate at all times.

The water and the air were separated in a small tank placed at the outlet of the riser. Air was vented to the atmosphere, and water was flowed back into the reservoir tank.

3.1.2 Instrumentation and Measurements

The gas flow rates for the system are measured using a float-meter. The float-meter was located 7.57 m from the riser base, and it was supplied with a scale that allowed conversion to actual flow rates using a table supplied by the manufacturer.

The water flow rates were supplied using a Hydra-Cell pump and measured using a SeaMetrics FT410 compact digital flow monitor, with an accuracy of $\pm$ 1.0% of the full scale. The pressures in the pipeline were measured using a Validyne differential pressure transducer with a range of $\pm$ 12.5 psi, and accuracy of $\pm$ 0.5% absolute. The pressure transducer was located near the gas and liquid inlet (See Figure 3-1).

An IBM compatible PC with a Labview^{TM} data acquisition package was used to collect the data from the pressure transducer. The voltage output from the transducer was read by the Labview^{TM} package and converted to binary numbers that could be processed by the computer. The computer program controlled the data acquisition process and converted the raw data into actual pressures.

3.1.3 Experimental Procedure

The data acquisition speed was set to one pressure data point per second. This data acquisition speed was considered sufficient based on the severe slugging cycle times expected from the experiments.

The liquid and gas flow rates were set in the range of 0.02 to 0.45 m/s and 0.01 to 0.3 m/s, respectively. The lower limits were set because of the meter accuracy and the higher limits were set by the slug/surging limitations, and the flow capacity of the system. The gas and liquid were allowed to flow for about 5-10 minutes prior to data acquisition, in order to eliminate transients due to start-up. After this flow period, the data acquisition was started and data is collected for the next 10 minutes.

3.1.4 Analysis of a Typical Test Run

Two different scenarios were studied: the severe slugging with no elimination, and the elimination using the external bypass. Typical pipeline pressure versus time plots for both scenarios are shown in Figure 3-2.
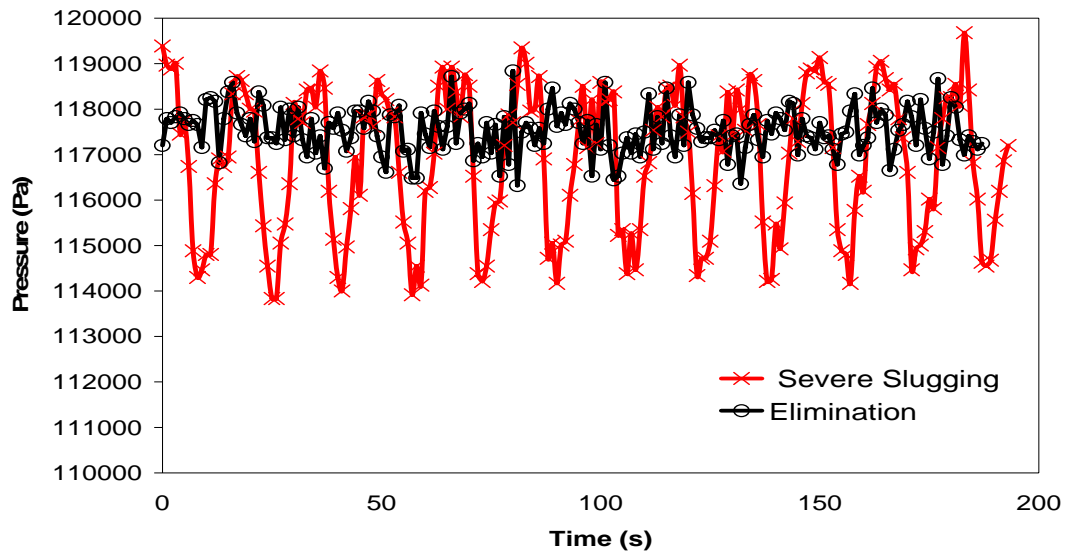
Figure 3–2: Pipeline pressure fluctuations versus time for an experimental run performed

For no elimination, the typical severe slugging characteristics were observed with liquid buildup in the riser followed by a sudden blowout of liquid and gas as soon as the gas reached the riser base. For the elimination part of the experiment, the gas was passed through the bypass via a variable ball valve, and introduced into the riser at a location of 0.23 m from the riser base. When the gas was passed through the bypass without a choke, a severe slugging cycle was still observed because the liquid blocked the pipeline to a point beyond the take-off of the gas bypass. It was observed that by regulating the choke and controlling the pressure in the pipeline, a total severe slugging elimination could be obtained. The experiments showed that a ball-valve on the bypass line increases the back-pressure in the pipeline by the amount of the differential hydrostatic head between the bypass inlet and outlet points. The pressure control induced at the bypass take-off also influences the length of blockage of liquid in the pipeline. It is found that it is desirable to have a certain range of lengths of liquid blockage in the pipeline to avoid

any gas entering through the riser base, thereby creating unstable oscillations. After a steady state process was reached, the liquid length in the pipeline remained constant.

3.2 Modeling

An existing model by Sarica and Shoham[27] has been modified to investigate the feasibility of the novel approach to eliminate severe slugging.

The modified model allows gas entry from any point along the riser. During the transfer of gas from pipeline to riser through a bypass pipe, the pressure losses in the bypass pipe are ignored for simplicity. No flow or pressure control is incorporated in the model.

The development of the model is based on one-dimensional gravity-dominant flow in both the pipeline and the riser. The system variables in the riser are functions of both time and space, while in the pipeline they are only a function of time. A drift flux formulation is used for the flow in the riser. The calculation of void fraction in the pipeline under stratified flow is based on inlet conditions using a local equilibrium concept. No mass transfer between the phases is considered.

Flow equations for the pipeline. The continuity equations for liquid and gas phases, respectively, are given by:

$$v_{SL,in} = v_{SL,sc} - \alpha_p \frac{dx}{dt} \qquad (3)$$

$$v_{Sg,in} = \frac{1}{P_P} \left\{ v_{Sg,sc} P_{sc} - \alpha_p \frac{d[(\ell_p - x)P_P]}{dt} \right\} \qquad (4)$$

Where incompressible liquid and ideal gas assumptions are made. Pressure losses in the pipeline due to flow are ignored.

Flow equations for the riser. The local liquid and gas continuity equations, and the mixture momentum equation can be expressed, respectively, as:

$$\frac{\partial(1-\alpha_r)}{\partial t}+\frac{\partial v_{SL}}{\partial z}=0 \qquad (5)$$

$$\frac{\partial(\rho_g\alpha_r)}{\partial t}+\frac{\partial(\rho_g v_{Sg})}{\partial z}=0 \qquad (6)$$

$$\rho_g=\rho_{sep}+\left\{z_n-z-\int_z^{z_n}\alpha_r dz\right\}\frac{\rho_L gM}{RT} \qquad (7)$$

Eqs. (5), (6) and (7) have four unknowns, namely, v_{Sg}, v_{SL}, α_r and ρ_g. To close the model, a constitutive drift flux relationship given by Zuber and Findlay[44] is used to obtain local void fractions in terms of superficial phase velocities.

$$v_g=C_o\left(v_{SL}+v_{Sg}\right)+v_d \qquad (8)$$

A minor modification of the Sarica and Shoham[27] model is done to account for the injection point on the riser. The injection point is assumed to be the starting point from which gas enters, and it is assumed no gas will enter through the riser base. An elaborate procedure to solve the above equations is given by Sarica and Shoham[27]. The solution procedure utilizes the method of characteristics to solve the hyperbolic PDE system in the riser.

3.3 Model Performance and Validation

Some example cases from literature, as well as, laboratory experimental data are examined by the model for validation purposes. The model results seem to agree reasonably well with observations in the laboratory and the available data on severe slugging existing in the literature.

3.3.1 Literature Data

Fabre et al.[9] conducted several severe slugging experiments using a 2" ID test facility consisting of a 25 m. long, -0.57° inclined pipeline, and a 13.5 m high vertical riser system, using air and water. The two experiments from their study, Case-1, and Case-2, are used here. Case-1, and Case-2 superficial liquid and gas velocities at standard conditions were given as v_{SL}=0.13 m/s and v_{SG}=0.45 m/s, and v_{SL}=0.13 m/s and v_{SG}=0.20 m/s, respectively.

Case-1 Results. In Figure 3-3 the cyclic pressure fluctuations (one of the characteristics of severe slugging) are shown for Case-1. The no elimination line and solid dots represent the model predictions and experimental data, respectively, for the no-elimination case. The model prediction and experimental data match quite well. Presented on Figure 3.3 are also the model performance predictions when the gas entry point to the riser is above the riser base for three different locations of 5, 10 and 20 cm. above the riser base, respectively. It is clearly shown from these responses that moving the gas entry point above the riser base can significantly change the nature of the flow. The magnitude of the pressure fluctuations was drastically reduced for the L_{inj} = 5 cm case, and eliminated for the L_{inj} = 10 cm case and the L_{inj} = 20 cm case.
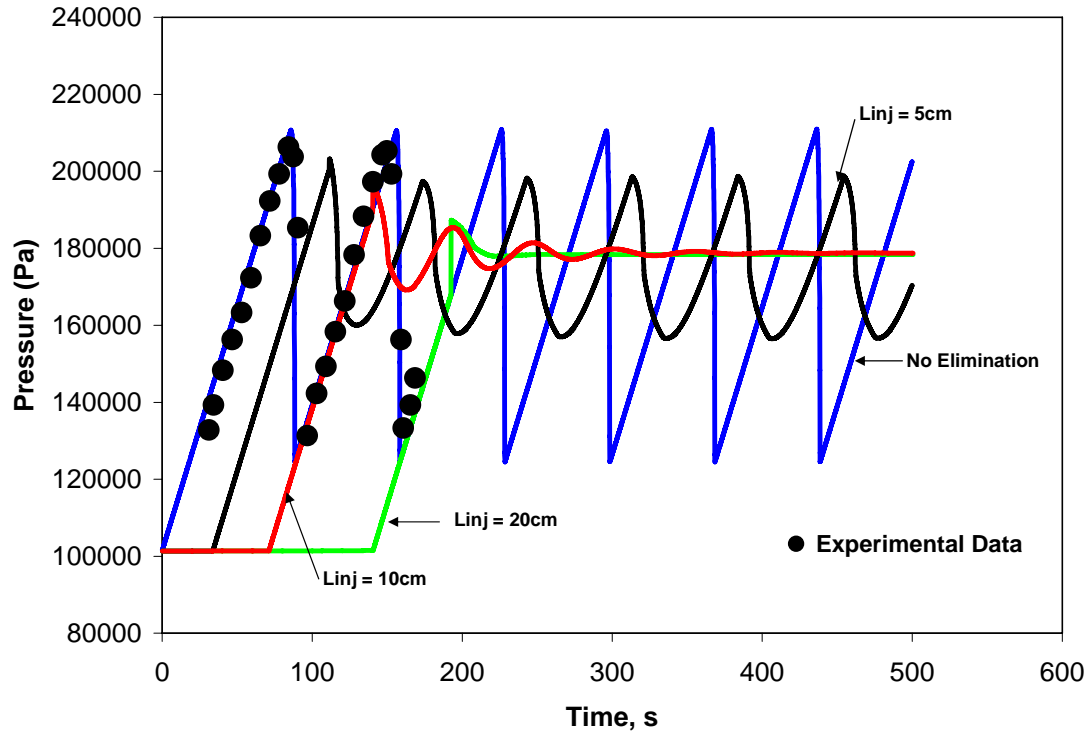
Figure 3–3: Pipeline pressure behavior for different gas entry locations (v_{SL} = 0.13 m/s, v_{Sgo} = 0.45 m/s)

In Figure 3-4, the lengths of the accumulated liquid in the pipeline versus time are presented. The accumulation increases as the location of the riser entry point moves up. For L_{inj} = 20 cm case, the liquid accumulation length reached up to 15.5 m., this indicates that the gas take-off point (by-pass connection to the pipeline) on the pipeline should be at least 16 m away from the riser base for the 20 cm case. The accumulated liquid volume can exceed the volume of the pipeline indicating a theoretical limit on the location of the riser entry point.

Figures 3-3 and 3-4 show that elimination can be accomplished with a riser entry point significantly lower than what Barbuto[2] proposed, 1/3 of the total riser height from

the riser base. The entry location depends on the system parameters and should be determined using a rigorous model.
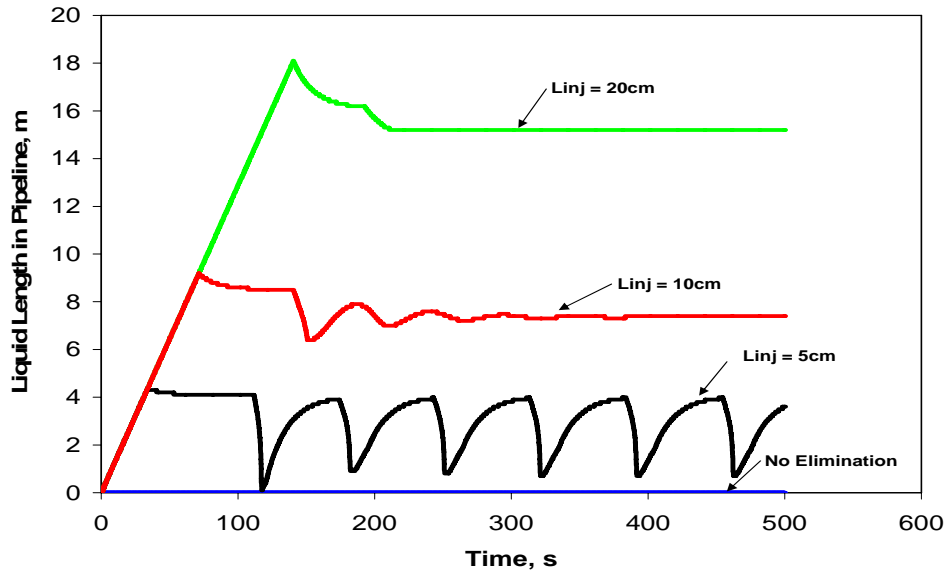
Figure 3–4: Liquid length in pipeline for different gas entry locations (v_{SL} = 0.13 m/s, v_{Sgo} = 0.45 m/s)

Case-2 Results. In Figure 3-5 the cyclic pressure fluctuations are shown for Case-2. The no elimination line and solid dots represent the model predictions and experimental data, respectively, showing a good match. Figure 3-5 also shows the system responses for the gas entry locations of 5, 10, and 20 cm. above the riser base, respectively. Similar to the Case-1 results, it is clear that the gas entry point above the riser base can significantly change the flow behavior. Figure 3-5 reveals that L_{inj} = 5 cm and L_{inj} = 10 cm is not sufficient to cause a significant change while the 20 cm location shows practically a complete elimination of severe slugging.

The lengths of the accumulated liquid in the pipeline versus time are shown in Figure 3-6. Comparing Figures 3-4 with 3-6, it is clear that the liquid accumulation is higher for lower superficial gas velocities at constant superficial liquid velocity. For the

no elimination case, fluctuations not only in pipeline pressure but also in liquid accumulation are observed.

The above analysis of Case-1 and Case-2 clearly shows that severe slugging can be eliminated with the proposed technique.
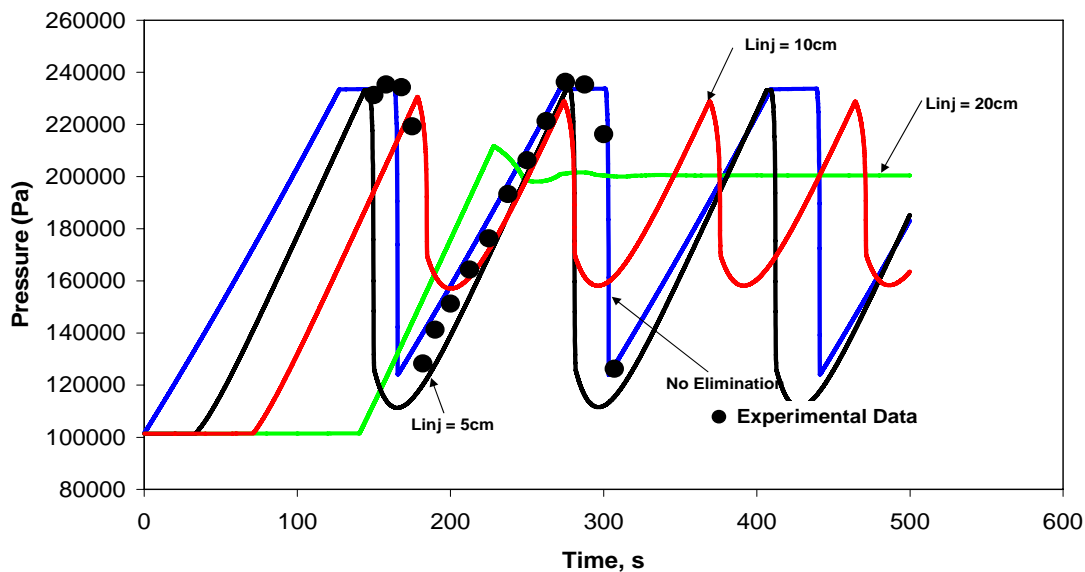
Figure 3–5: Pipeline pressure behavior for different gas entry locations (v_{SL} = 0.13 m/s, v_{Sgo} = 0.20 m/s)
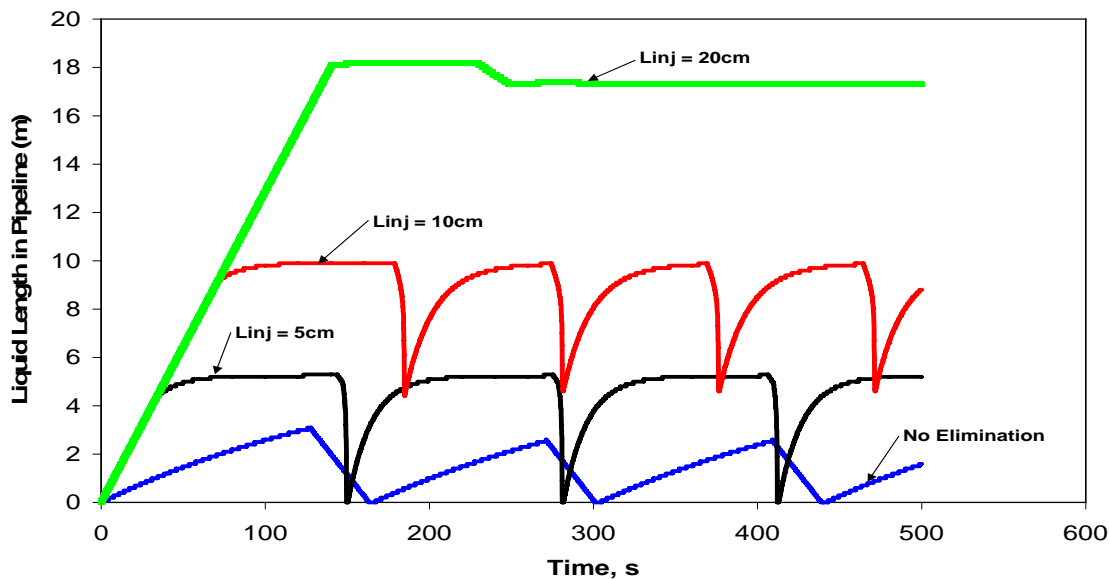
Figure 3–6: Liquid length in pipeline for different gas entry locations (v_{SL} = 0.13 m/s, v_{Sgo} = 0.20 m/s)

3.3.2 Experimental Data

Several severe slugging experiments were conducted using a test facility consisting of a 7.57 m. long, -3.0° inclined pipeline, and a 1.88 m high vertical riser system.

The experimental observations together with model predictions and Bøe[5] and Taitel's[35] stability criteria are shown for the severe slugging envelope in Figure 3-7. The model prediction agrees very well with the observed data and confirms that Bøe's[5] criteria does not fully predict the whole region of severe slugging.

The results of the two experimental runs Case-3 and Case-4 are presented. For Case-3, and Case-4 the superficial liquid and gas velocities at standard conditions are given as v_{SL}=0.207 m/s and v_{Sgo}=0.0507 m/s, and v_{SL} = 0.115 m/s and v_{Sgo} = 0.0507 m/s, respectively. Also, included in Figure 3-7 are the two operational points of the Case-3 and Case-4.
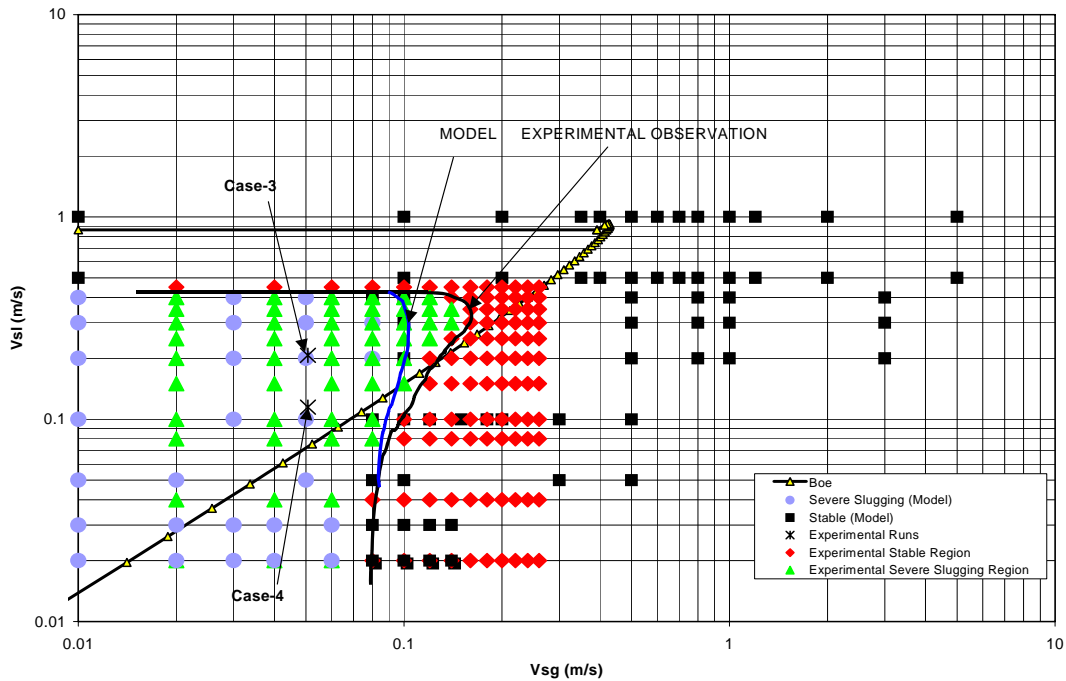
Figure 3–7: Severe slugging envelop for the small-scale facility

Case-3 Results. In Figure 3-8, the cyclic pressure fluctuations of flow conditions operating in the severe slugging region are shown. Figure 3-8 shows the model predictions together with the experimental data. The model prediction and the experimental data match quite well, but the experimental data shows a slugging frequency that is slightly lower than the model. Figure 3-9 show the experimental and model responses with bypass for a gas entry located 23 cm above the riser base. It is clearly seen from both experimental data and model predictions that severe slugging has been eliminated. The current model assumes that the gas take off point is free of liquids, and insensitive to the pressure losses through the bypass. However, experimentally, it is observed that the elimination depends on the liquid penetration length into the pipeline and pressure losses in the bypass. Therefore, either the pressure at the inlet of the bypass
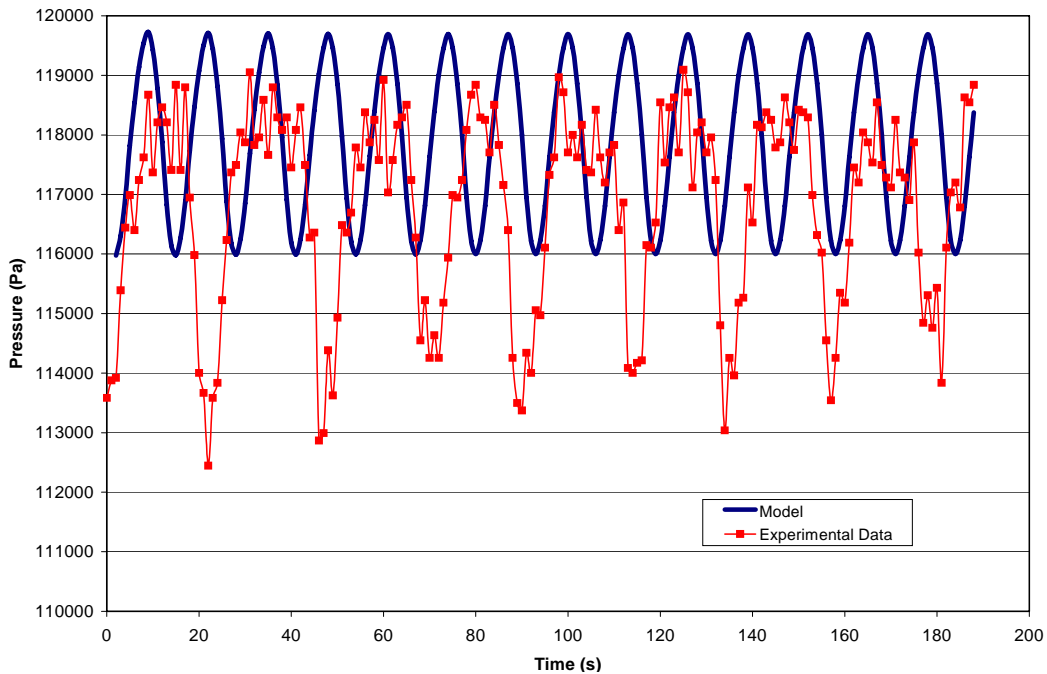
Figure 3–8: Pipeline pressure behavior for severe slugging (v_{SL} = 0.207 m/s, v_{Sgo} = 0.0507 m/s)
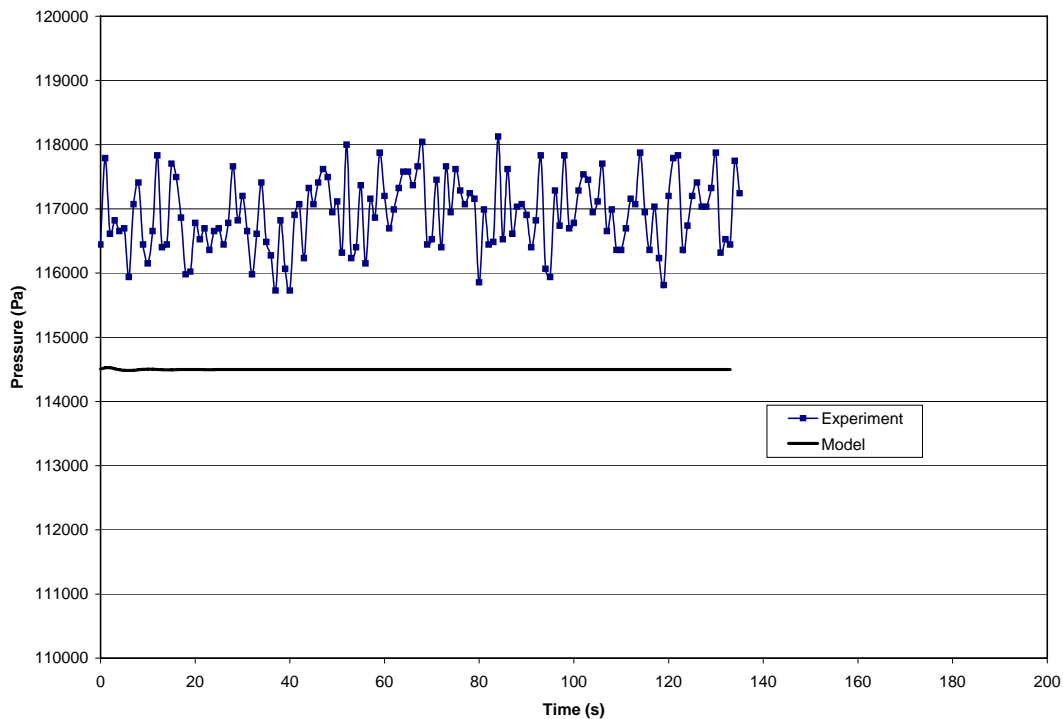
Figure 3–9: Pipeline pressure behavior for gas entry located 23 cm above riser base (v_{SL} = 0.207 m/s, v_{Sgo} = 0.0507 m/s)

needs to be controlled or the take off point should be further away from the riser base to ensure the elimination of severe slugging.

   Case-4 Results.   Both the model predictions and experimental data are shown in Figure 3-10 for Case-4.   The model prediction and the experimental data match quite well, but the experimental data shows a slugging frequency that is slightly lower than the model prediction.   Figure 3-11 shows the system responses for the gas entry locations of 23 cm above the riser base. The model prediction and experimental data match quite well. Figure 3-11 shows a complete elimination of severe slugging.
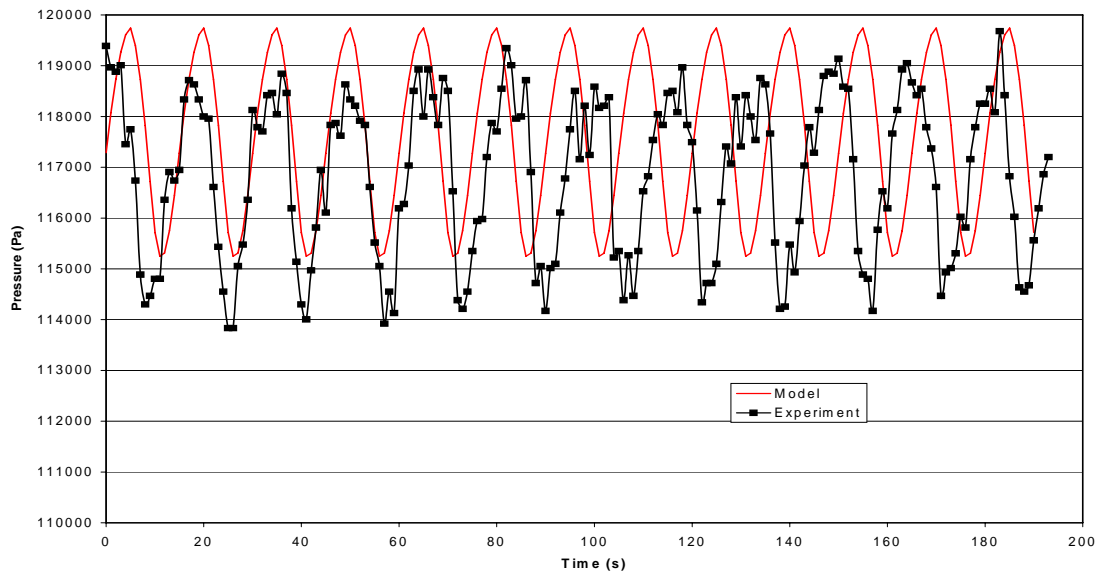
Figure 3–10: Pipeline pressure behavior for severe slugging (v_{SL} = 0.115 m/s, v_{Sgo} = 0.0507 m/s)
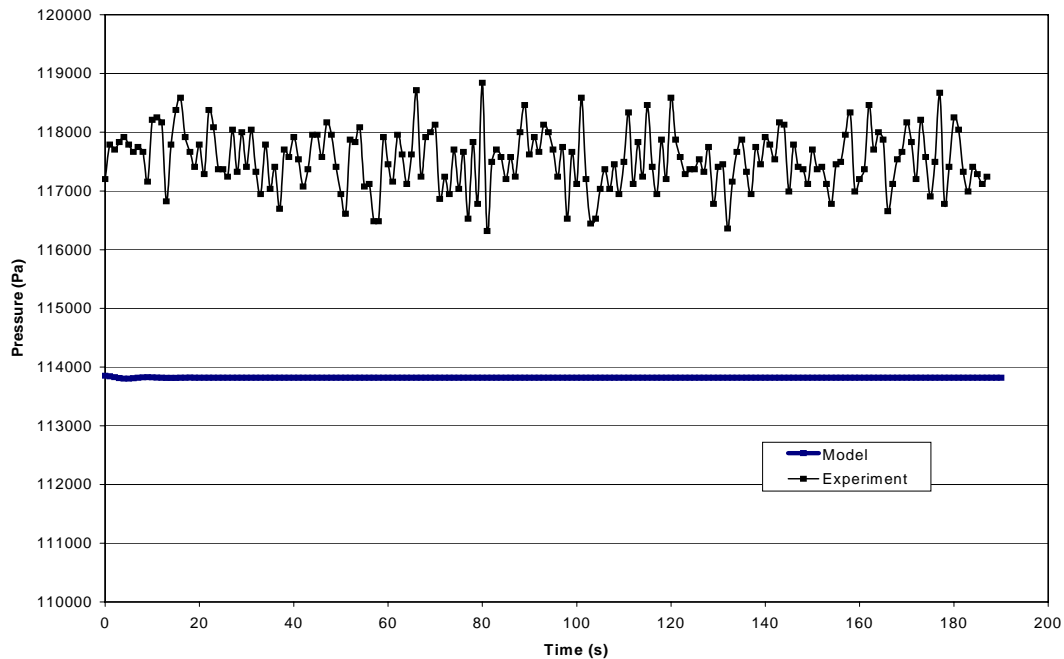
Figure 3–11: Pipeline pressure behavior for gas entry located 23 cm above riser base (v_{SL} = 0.115 m/s, v_{Sgo} = 0.0507 m/s)

A novel approach to lessen or eliminate severe slugging in pipeline-riser systems, by transferring the pipeline gas to the riser at a point above the riser base is proven both experimentally and theoretically. This transfer process reduces both the hydrostatic head in the riser and the pressure in the pipeline, consequently lessening or eliminating severe slugging occurrence. This approach can be considered as self-gas lifting (i.e., no additional gas injection is required from the platform). An existing severe slugging model based on a one-dimensional drift flux formulation, has been modified to simulate the flow behavior of the new severe slugging elimination method. The modified model has been verified by comparing it to the existing laboratory severe slugging data from several sources. The next chapter focuses on the experimental and modeling studies to further investigate the proven technique.

Chapter 4 EXPERIMENTAL PROGRAM

In the proof of concept study, a small facility was utilized to verify whether the concept is feasible. A thorough experimental study was needed to investigate the problem of severe slugging and elimination with the proposed technique and to help develop a model as a design tool. A larger and more versatile facility was needed to facilitate further studies.

4.1 Test Facility

An existing two-phase flow facility at Tulsa University Fluid Flow Projects was modified for this study. The modified facility consisted of a 65 ft pipeline followed by a 49 ft riser. The pipeline and the riser were made out of 3 in ID transparent acrylic pipe. Additional variable volume tanks were available to increase the effective pipeline length to 280 ft. The liquid and gas flow rates could be varied between 0.1 – 2.0 m/s and 0.1 – 5.0 m/s, respectively. Two different scenarios are studied: the severe slugging cycle with no elimination, and the elimination using an external bypass. Several connection points for the bypass, both on the pipeline and the riser are studied. The modified facility accommodated pipeline inclination angles ranging from 0 – 5° downwards. A schematic of the new large-scale facility is shown in Figure 4-1.
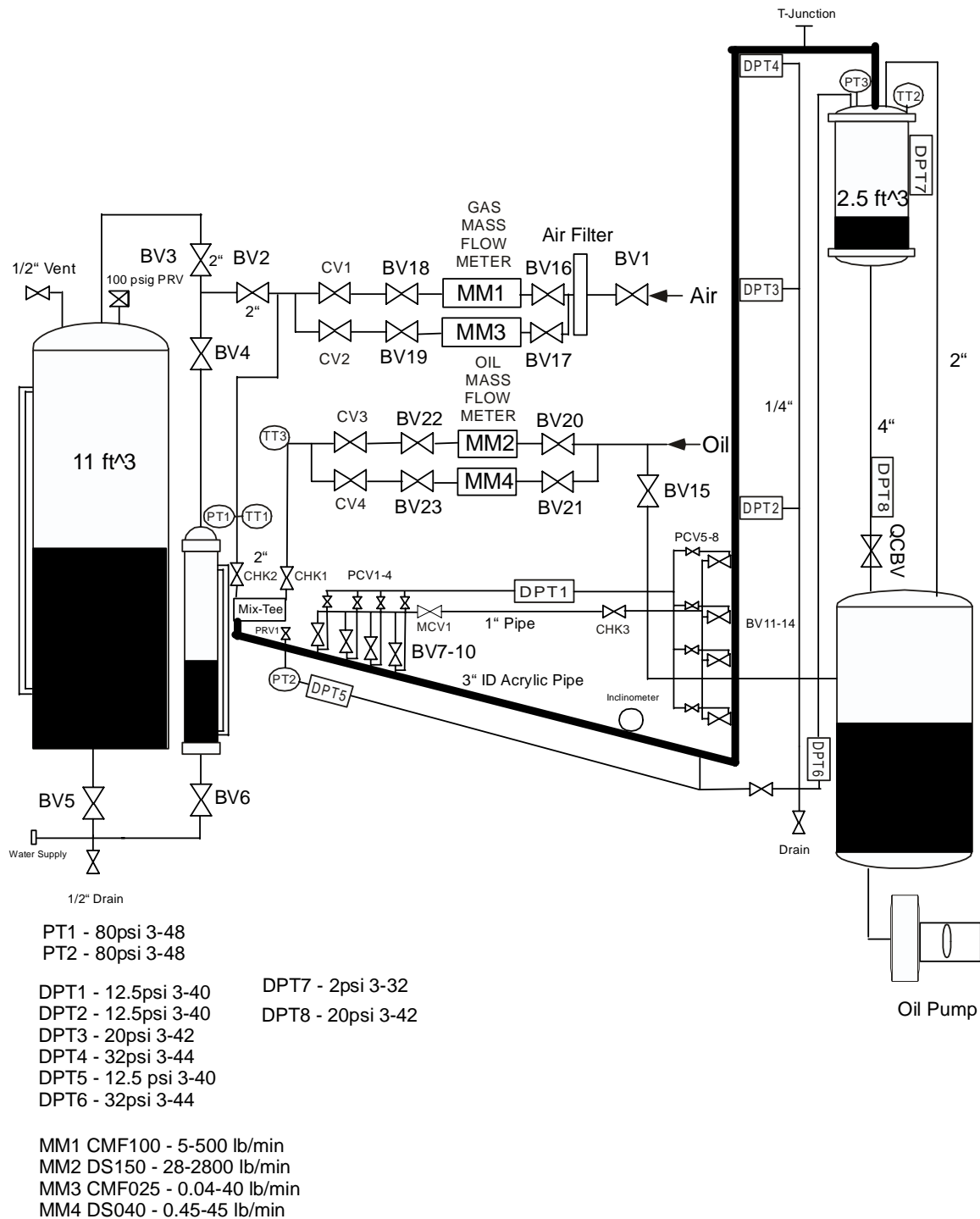
Figure 4–1: Large-scale facility

4.1.1 Fluid Handling System

A refined clear mineral oil, Crystex AF-M was used as the liquid phase, and it was supplied from a tank that acts as a reservoir and circulation tank. The properties of the oil as provided by the manufacturer are given in Table 4-1. Before entering the pipeline, the oil is flowed through a filter to remove any unwanted particles.

Table 4-1: Properties of the Crystex AF-M Oil

Physical Properties	ASTM Test	Crystex AF-M
Gravity (API)	D287	33.6
Specific Gravity @ 77 °F	D1298	0.856
Flash Point	D92	385 °F
Viscosity, cSt @ 104 °F	D445	18.9
Pour Point	D97	10 °F

The gas phase (compressed air), was supplied by a two-stage compressor with a maximum capacity of 0.7 MMSCF/D. The air was passed through air filters to ensure that there were no impurities when it enters the pipeline.

4.1.2 Instrumentation and Measurements

The gas flow rates were measured using a CMF025 micromotion meter. The micromotion meter was located upstream of the regulator valve to minimize pressure fluctuations. The oil flow rate was measured using a DS150 micromotion meter.

Pressure transducers were located at the inlet and outlet of the bypass and along the riser as shown in Figure 4-1.

A choke was placed at the bypass inlet in order to control the pressure in the pipeline, if the liquid penetration length were to exceed that of the bypass inlet in the pipeline.

A PC based data acquisition system from National Instruments, Inc. was utilized to acquire the data into text files. The hardware consisted of a PC and a multifunction I/O board. The analog signals from the measurements devices were converted to digital signals by the multifunction I/O board. A software package from Labview[TM] was used to perform the data acquisition and processing tasks.

4.1.3 Experimental Grid

With the large-scale experimental facility, several variables were investigated. These were: inclination angle, gas and liquid flow rates, bypass-pipeline take-off points and bypass-riser injection points. To capture the physics of severe slugging thoroughly, a large amount of data were needed with varying configurations and flow conditions. The bypass system consisted of four take-off points, and four injection points. Three different angles, 1°, 3°, and -5° were investigated.

The Bøe[5] region for a pipeline and inclination angle of 1 degree downwards is shown in Figure 4-2. In this figure, a grid system of the test points is shown. This inclination angle had 49 different combinations of liquid and gas flow rates that were investigated, and since there are 3 different bypass connection points on the pipeline and on the riser, the total amount of data points gathered for this angle were about 400 points.

These numbers are representative for this angle only. The Bøe[5] stability criteria for each of the five angles using the dimensions of the new facility are presented in Figure 4-3. It is clear from Figure 4-3 that the severe slugging envelope increases as the angle increases. Therefore, the test matrix was modified for increasing angles.
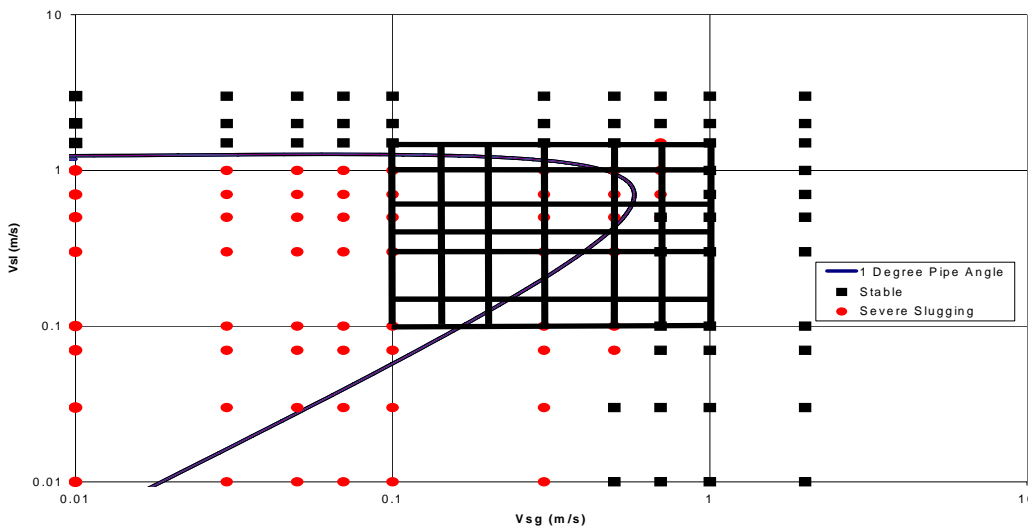
Figure 4–2: Visual schematic of superficial gas and liquid velocities investigated for a downward angle of 1 degree
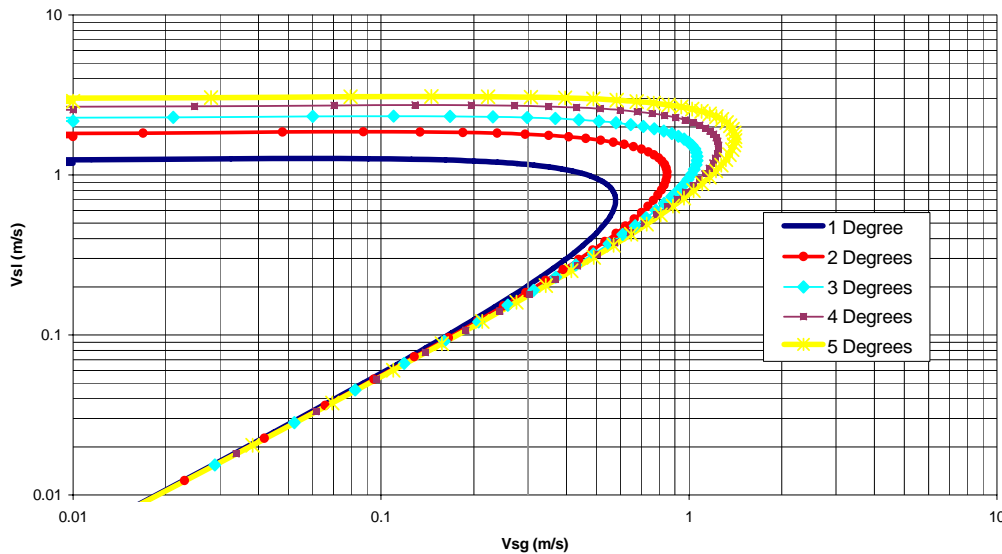
Figure 4–3: The Bøe[5] stability region for pipeline angles ranging from 1-5 degrees downward

4.2 Uncertainty Analysis

An uncertainty analysis was performed on the measured physical parameters in the experiments, such as the pressure, temperature and flow measurement devices to quantify the quality of the data and to estimate the uncertainty of the measurements gathered. An error propagation analysis on the superficial liquid and gas velocities was also performed.

In general, errors can be divided into two parts, systematic and random errors. Systematic error is an error that shifts the measurements in a systematic way, so that their mean value is displaced. Systematic error includes incorrect calibration of equipment and improper use of equipment or failure to account for certain effects present in the device. In any experimental work, it is important to try to eliminate as much as possible the effect of the systematic error. In this study, the failure to account for the important effects of systematic errors are assumed to be absent due to good engineering practices. However, regardless of the care taken in calibrating a device, there will always be a small systematic error present in the device.

The random error is directly related to the scatter of the data around its average value, which can be defined as a displaced measurement in any direction, as opposed to the systematic error that displaces the measurement in one direction. Random errors are always represented using a distribution, such as Normal, Gaussian or other distribution functions.

4.2.1 Systematic Uncertainty

As stated earlier, the systematic error uncertainty can come from various sources. For this study, the instrument calibration is considered as the only source of the systematic error, since it is the dominant error in the system. Each of the calibration errors can be a source of the elemental systematic uncertainty, expressed as b_i, which needs to be combined using the square root of the sum of the errors squared, and is expressed as:

$$B_R = \sqrt{\sum (b_i)^2} \qquad (9)$$

B_R is the combined systematic uncertainty component of the overall uncertainty analysis.

4.2.2 Random Uncertainty

A sample of the data is used to determine the random uncertainty, as opposed to the whole population. Using the whole population is almost always impossible due to the nature of the data. Therefore, a sample of the data is used to estimate the population properties such as the central tendency and spread from the data sample. It is easily proven that this method is an unbiased estimation of the population mean.

The scatter of the data around its average can be defined as the sample variance or sample standard deviation squared. In order to determine the random uncertainty, we need to determine the variance of the sample data, expressed as follows:

$$S_X = \sqrt{\frac{1}{N-1} \sum_{i=1}^{N} (x_i - \bar{x})^2} \qquad (10)$$

The actual sample data scatter is rarely of any interest in the uncertainty analysis. It is more desirable to find the scatter of the mean values or the variance of the group means. Because it is difficult to determine the mean distribution using numerous tests, it has been estimated from one test of actual data. The mean variance can be expressed as:

$$S_{\bar{X}} = \frac{S_X}{\sqrt{N}}$$
(11)

In order to continue the uncertainty analysis a distribution function needs to be selected. Since the sample data are used as opposed to the total population, the "Student's t" distribution is selected. From Figure 4-4 it can be seen that the sample presented shows a normal distribution, therefore, the "Student's t" distribution can be used with confidence. A significance level needs to be chosen in order to obtain the random uncertainty. This significance level is used to look up the value of the t-statistics from a statistics table.
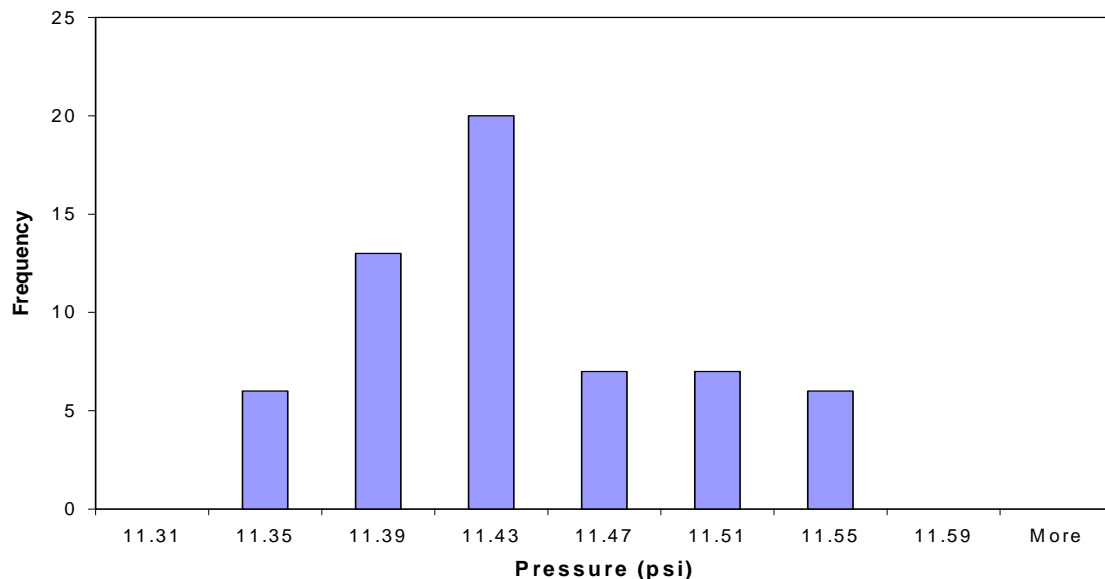
Figure 4–4: Distribution of one data sample

In this study a confidence interval of 95% is chosen as the value of which the desired accuracy being sought, in the statistics table this value is represented as the 5% significance level. The t-distribution can be expressed as:

$$t = \frac{\overline{x} - \mu}{S_X / \sqrt{N}} \sim t(N-1) \tag{12}$$

(N-1) degrees of freedom are used to obtain the t-statistics. The random uncertainty component is expressed as:

$$t_{95} S_{\overline{X}} \tag{13}$$

Now the systematic and the random components can be combined into an overall uncertainty. This requires the computation of the proper degrees of freedom to be used.

4.2.3 Degrees of Freedom

A proper degree of freedom parameter needs to be computed to use the 95% t-statistics from the statistics table. By combining the systematic and random uncertainties we can obtain the combined degrees of freedom. In this study the Welch-Satterthwaite[8] approximation is used, and is expressed as follows:

$$df = \frac{\left(\sum (S_{\overline{X},i})^2 + \sum \left(\frac{b_i}{2}\right)^2 \right)^2}{\left[\sum \left((S_{\overline{X},i})^4 / df_i\right) + \left(\sum \left(\frac{b_i}{2}\right)^4 / df_i \right) \right]} \tag{14}$$

There are several models to compute the measurement uncertainty available in the literature. In this study, the model of ASME is selected because of its robustness. The ASME model states the uncertainty as follows:

$$\left(\overline{X} - U_{ASME}\right) \le \mu \le \left(\overline{X} + U_{ASME}\right) \tag{15}$$

where,

$$U_{ASME} = t_{95}\left[\left(B_R/2\right)^2 + \left(S_{\overline{X}}\right)^2\right]^{0.5} \tag{16}$$

The above statement is not a probability statement, but rather a confidence level for the data or population that the uncertainty analysis has been performed on. The best interpretation for the above statement is "Either the population mean (μ) is within the interval or we have unusual data". Table A-1 in Appendix A summarizes the overall uncertainty of all the instruments or devices used in the experimental part of this study. The inclination angle random uncertainty is not reported because the angle is set at a certain level, and thus there are no random errors associated with this parameter. To obtain the uncertainty for composite measured parameters, such as volumetric flow rate or superficial velocities, an investigation of uncertainty propagation is needed.

4.2.4 Uncertainty Propagation

It is essential to measure the combined effects of the elemental uncertainty to obtain the composite experimental parameters. The propagation of the systematic and random uncertainty components of the elemental uncertainty as required in this process is calculated. Three common methods are used for the uncertainty propagation, these are, Taylor's Series uncertainty propagation, "Dithering", and Monte Carlo simulation. In this study, the method of Taylor's Series was adopted to calculate the uncertainty propagation into the superficial liquid and gas velocity calculations. Only the first-order

terms are considered significant in the Taylor series method. For this study, an evaluation of the uncertainty propagation for the gas and liquid flow rates is performed.

The density value in the equation below is the reported liquid density from the experiment. The density of the liquid is correlated with temperature to obtain the density at different temperatures, assuming insignificant pressure variations to influence the density measurements. Therefore, the uncertainty on the density needs to be propagated based on the temperature. The expression for the liquid density is shown below:

$$\rho_L = (-0.0004T + 0.8905)*62.4 \qquad (17)$$

The overall uncertainty propagation based on the temperature can be expressed as:

$$U_{\rho_L} = \left[\left(\frac{\partial \rho_L}{\partial T}\right)^2 U_T^2\right]^{0.5} \qquad (18)$$

$$U_{\rho_L} = \left[(-0.0004*62.4)^2 U_T^2\right]^{0.5} \qquad (19)$$

The following are the expressions for the liquid and gas flow rates and their associated uncertainty values:

$$Q_L = \frac{\dot{m}}{\rho_L} \qquad (20)$$

$$U_{Q_L} = \left[\left(\frac{\partial Q_L}{\partial \dot{m}}\right)^2 U_{\dot{m}}^2 + \left(\frac{\partial Q_L}{\partial \rho_L}\right)^2 U_{\rho_L}^2\right]^{0.5} \qquad (21)$$

$$U_{Q_L} = \left[\left(\frac{1}{\rho_L}\right)^2 U_{\dot{m}}^2 + \left(-\frac{\dot{m}}{\rho_L^2}\right)^2 U_{\rho_L}^2\right]^{0.5} \qquad (22)$$

For the gas flow rate the following uncertainty propagation equations based on the ideal gas law are used:

$$Q_g = \frac{RT\dot{m}_g}{pM} \tag{23}$$

$$U_{Q_G} = \left[\left(\frac{\partial Q_g}{\partial T} \right)^2 U_T^2 + \left(\frac{\partial Q_g}{\partial \dot{m}_g} \right)^2 U_{\dot{m}_g}^2 + \left(\frac{\partial Q_g}{\partial p} \right)^2 U_p^2 \right]^{0.5} \tag{24}$$

$$U_{Q_g} = \left[\left(\frac{R\dot{m}_g}{pM} \right)^2 U_T^2 + \left(\frac{RT}{pM} \right)^2 U_{\dot{m}_g}^2 + \left(-\frac{RT\dot{m}_g}{p^2 M} \right)^2 U_p^2 \right]^{0.5} \tag{25}$$

Using the overall gas and liquid flow uncertainties as expressed above, the uncertainties in the superficial gas and liquid velocities can be calculated assuming a constant value of pipe ID as follows:

$$U_{v_{SL}} = \left[\left(\frac{1}{A} \right)^2 U_{Q_L}^2 \right]^{0.5} \tag{26}$$

$$U_{v_{Sg}} = \left[\left(\frac{1}{A} \right)^2 U_{Q_g}^2 \right]^{0.5} \tag{27}$$

The results of this analysis for all flow rate combinations for all angles are presented in Tables A1 through A4 in Appendix A.

4.3 Experimental Results and Analysis

The main objective of the experimental part of this study was to investigate the severe slugging phenomenon with and without an external bypass conduit between the pipeline and the riser.

Several variables such as pipeline inclination angle, gas and liquid flow rates, and bypass, take-off and injection points have been investigated. Tests were conducted for -1°, -3°, and -5° pipeline inclination angles.

Several tests were performed for each pipeline inclination angle. First, the facility was operated without the bypass to obtain the severe slugging occurrence characteristics of the flow. Then, the tests with bypass for several combinations of the take-off and injection points were conducted for a given gas and liquid flow rate combination. The tests with bypass have included both fully and partially open take-off valve cases. In all the figures presented, (SS) denotes the experimental severe slugging pressure fluctuations in the pipeline, unless otherwise specified.

4.3.1 Severe Slugging Occurrence

Experimental observations of severe slugging were made during the experimental phase of this study, and the result for the -1° inclination angle case is presented in Figure 4-4. There are several proposed models to predict the severe slugging region or envelope. These models have been discussed previously under the literature review. Here, the Bøe[5] prediction method is shown for comparison in Figure 4-4. The experimental data show severe slugging well outside the Bøe[5] region. Similar behavior has also been observed for the –3° and –5° inclination angles as shown in Figures 4-5 and 4-6, respectively. Figure 3.7 of chapter 3.3.2 shows the comparison of the severe slugging data obtained by the small-scale facility with the Bøe[5] prediction model. Severe slugging observation made with the small-scale facility agrees with the observations of both Vierkandt[40] and Jansen[17] for a 2.54 cm diameter pipe. This study used a larger

diameter pipe of 7.62 cm, and observations showed that the Bøe[5] criterion cannot accurately predict the severe slugging region for a larger scale test facility.

The flow pattern maps in Figures 4-4 and 4-5 show the experimental data for -1° on a vertical and one degree downward flow pattern map, respectively. Also shown on these figures is the Bøe[5] stability region. From these figures it can be seen that most of the data fall into the slug region in the vertical flow pattern regime and in the stratified wavy region of the one-degree flow pattern regime.
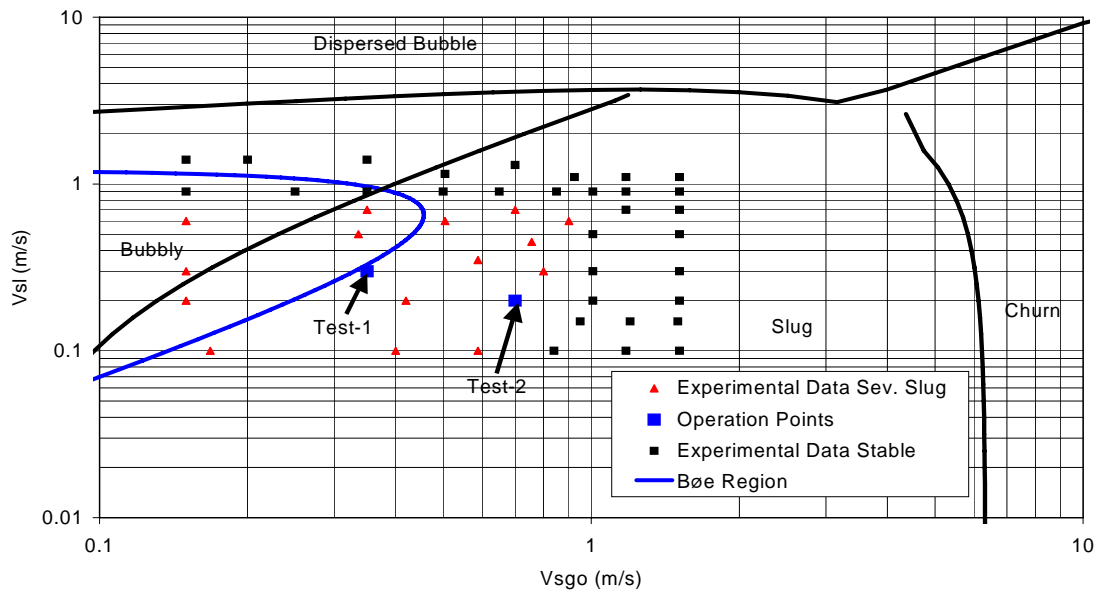
Figure 4–5: Severe slugging data shown on a vertical flow pattern map
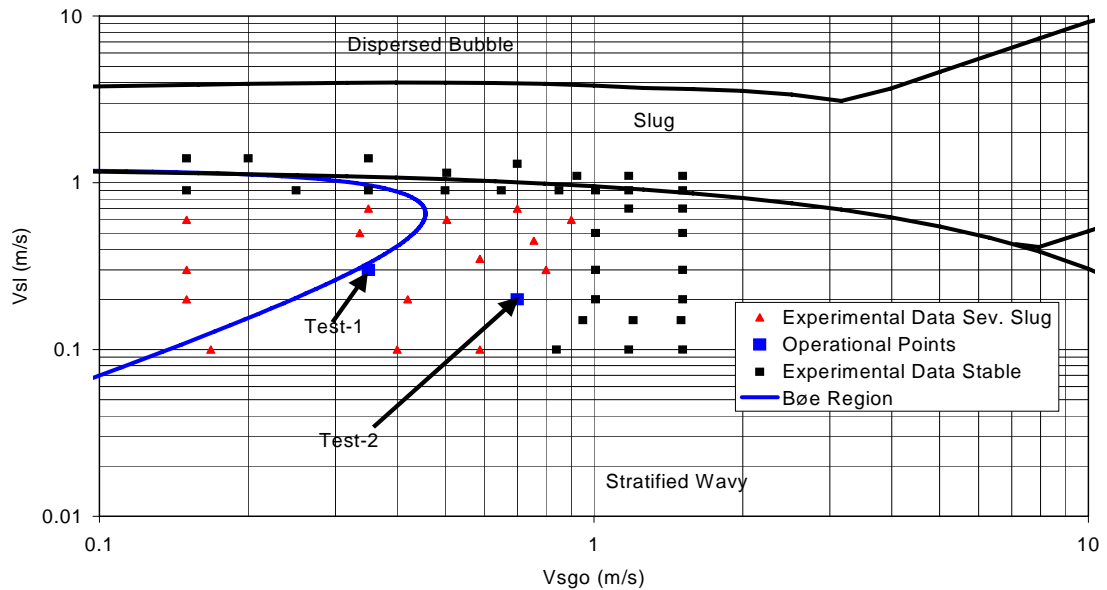
Figure 4–6: Severe slugging data shown on a flow pattern map

4.3.2 Severe Slugging Elimination

158 tests were conducted. The results of four tests, test-1, test-2, test-3 and test-4 are presented to describe the physics of both the severe slugging and the lessening and/or elimination of severe slugging. The operational points of Test-1, Test-2, Test-3 and Test-4 are shown in Figures 4-6 to 4-8.
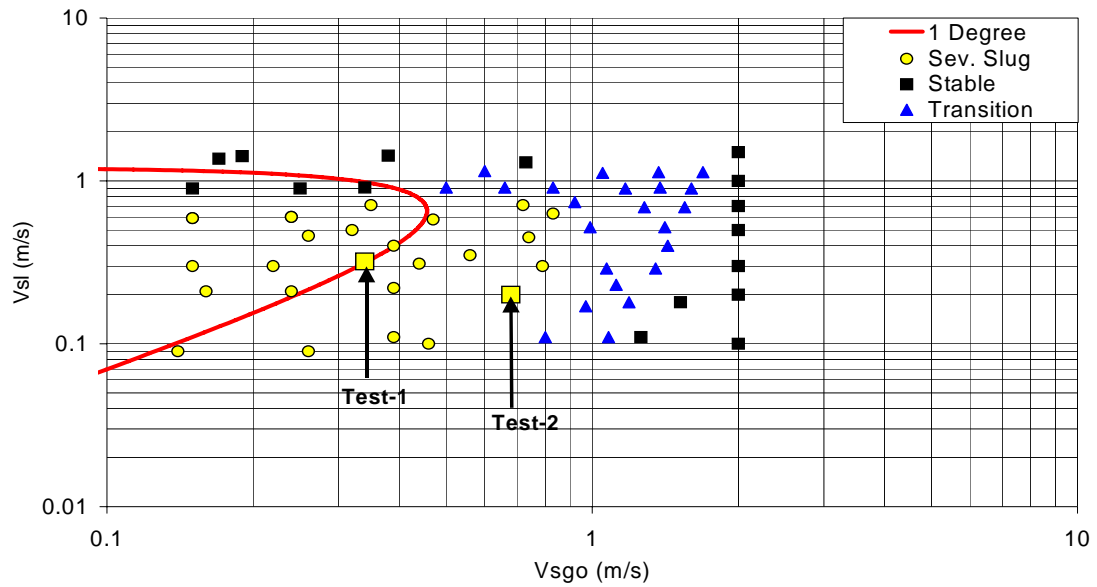
Figure 4–7: Experimental severe slugging region for -1°-pipeline inclination angle
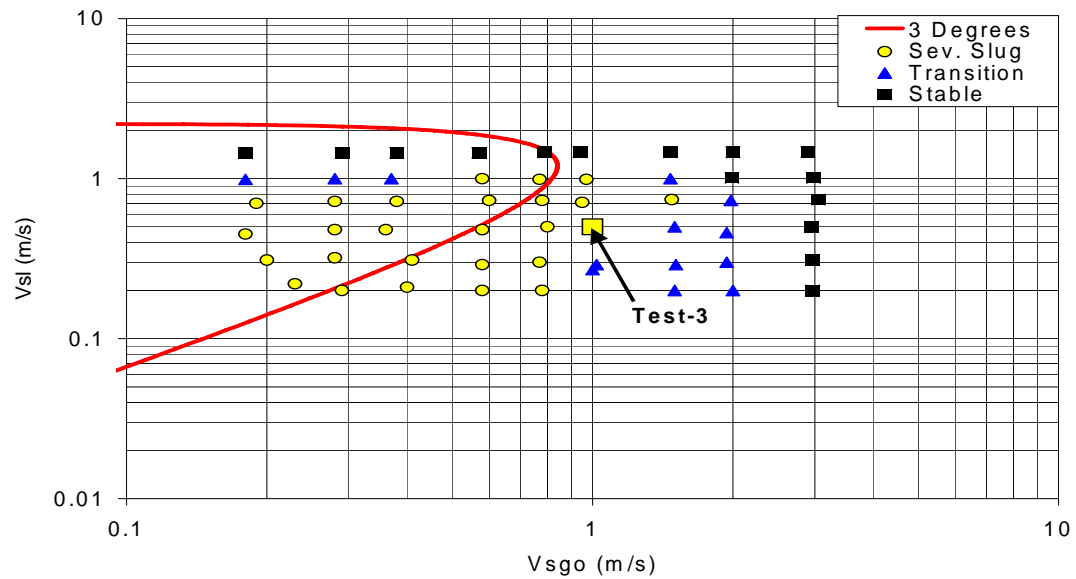
Figure 4–8: Experimental severe slugging region for -3° pipeline inclination angle
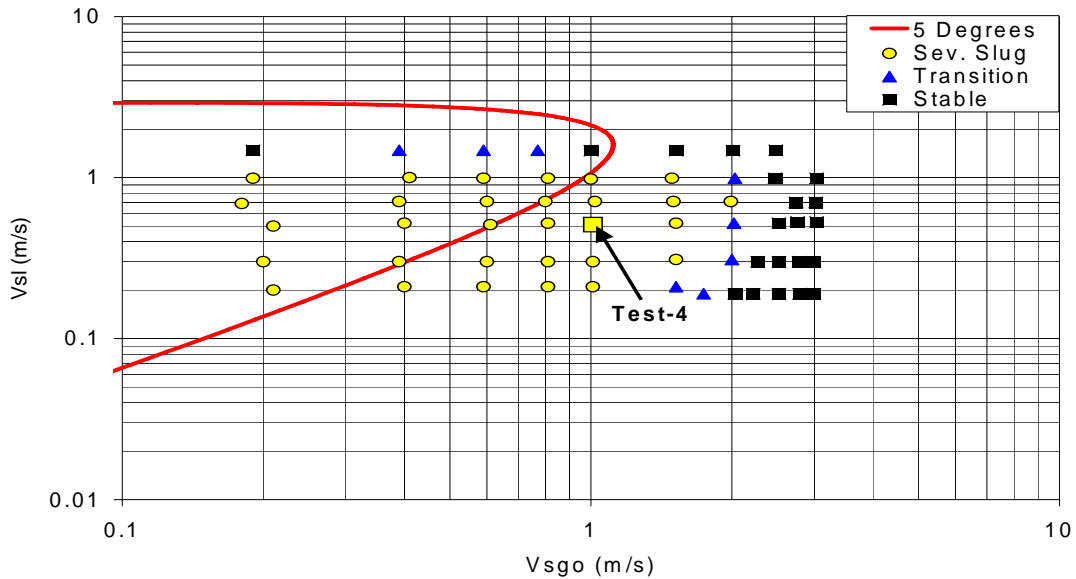
Figure 4–9: Experimental severe slugging region for -5° pipeline inclination angle

4.3.2.1 Analysis of Test Runs for -1° Pipeline Angle

Test-1 is located in the middle of the severe slugging region while Test-2 is near the boundary between the severe slugging and stable regions as shown in Figure 4-6. Two different cases, fully and partially open take-off valves, were studied for the lessening or elimination of severe slugging.

4.3.2.1.1 Fully Open Take-off Valve

The superficial velocities for Test-1 $v_{SL} = 0.32$ m/s, and $v_{SG} = 0.35$ m/s. Figure 4-9 shows the pressure vs. time response using the injection point of 27 in. above the riser base with the different take-off points. This figure shows that severe slugging has been

slightly lessened, but not eliminated due to liquid blockage of the take-off points. It is postulated to occur because the injection point is higher than all the take-off points. This creates a lesser degree severe slugging when compared to the base case (no elimination).

Figure 4–10: Experimental data for severe slugging (SS), using different fully open take-off points and injection point BV13 (v_{SL} = 0.32 m/s, v_{Sg} = 0.35 m/s)

Figure 4-10 is similar to Figure 4-9, but now the injection point is 13.5 in. above the riser base. From Figure 4-10 it can be observed that severe slugging has been lessened further for this injection point as compared to the 27 in. above the riser case, showing as the injection points are lowered a more stable operation is achieved using the current take-off valve.

Figure 4–11: Experimental data for severe slugging (SS), using different fully open take-off points and injection point BV12 (v_{SL} = 0.32 m/s, v_{Sg} = 0.35 m/s)

Figure 4-11 shows the pipeline pressure vs. time behavior for the lowest injection point of 7 in. above the riser base. One would expect that this point would lessen the severe slugging pressure oscillations even further than the previous case, however, that is not the case. When using the lowest injection point it is observed that the cycles are not governed by the blockage of the take-off points as is the case with the two previous injection ports. The governing mechanism for the pressure oscillations is that the pressure at the take-off point is lower than the pressure at the injection point into the riser, so liquid flows back through the injection port and thus blocks the flow of gas through the bypass line. Therefore, no matter where the gas is taken off, the pressure fluctuation magnitude as well as the severe slugging cycle is the same.

Figure 4–12: Experimental data for severe slugging (SS), using different fully open take-off points and injection point BV11 (v_{SL} = 0.32 m/s, v_{Sg} = 0.35 m/s)

The cycle times and pressure fluctuations for the different take-off and injection combinations are shown in Figure 4-12.
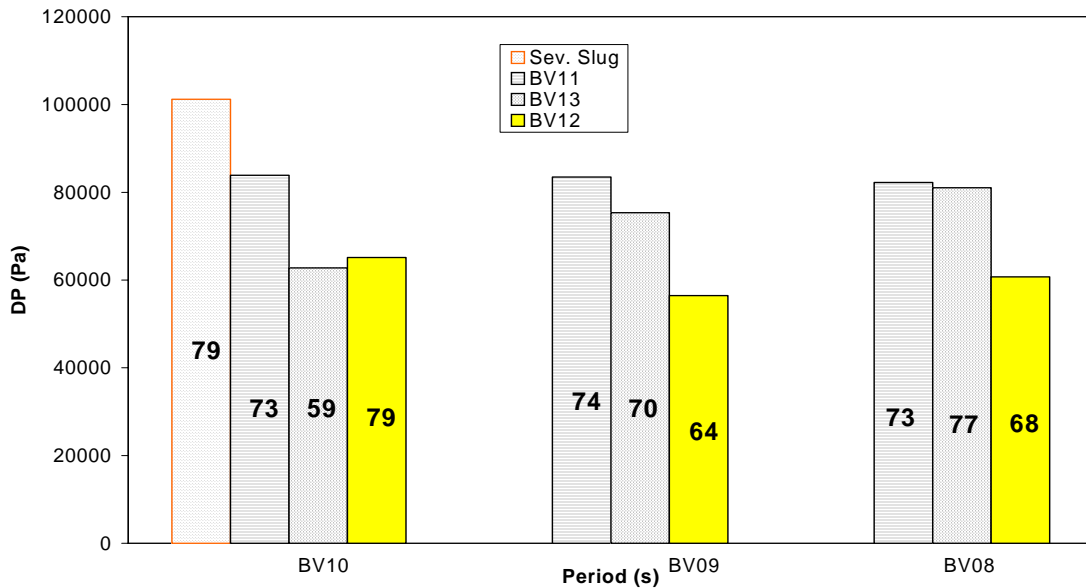
Figure 4–13: Period and differential pressures for severe slugging and different take-off and injection combinations (v_{SL} = 0.32 m/s, v_{Sg} =0.35 m/s)

A differential pressure transducer was located on the tank acting as a separator, measuring the liquid level in the tank during flow. The tank level expressed in terms of pressure will be presented as a function of time.

Figure 4-13 shows the tank level pressure as a function of time for injection port BV13 for Test-1 (v_{SL} = 0.32 m/s, and v_{Sg} = 0.35 m/s). This figure indicates that the pressure differential and frequency are reduced when the different take-off ports are used.
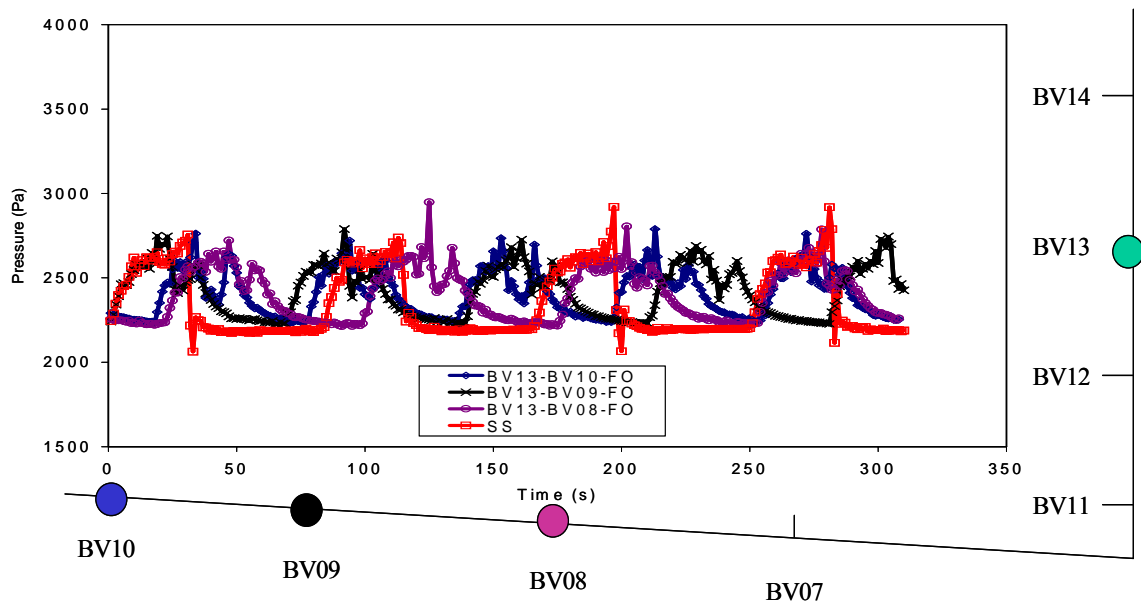
Figure 4–14: Pressure differential in separator for injection point BV13 and different fully open take-off points (v_{SL} = 0.32 m/s, v_{Sg} = 0.35 m/s)

The take-off point furthest away from the riser base displays the least pressure differential and frequency compared to the other ports and the severe slugging base-case. Figure 4-14 shows the tank level pressures as in the previous case, but using the injection port BV12. Similar behavior is observed in this case.
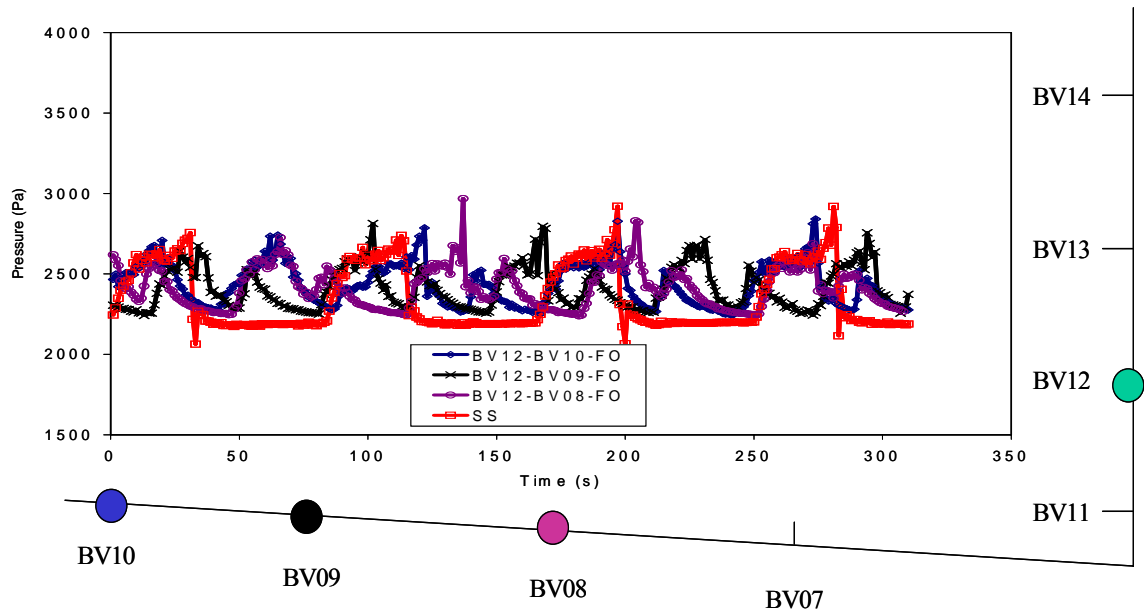
Figure 4–15: Pressure differential in separator for injection point BV12 and different fully open take-off points (v_{SL} = 0.32 m/s, v_{Sg} = 0.35 m/s)

For the last injection port, BV11, the pressure behavior and frequency are the same for all take-off ports used, shown in Figure 4-15.
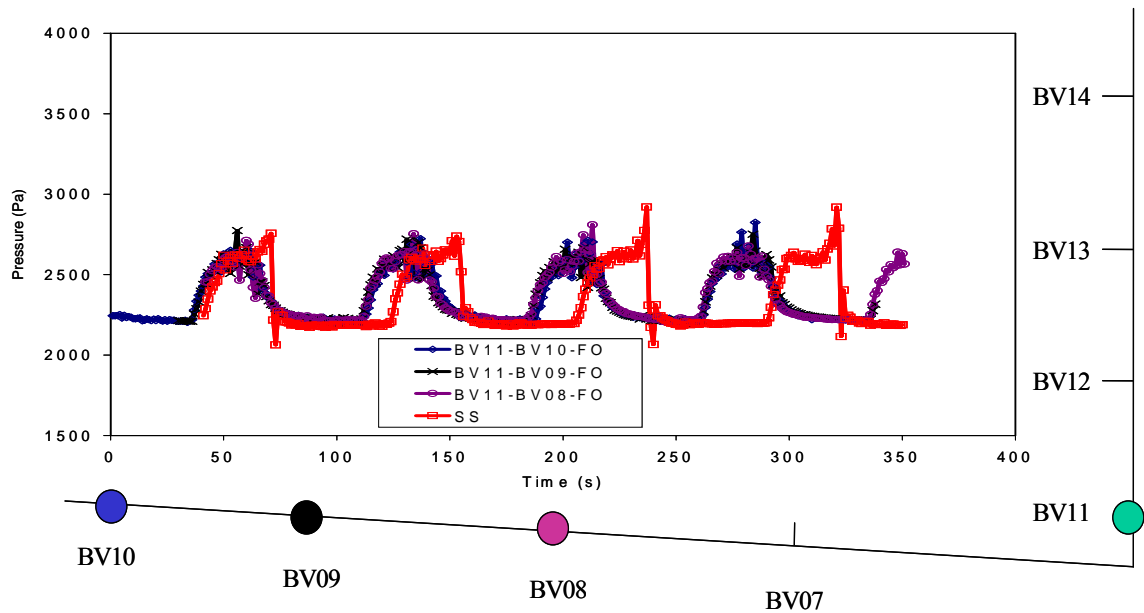
Figure 4–16: Pressure differential in separator for injection point BV11 and different fully open take-off points (v_{SL} = 0.32 m/s, v_{Sg} = 0.35 m/s)

As discussed earlier, this is because the governing mechanism for blockage of the bypass line occurs at the injection port not at the take-off point as was the case for the other injection ports.

The superficial velocities for Test-2 were v_{SL} = 0.2 m/s, and v_{Sg} = 0.68 m/s. Figure 4-16 shows the experiments results for the injection point of 27 in. above riser base with the different take off points. Plotted is the pipeline pressure vs. time.
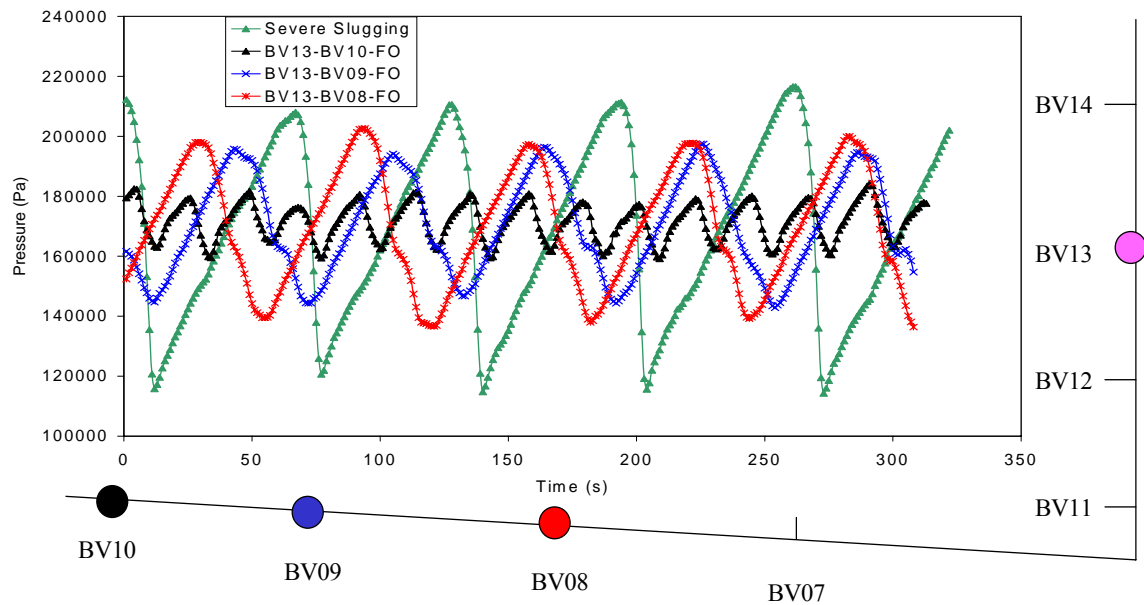
Figure 4–17: Experimental data for severe slugging (SS), using different fully open take-off points and injection point BV13 (v_{SL} = 0.2 m/s, v_{Sg} = 0.68 m/s)

This figure displays characteristics similar to the previous case, i.e., that severe slugging has been lessened, but not eliminated. However, it can be observed that the severe slugging pressure fluctuations were significantly reduced for both the maximum and minimum pressure at the riser base. Since the gas flow rate is high compared to the liquid flow rate, the liquid does not come back and block the take off point as fast as in the lower gas rate case shown before. This causes the system to become more stable and shows less magnitude in the riser base pressure fluctuations.

Figure 4-17 is similar to Figure 4-16, but now the injection point is 13.5 in. above the riser base. From Figure 4-17, it can be observed that severe slugging has been lessened further for this injection point as compared to the 27 in. above the riser case. It is observed that the liquid penetration length in the pipeline never exceeded that of the take-off point furthest away from the riser base, and hence the stable conditions are observed.

Figure 4–18: Experimental data for severe slugging (SS), using different fully open take-off points and injection point BV12 (v_{SL} = 0.2 m/s, v_{Sg} = 0.68 m/s)

Figure 4-18 shows the lowest injection point of 7 in. above the riser base. Again when using the lowest injection point it is observed that the cycles are not governed by the blockage of the take off points, but rather the liquid flow back through the injection port. Therefore, no matter where the gas is taken off, the pressure fluctuation magnitude as well as the severe slugging cycle remain the same.
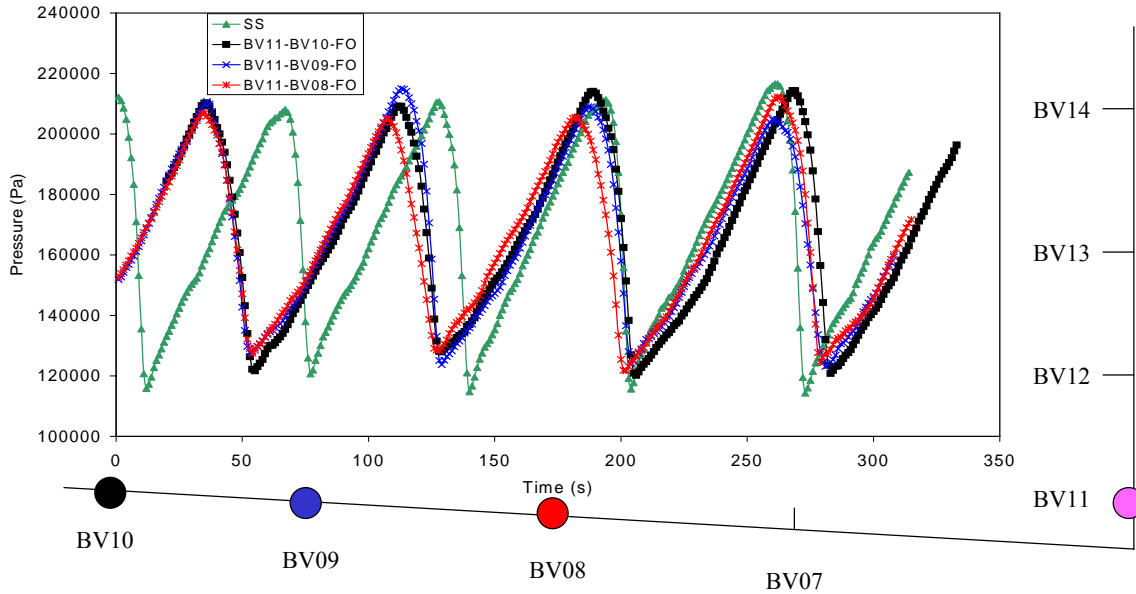
Figure 4–19: Experimental data for severe slugging, using different fully open take-off points and injection point BV11 (v_{SL} = 0.2 m/s, v_{Sg} = 0.68 m/s)

The cycle times and magnitude of the pressure fluctuations for the different take-off injection-point combinations are shown in Figure 4-19.
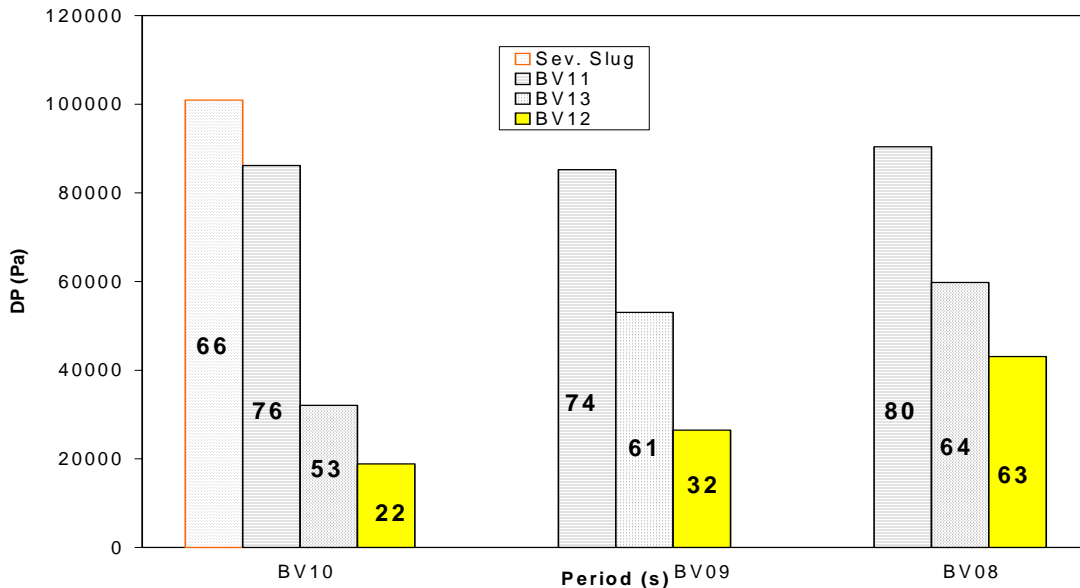
Figure 4–20: Period and differential pressures for severe slugging and different take-off and injection combinations (v_{SL} = 0.2 m/s, v_{Sg} =0.68 m/s)

Figure 4-20 shows the tank level pressure as a function of time for injection port BV13 for Test-2 (v_{SL} = 0.2 m/s, and v_{Sg} = 0.68 m/s). This figure shows similar behavior as with the previous case in that the pressure differential and frequency are reduced when the different take-off ports are used. The take-off port farthest away from the riser base shows the least pressure differential and frequency compared to the other ports and the severe slugging base-case.
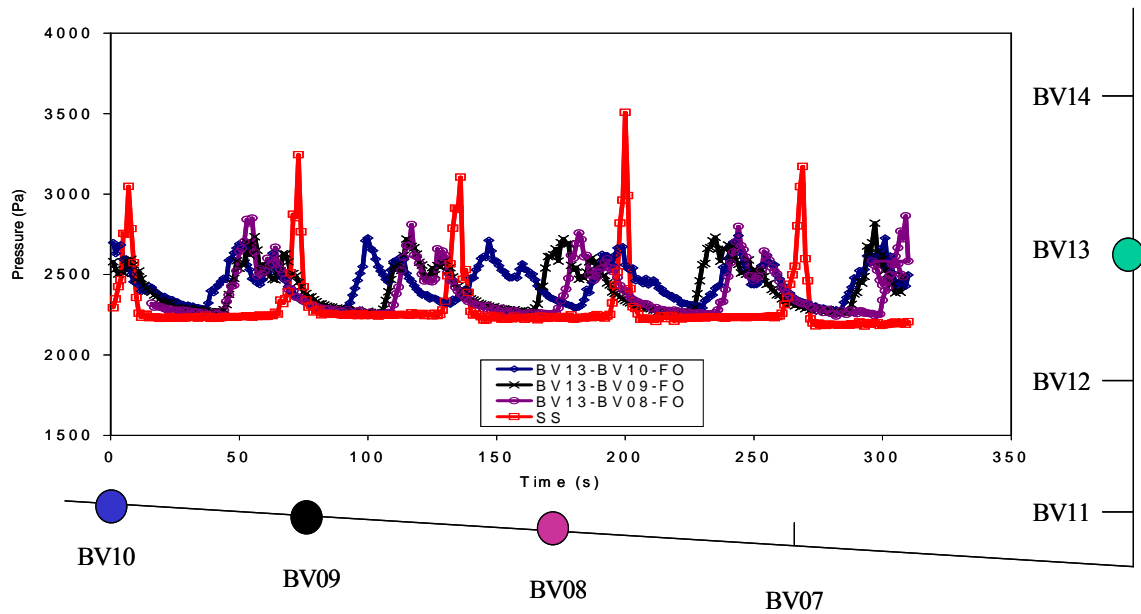
Figure 4–21: Pressure differential in separator for injection point BV13 and different fully open take-off points (v_{SL} = 0.2 m/s, v_{Sg} = 0.68 m/s)

Figure 4-21 shows the tank level pressure as in the previous case, but using the injection port BV12. Similar behavior is observed in this case.
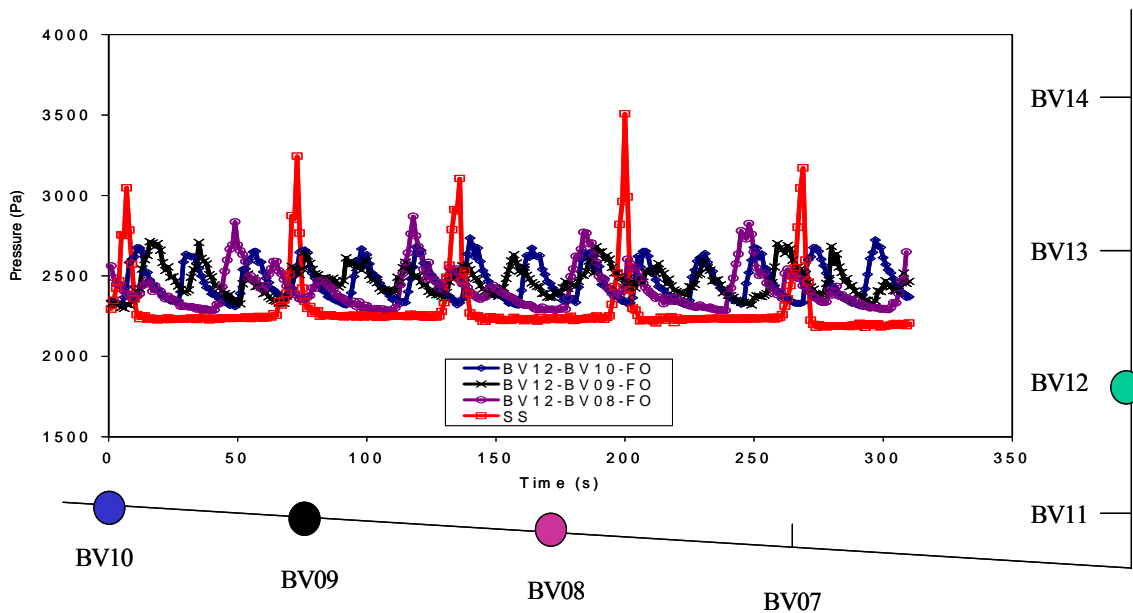
Figure 4–22: Pressure differential in separator for injection point BV12 and different fully open take-off points (v_{SL} = 0.2 m/s, v_{Sg} = 0.68 m/s)

For the last injection port, BV11, the pressure behavior and frequency are the same for all take-off ports used, as shown in Figure 4-22.
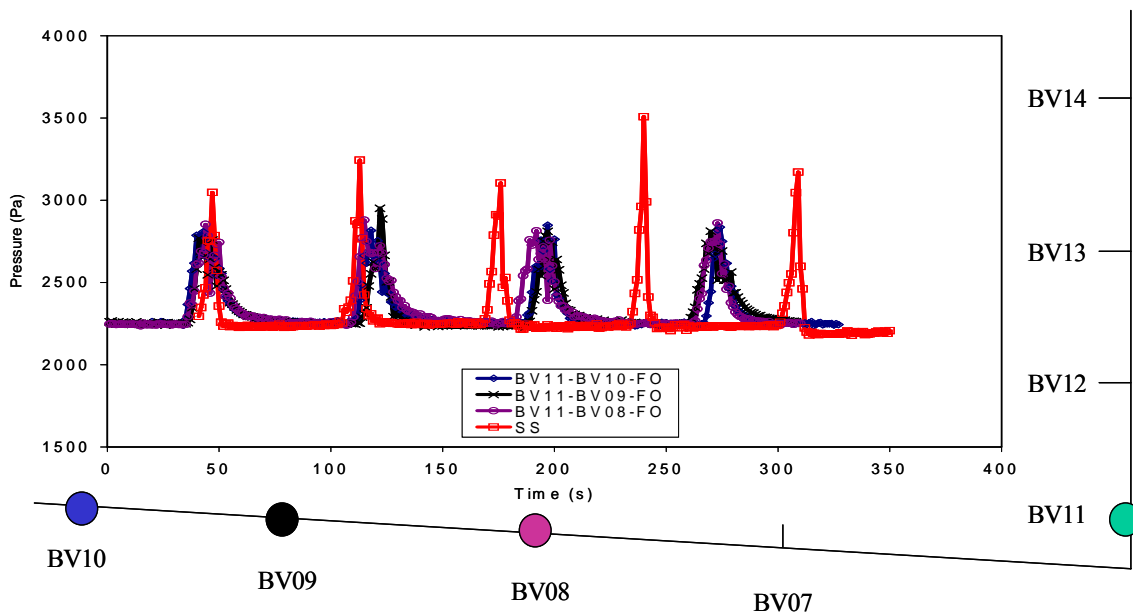
Figure 4–23: Pressure differential in separator for injection point BV11 and different fully open take-off points (v_{SL} = 0.2 m/s, v_{Sg} = 0.68 m/s)

As discussed earlier, this is because the blockage of the bypass line occurs at the injection port not at the off-take point as is the case for the other injection ports. Similar behavior was observed for all inclination angles investigated.

4.3.2.1.2 Partially Open Take-off Valve

As observed in the preliminary study, a partial choking of the valves can stabilize the pressure fluctuations in the pipeline as well as the flow rate fluctuations in the separator. Figure 4-23 shows the severe slugging pressure fluctuations together with the stabilized pressure in the pipeline for Test-1 ($v_{SL} = 0.32$ m/s, and $v_{Sg} = 0.35$ m/s) when the take-off point was partially choked.
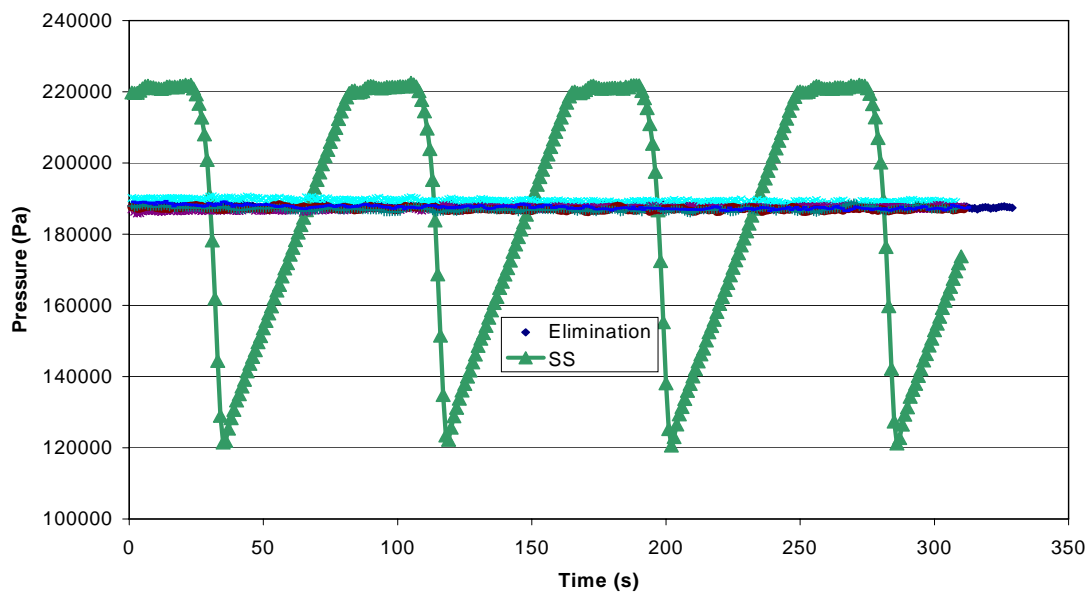
Figure 4–24: Experimental data for severe slugging (SS), using different partially-choked take-off points and all injection points ($v_{SL} = 0.32$ m/s, $v_{Sg} = 0.35$ m/s)

It is observed that by creating an additional small pressure drop across the valve it is possible to eliminate severe slugging.

Figure 4-24 shows the pressure in the pipeline, and the pressure level in the separator for the severe slugging case, and also the stabilized pressure level in the tank for the elimination cases. The pressure level in the tank is constant for the elimination cases, indicating a constant flow rate coming into the tank, where the inlet and outlet flow rates are the same.
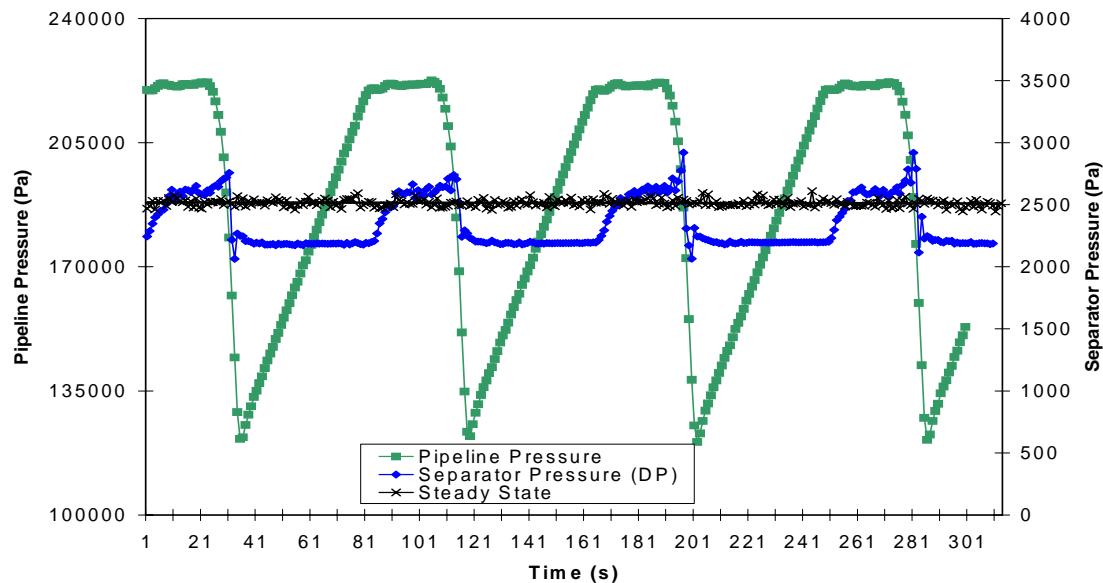
Figure 4–25: Pressure differential in separator during severe slugging cycle and at stable operations (v_{SL} = 0.32 m/s, v_{Sg} =0.35 m/s)

Table 4-2 shows the pressure drop over the bypass line with choking and the stabilized liquid penetration length in the pipeline. Also shown is the hydrostatic pressure from the riser base to the injection port accounting for the liquid penetration length in the pipeline. From Table 4-2, it can be observed that as the injection point is moved to a distance higher than the take-off point, more pressure drop over the bypass valve is needed to stabilize the flow. By increasing the vertical distance between the take-off and injection points, the hydrostatic head becomes greater. To create a balance

between the forces, an additional pressure increase in the pipeline is necessary. This is

obtained by increasing the pressure loss through the bypass valve.

Table 4-2: Bypass pressure drop and liquid penetration lengths for different take-off-injection point combinations

Ports Used	DP$_{Measured}$ Total (Pa)	DP$_{Calculated}$ Hydrostatic (Pa)	Liquid Penetration length (ft)
BV13-BV10	4785	4409	27.8
BV13-BV09	4839	5378	30.8
BV13-BV08	3993	4365	23.8
BV12-BV10	2277	1790	29.8
BV12-BV09	2029	1482	6.8
BV12-BV08	2286	1614	28.8

Similar results are found for Test-2 (v_{SL} = 0.2 m/s, and v_{Sg} = 0.68 m/s), and shown in
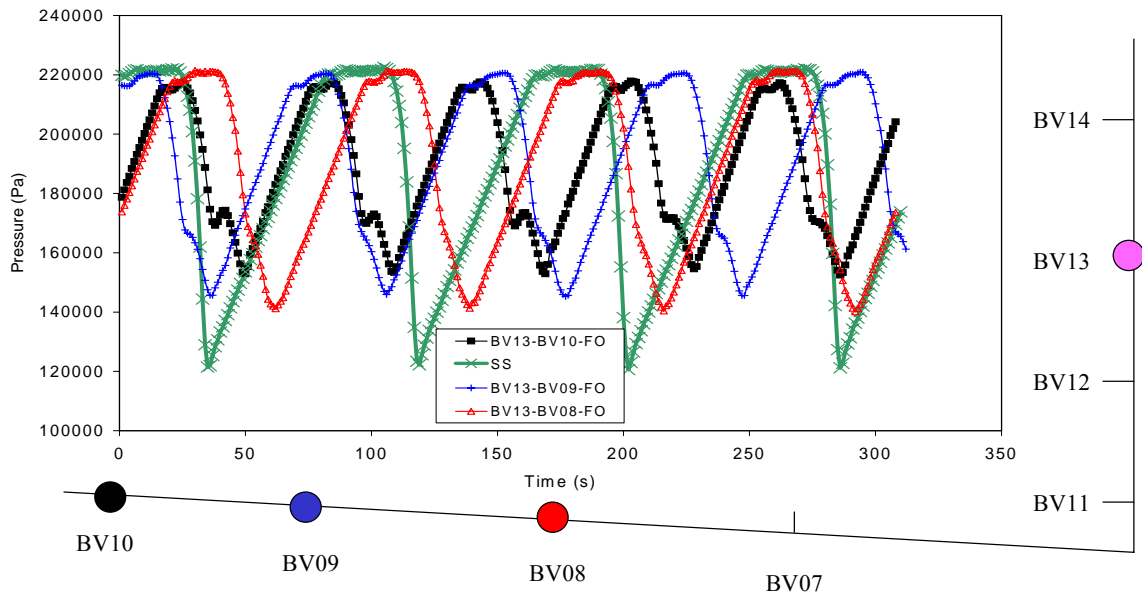
Figure 4-25.
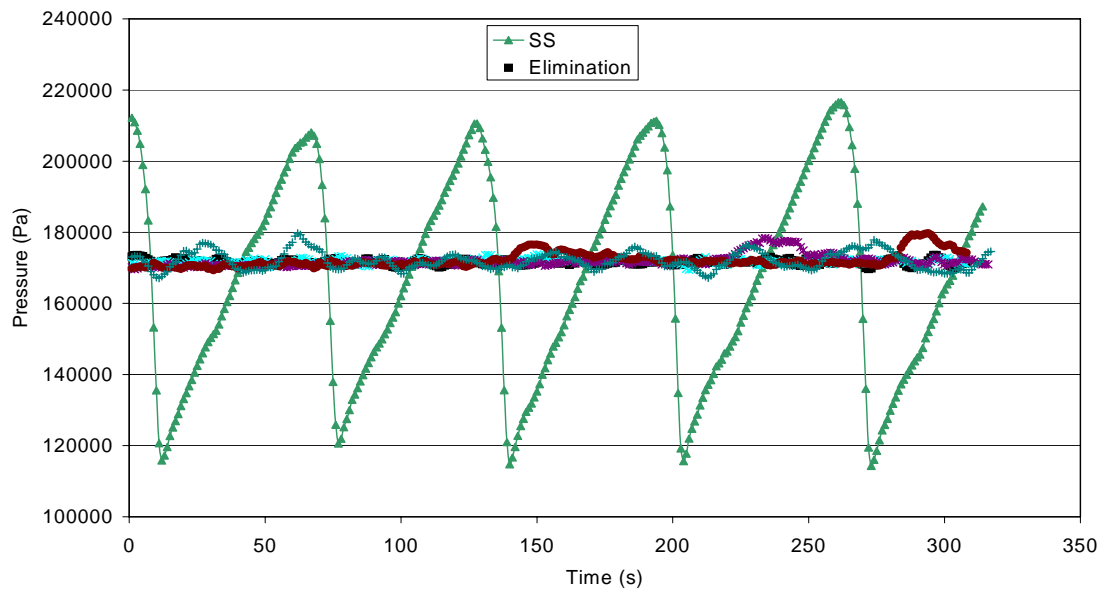
Figure 4–26: Experimental data for severe slugging (SS), using different partially-choked take-off points and all injection points (v_{SL} = 0.2 m/s, v_{Sg} = 0.68 m/s)

Figure 4-26 shows the pressure in the pipeline, and the pressure level in the separator for the severe slugging case, and also the stabilized pressure level in the tank for the elimination cases. Again, the pressure level for the elimination cases indicates a steady state flow rate coming in and leaving the separator.
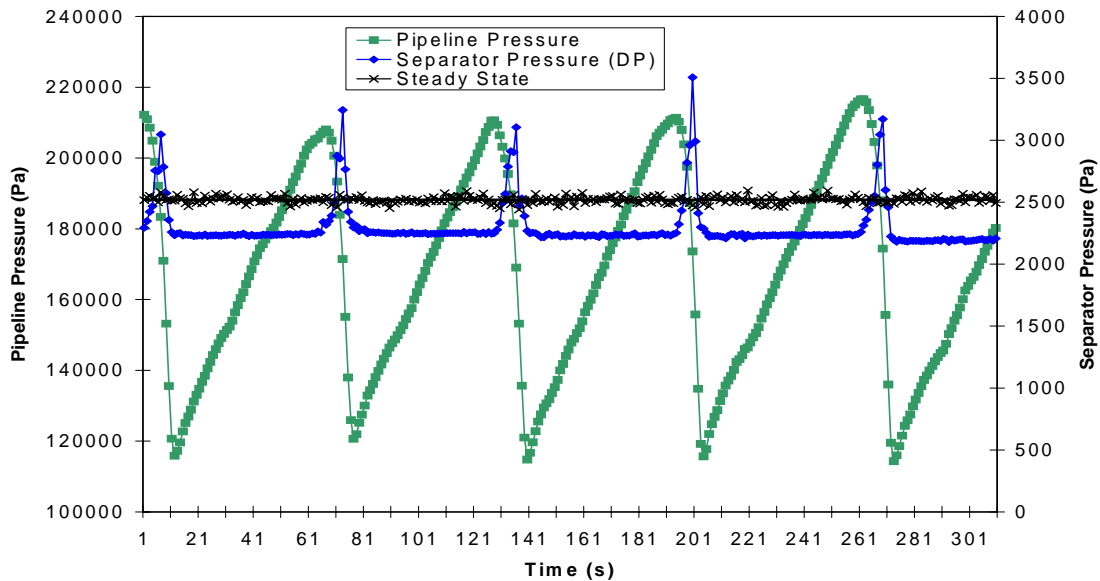
Figure 4–27: Pressure differential in separator during severe slugging cycle and at stable operations (v_{SL} = 0.2 m/s, v_{Sg} =0.68 m/s)

4.3.2.2 Analysis of a Test Run for -3° Pipeline Angle

The severe slugging region for Test-3 determined by the Bøe[5] criteria for - 3° case is shown in Figure 4-7. 54 different combinations of liquid and gas flow rates were investigated.

Figure 4-27 shows the results of the severe slugging cycle and the injection point BV 14 and the take-off valves BV 8-10 for v_{SL} = 0.5 m/s and v_{Sg} = 1.0 m/s, with all ball valves fully open. The data shows that as the take-off points are moved away from the riser base, the pressure fluctuations are lessened. The take-off point closest to the riser

base shows similar behavior to that of the severe slugging cycle, but the take-off point farthest away from the riser shows that the flow is moving towards the stable region.
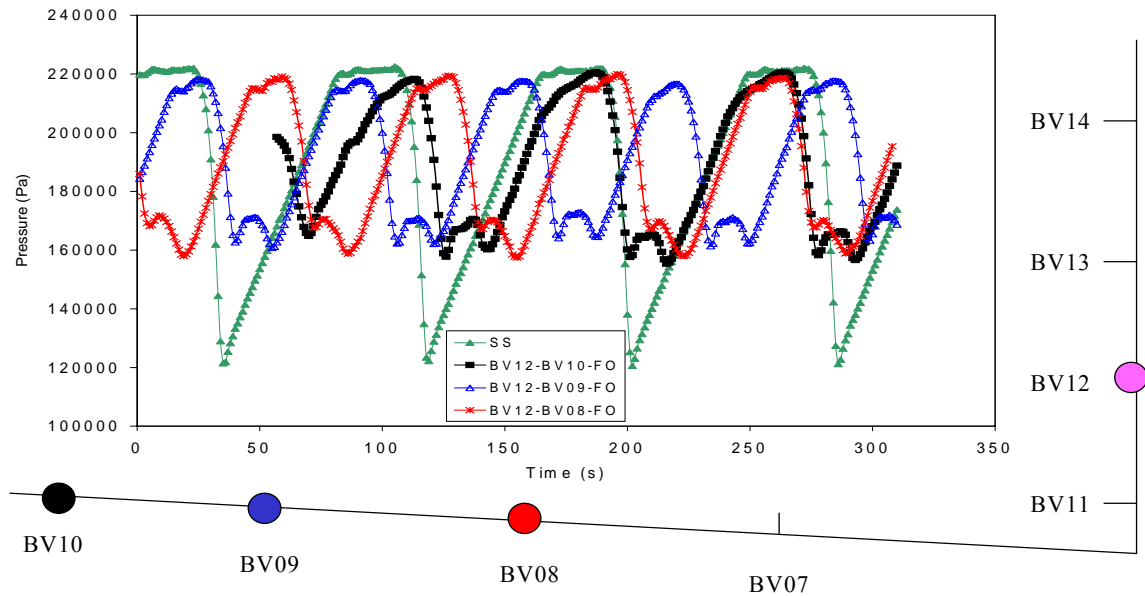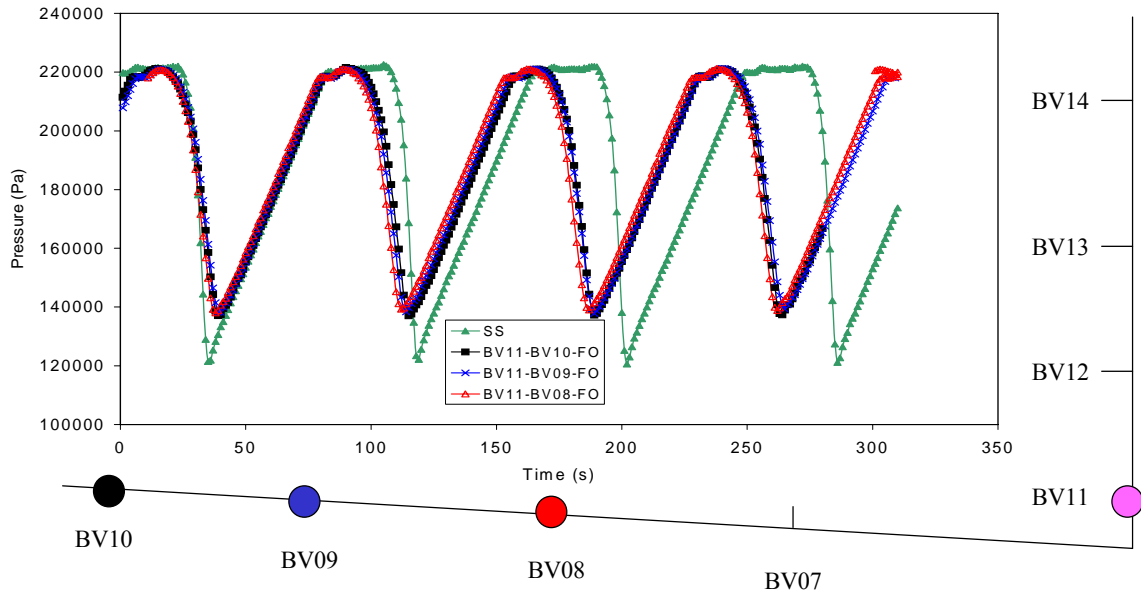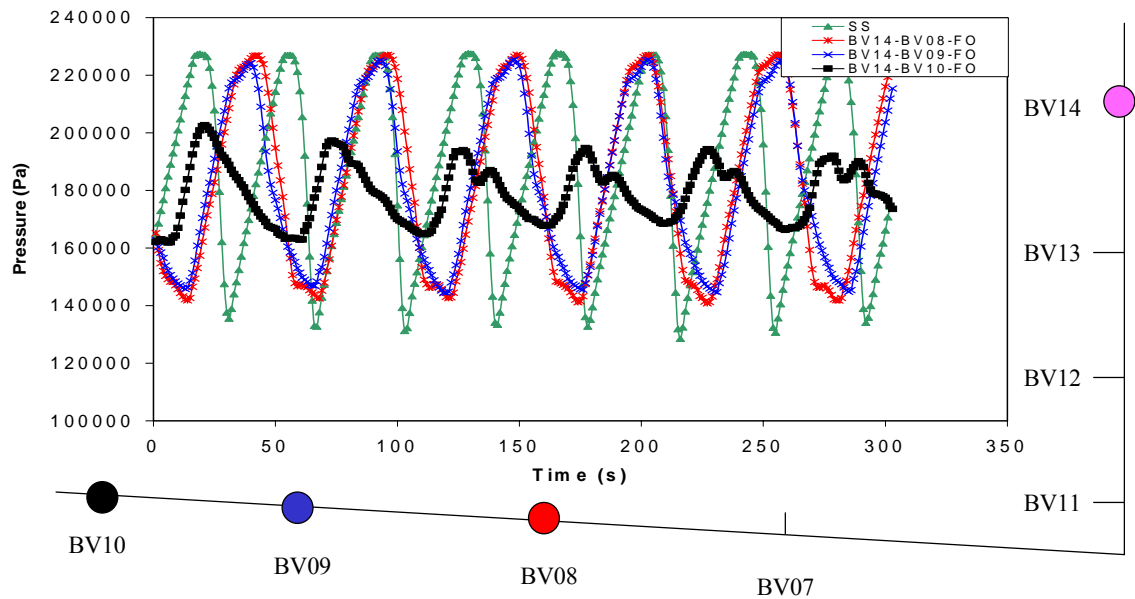

Figure 4–28: Experimental results for severe slugging (SS), using different fully open take-off points and injection point BV14 (v_{SL} = 0.50 m/s, v_{Sg} = 1.0 m/s, -3°)

Figure 4-28 shows the results for the injection point of BV13. By lowering the injection point on the riser, stable flow is obtained for the two take-off points farthest away from the riser using fully open ball valves. Although stable flow can be achieved even for fully open ball valves, experiments have shown that this is flow rate specific. At higher gas flow rates, stable operations can be obtained using fully open ball valves because the pressure drop through the bypass line becomes equal to or greater than that of the difference in hydrostatic height between the injection point and the take-off points. From Figure 4-29 the same behavior can be seen using BV12 as injection point.
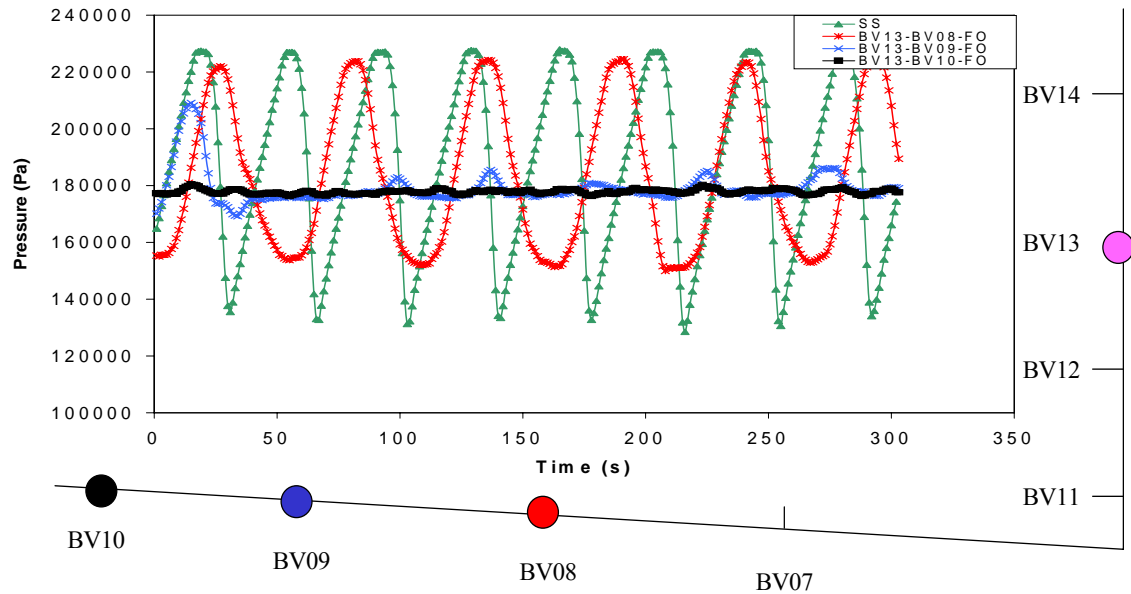
Figure 4–29: Experimental results for severe slugging (SS), using different fully open take-off points and injection point BV13 (v_{SL} = 0.50 m/s, v_{Sg} = 1.0 m/s, -3°)
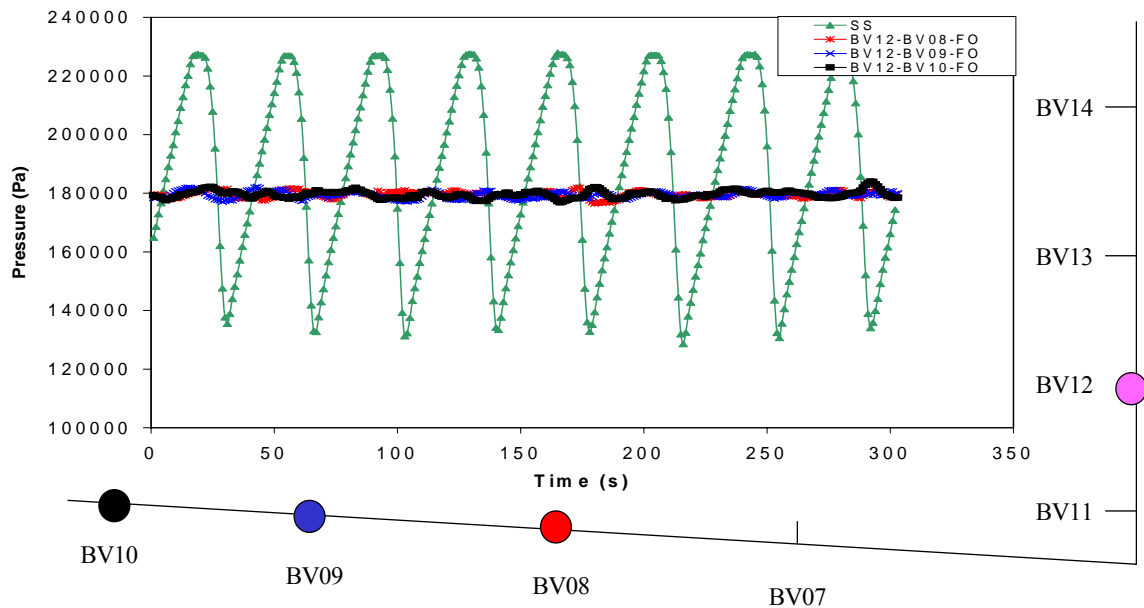
Figure 4–30: Experimental results for severe slugging (SS), using different fully open take-off points and injection point BV12 (v_{SL} = 0.50 m/s, v_{Sg} = 1.0 m/s, -3°)

Figure 4-30 shows the results of the injection point of BV14 and partially choked take-off valves. This figure shows that stable flow is achieved using all the different

take-off points. A similar behavior is also shown in Figure 4-31. Again, all take-off

points show stable behavior for partially choked take-off valves and using BV13 as
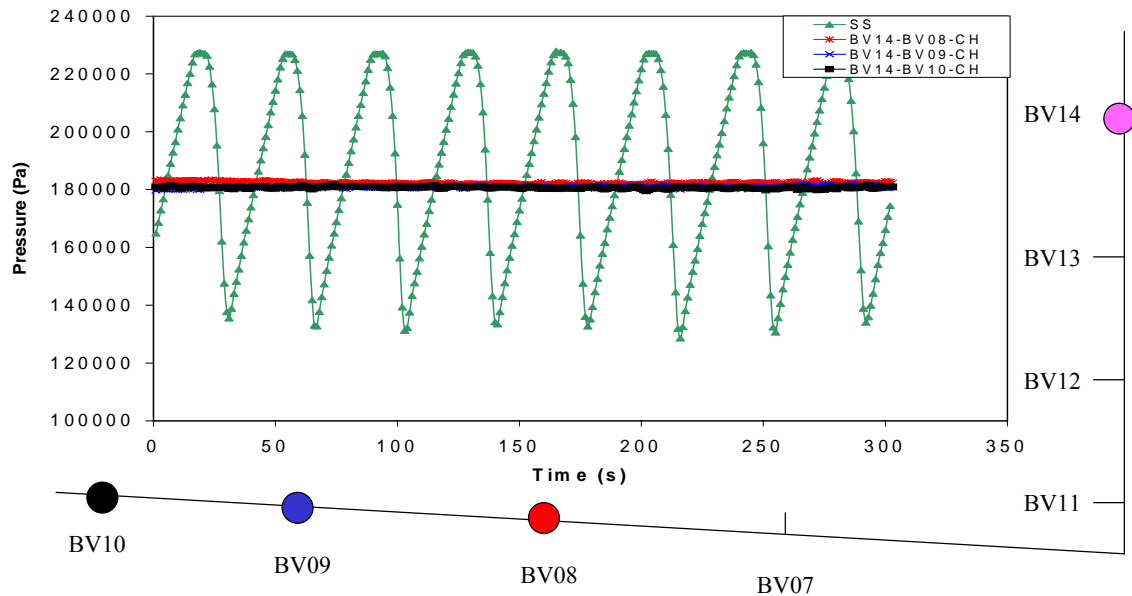
injection point.

Figure 4–31: Experimental results for severe slugging (SS), using different
partially-choked take-off points and injection point BV14
(v_{SL} = 0.50 m/s, v_{Sg} = 1.0 m/s, -3°)

Figure 4-31 using partially choked valves shows a smoother stable region

compared to that of the two stable cases of Figure 4-28 using fully open valve. Also, by

using partially choked valves it is possible to move the liquid penetration length in the

pipeline closer to the riser base by applying more pressure drop through the choke. Flow

into the separator shows similar behavior as shown in the -1° case.
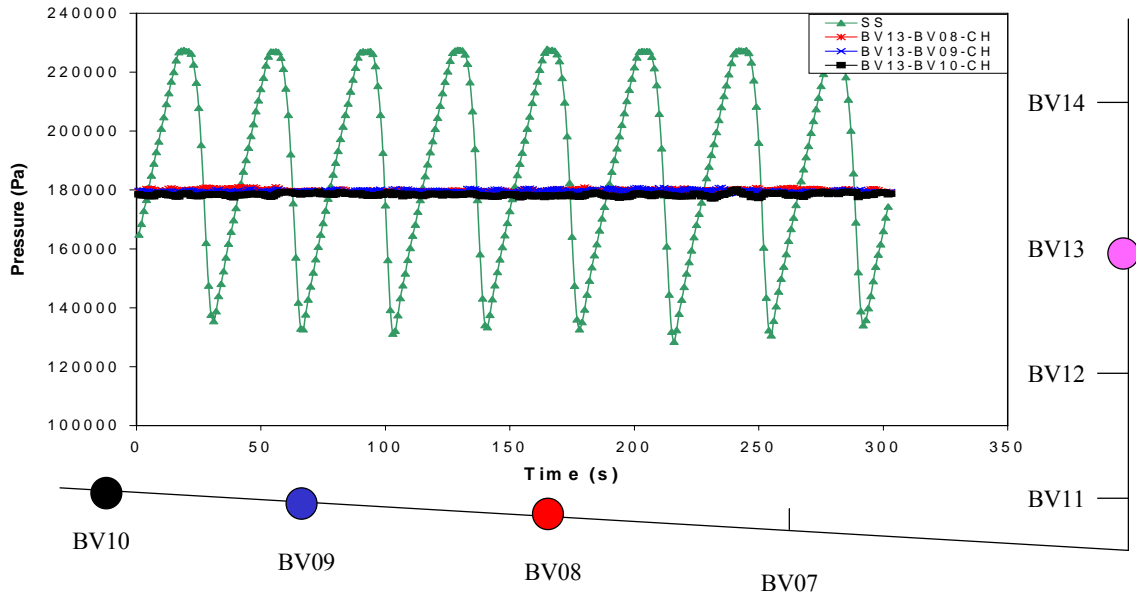
Figure 4–32: Experimental results for severe slugging (SS), using different partially-choked take-off points and injection point BV13
(v_{SL} = 0.50 m/s, v_{Sg} = 1.0 m/s, -3°)

4.3.2.3 Analysis of a Test Run for -5° Pipeline Angle

The severe slugging region for Test-4 determined by the Bøe[5] criteria for - 5° case is shown in Figure 4-8. 59 different combinations of liquid and gas flow rates were investigated. Similar observations are made as in the -1° and -3° cases. As the inclination angle is increased the relative distance between the take-off point and injection point is changed. For the same set of flow rates, the -5° case shows stable operations while the two other cases will show unstable flow behavior. Comparing to the two other cases, the take-off points move closer to the injection points. This is because the pressure losses through the bypass system using a fully open take-off valve accounts for the difference in height between the take-off and injection points, while for the 2 other cases the hydrostatic head between the injection point and take-off points was greater

than the pressure losses in the bypass system. When this occurs liquid penetrates the pipeline, and blocks the take-off point and a severe slugging like behavior is observed with lesser pressure fluctuations compared to no bypass case.

Figure 4-32 shows the results of the severe slugging cycle and the injection point BV 14 and the take-off valves BV 8-10 for v_{SL} = 0.5 m/s and v_{Sg} = 1.0 m/s, for all ball valves fully open. The data show that as the take-off points are moved away from the riser base, the flow becomes almost stable. The take-off point closest to the riser base shows behavior similar to that of the severe slugging, but the take-off point farthest away from the riser shows stable conditions.
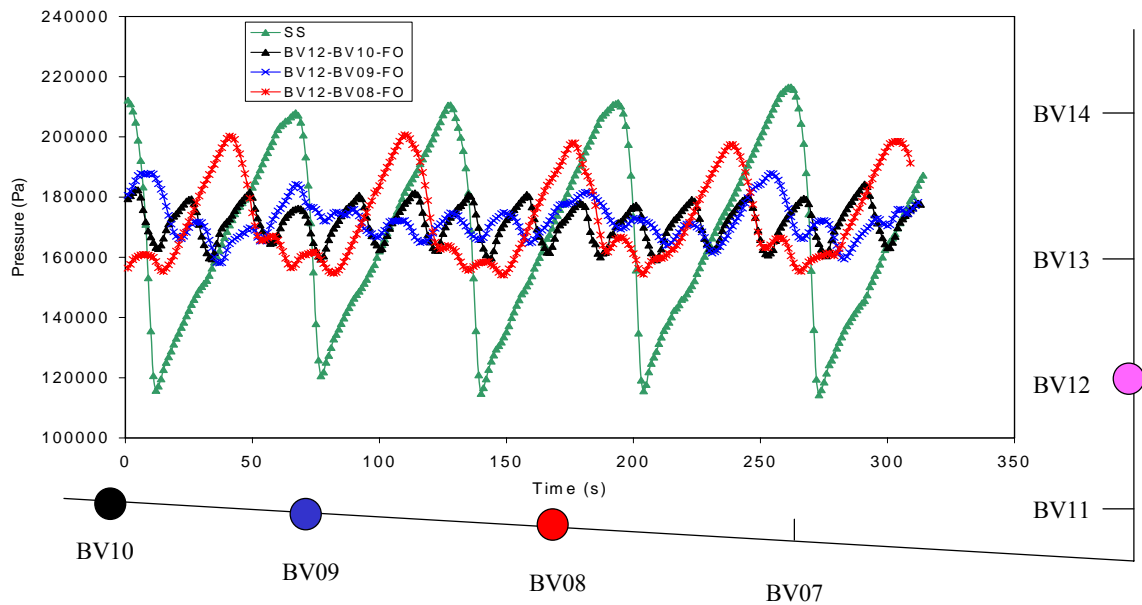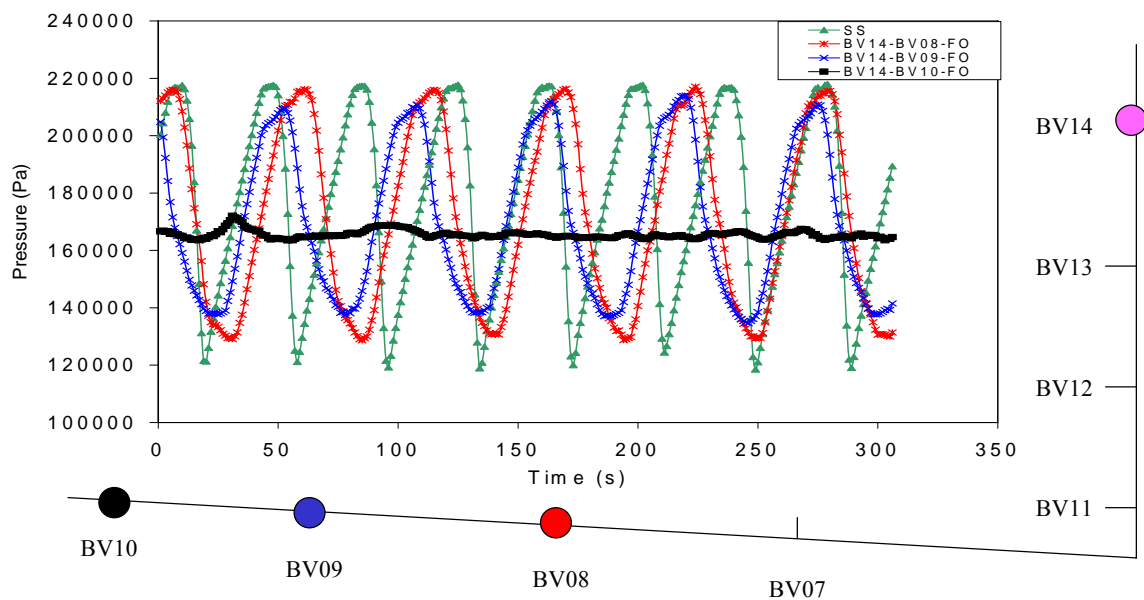

Figure 4–33: Experimental results for severe slugging (SS), using different fully open take-off points and injection point BV14 (v_{SL} = 0.50 m/s, v_{Sg} = 1.0 m/s, -5°)

Figure 4-33 shows the results for the injection point of BV13. By lowering the injection point on the riser, stable flow was obtained for all take-off points using fully open ball valves. Although stable flow can be achieved even for fully open ball valves, experiments showed that this is flow rate specific. At higher gas flow rates, stable

operations can be obtained using fully open ball valves because the pressure drop through the bypass line becomes equal to that of the difference in hydrostatic height between the injection point and the take-off points. The injection point of BV12 did not stabilize for any of the take-off points using fully open ball valves as shown in Figure 4-34.
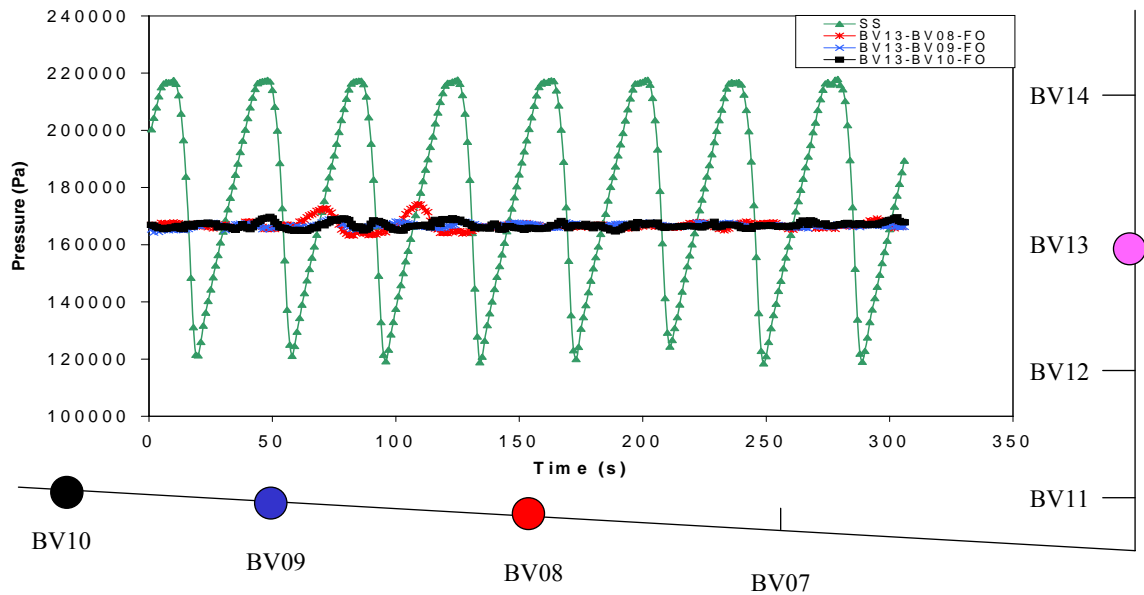
Figure 4–34: Experimental results for different fully open take-off points and injection point BV13 (v_{SL} = 0.50 m/s, v_{Sg} = 1.0 m/s, -5°)
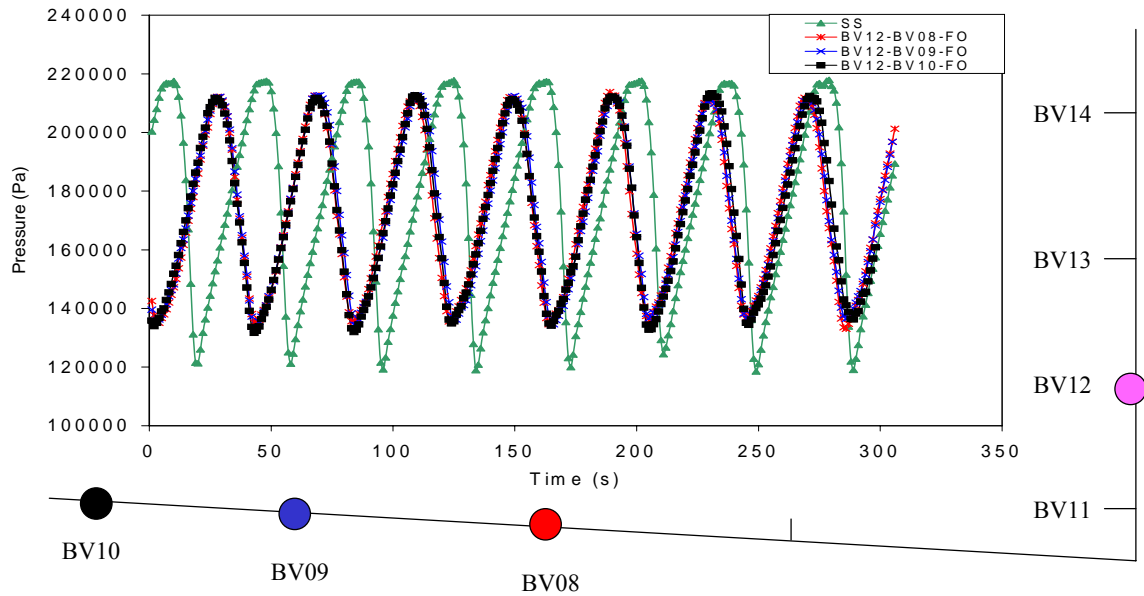
Figure 4–35: Experimental results for different fully open take-off points and injection point BV12 (v_{SL} = 0.50 m/s, v_{Sg} = 1.0 m/s, -5°)

Figure 4-35 shows the results of the injection point of BV14 and partially choked take-off valves. This figure shows that stable flow is achieved using all the different take-off points. A similar behavior is also shown in Figure 4-36. Again, all take-off points show stable behavior for partially choked take-off valves and using BV13 as injection point. Figure 4-36 using partially choked valves shows a smoother stable region compared to that of Figure 4-33 using fully open valve. Also, by using partially choked valves it is possible to move the liquid penetration length in the pipeline closer to the riser base by applying more pressure drop through the choke. Flow into the separator shows similar behavior as shown in the -1° case.
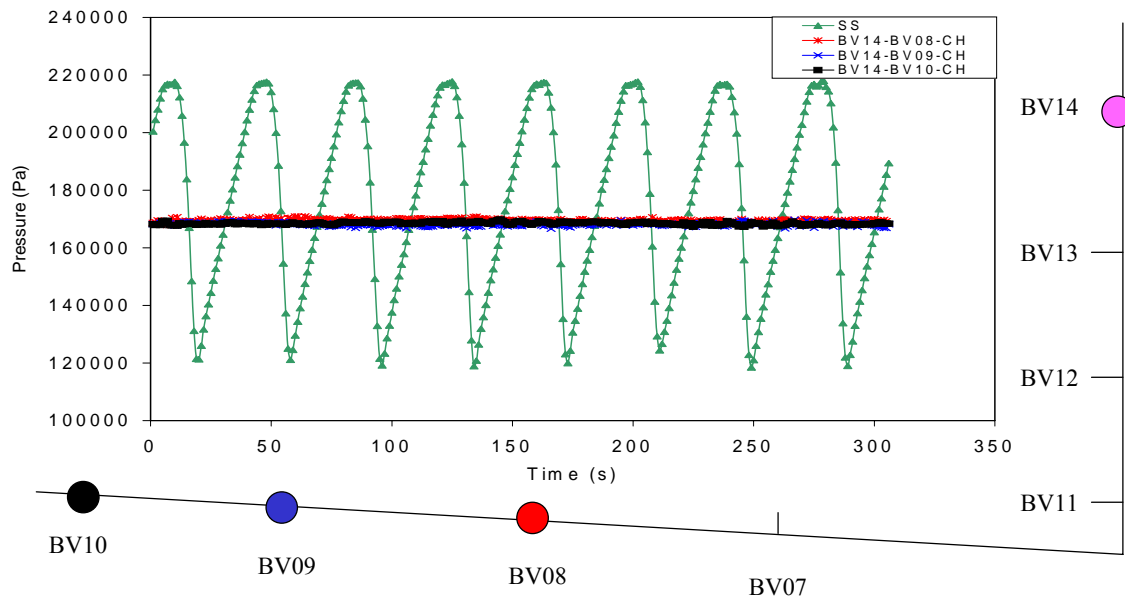
Figure 4–36: Experimental results for different partially choked take-off points and injection Point BV14 (v_{SL} = 0.50 m/s, v_{Sg} = 1.0 m/s, -5°)
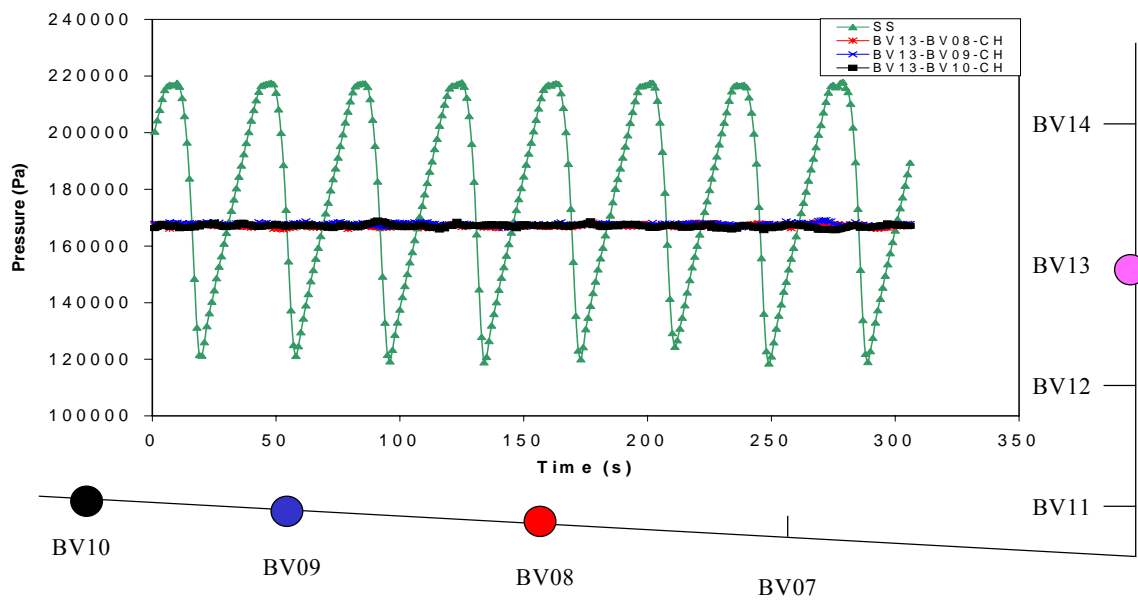
Figure 4–37: Experimental results for different partially choked take-off points and injection point BV13 (v_{SL} = 0.50 m/s, v_{Sg} = 1.0 m/s, -5°)

4.3.3 Flow Rate Sensitivity

A flow rate sensitivity test was performed to check the stability of the bypass option using the same choke setting and varying flow conditions. A base case of v_{SL} = 0.4 m/s and v_{Sg} = 0.4 m/s, for a -3° inclined pipe with the BV13-BV10 take-off and injection point option was used to perform the experiment. First the liquid and gas superficial velocity were set to 0.4 m/s. Then a choke setting was applied to stabilize the flow, where this choke setting was kept the same throughout the test. When the flow was stabilized, v_{SL} = 0.4 m/s was kept constant while the superficial gas velocity was varied. As can be seen from Figure 4-37, the bypass settings using the applied choking could handle changes in gas flow rates that were ±50% of the base case. Another test was performed by keeping v_{Sg} = 0.4 m/s constant and varying the liquid velocity.

Constant V_{SL} = 0.4 m/s
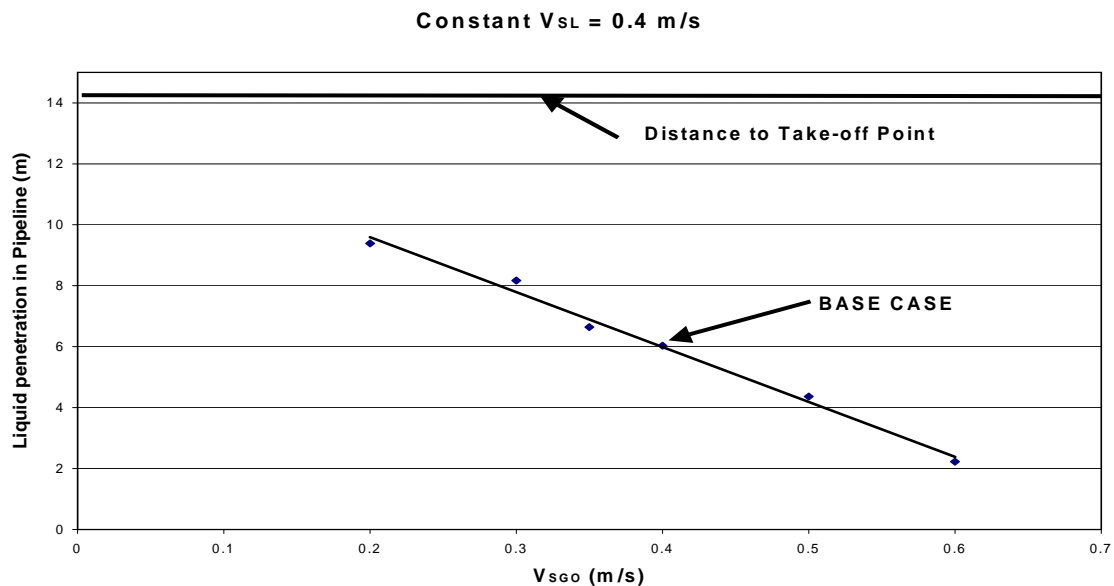
Figure 4–38: Gas flow rate sensitivity for BV13-BV10 injection/take-off combination (Base Case: v_{SL} = 0.40 m/s, v_{Sg} = 0.4 m/s, -3°)

Constant Vsᴳᴼ = 0.4 m/s
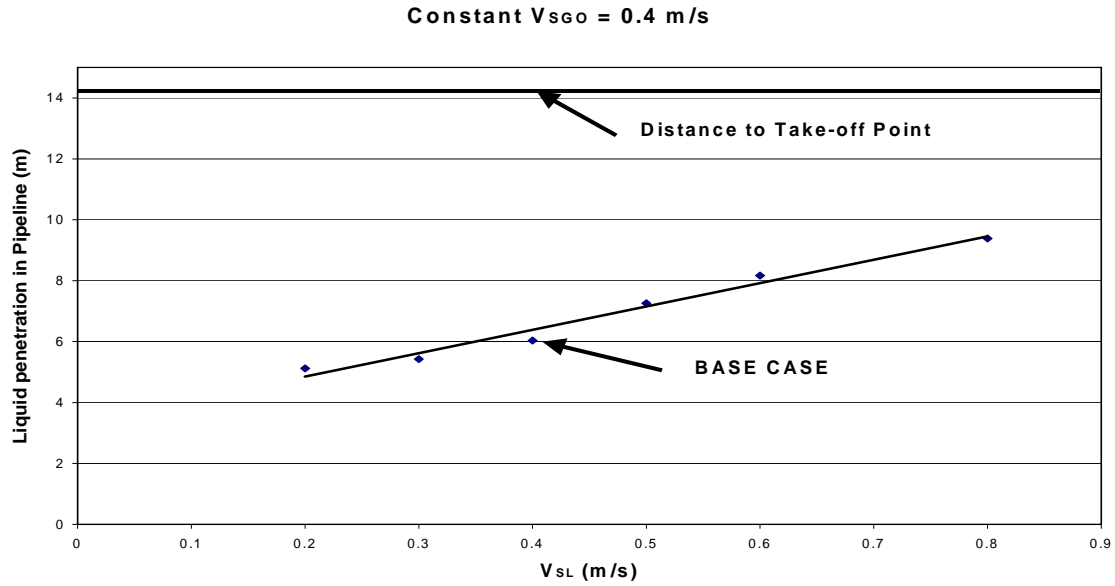
Figure 4–39: Liquid flow rate sensitivity for BV13-BV10 injection/take-off combination (Base Case: v_{SL} = 0.40 m/s, v_{Sg} = 0.4 m/s, -3°)

Figure 4-38 shows that changes in liquid velocity do not change the liquid penetration length significantly, and liquid flow rate variations of ±75% from the base case can be accommodated without disturbing the steady state flow that the bypass can achieve. Overall the elimination of severe slugging using the external bypass is not very rate sensitive and can be used over a wide range of flow rates keeping the same choke settings at the bypass take-off/injection point.

Further testing was performed to investigate the flow rate sensitivity by varying both gas and liquid flow rates. A base case of v_{SL} = 0.5 m/s and v_{Sg} = 0.5 m/s, for the -3° pipeline inclination angle with the BV13-BV10, and BV13-BV08 take-off and injection point combination was used to perform the experiments. Figure 4-39 shows the Bøe[5] envelope together with the experimental data gathered for the closest take-off point. For

a constant choke setting severe slugging is eliminated for a band of different gas and liquid flow rate combinations.
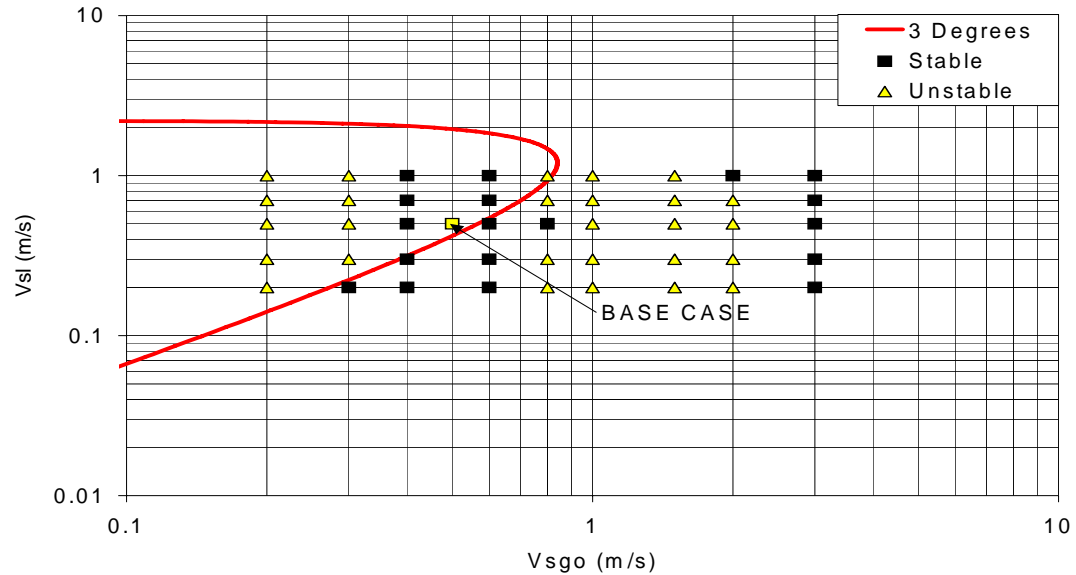
Figure 4–40: Elimination range with a constant choke setting for BV13-BV08 injection/take-off combination (Base Case: v_{SL} = 0.50 m/s, v_{Sg} = 0.5 m/s, -3°)

Figure 4-40 presents similar experimental results for the take-off farthest away from the riser base. From Figure 4-40, it can be seen that the region of elimination has significantly increased compared to the previous case. As the take-off point is moved away from the riser base, and at the same time, if the injection point is at the same level or slightly higher than the take-off point, there will be more differential pressure available to compensate for the elevation difference between the take-off and the riser base. Therefore, it may be desirable to have a take-off point that is not to close to the riser base. Moreover, in the unstable region, the pressure fluctuations and therefore the flow rate fluctuations were reduced significantly using the bypass option compared to using no bypass. Table 4-3 shows the different flow rate combinations together with the pressure fluctuations for the bypass case using the BV13-BV10 option, and no bypass case,

respectively. When the stable and unstable boundary presented in Figure 4-6 is crossed

fluctuations are not significant when compared to that of the no-bypass option.
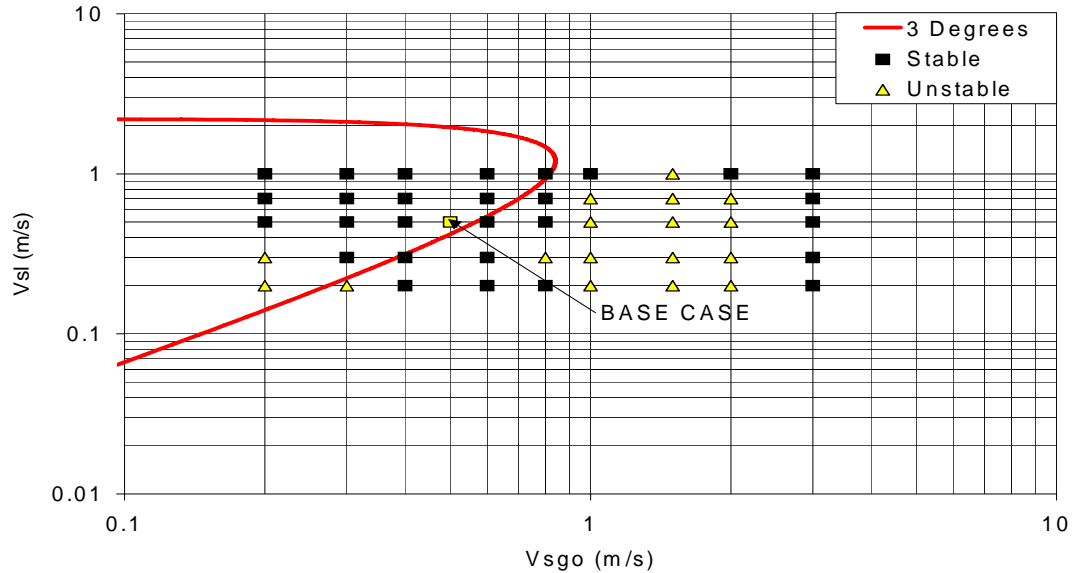
Figure 4–41: Elimination range with a constant choke setting for BV13-BV10 injection/take-off combination (Base Case: v_{SL} = 0.50 m/s, v_{Sg} = 0.5 m/s, -3°)

Table 4-3: Pipeline pressure fluctuations for bypass and no bypass options for unstable flow cases

Case	v_{SL} (m/s)	v_{Sgo} (m/s)	Δp (Max-Min) Bypass (Psi)	Δp (Max-Min) No Bypass (Psi)
1	0.2	0.2	5.7	14.3
2	0.2	0.3	5.6	15.3
3	0.2	1.0	7.2	10.5
4	0.2	1.5	5.1	6.4
5	0.2	2.0	5.4	4.5
6	0.3	0.2	5.3	14.0
7	0.3	0.8	4.6	13.8
8	0.3	1.0	6.2	12.0
9	0.3	1.5	8.6	7.4
10	0.3	2.0	4.7	6.0
11	0.5	1.0	7.3	14.0
12	0.5	1.5	8.0	11.1
13	0.5	2.0	8.7	8.1
14	0.7	1.0	5.6	12.5
15	0.7	1.5	7.4	12.5
16	0.7	2.0	8.5	9.0
17	1.0	1.5	7.4	6.0

4.3.4 Repeatability Tests

A repeatability test was performed to ensure that the facility gave similar results for the same settings when data were gathered at two different times. The following tests were performed during fall 2001 and spring 2002. Figure 4-41 shows that the facility can reproduce similar results for data gathered at two different times and thereby is consistent. More repeatability tests are presented in Appendix B.
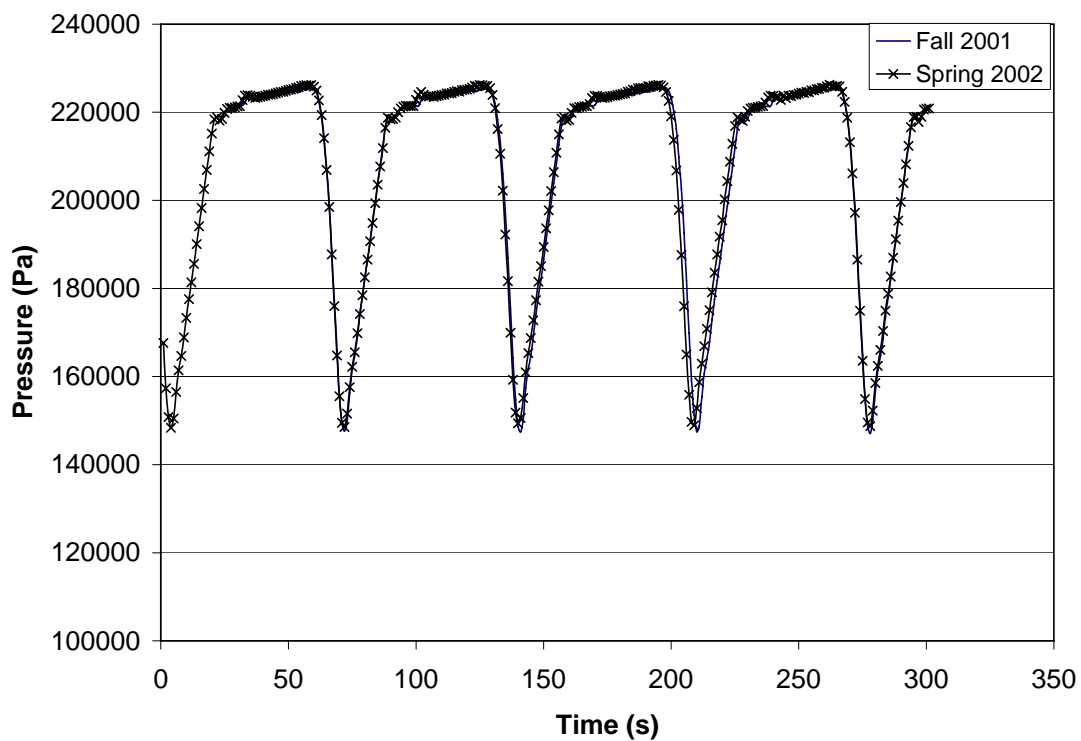
Figure 4–42: Severe slugging repeatability test for v_{SL} = 0.71 m/s, and v_{Sg} = 0.39 m/s, -5°

4.3.5 General Experimental Observations

During the experiments several interesting behaviors were observed. One of the most important observations was the relationship between the injection and the take-off

level relative to the riser base. If these two levels are very close, stabilized conditions are more easily obtained. Consider a case where the injection point and the take-off point are at the same level. The pressure at the injection point is the combination of the pressure at the take-off point and pressure losses through the bypass line. Considering the pipeline and the riser as a u-tube, the injection and take-off pressures are almost equal and the only part that influences the liquid penetration length in the riser is the level difference between the injection and take-off points, since the two points are equal, the liquid level will stay close to the take-off point. However, this behavior is dependent on the gas flow rate. If the gas flow rate is increased, the pressure losses through the bypass line are increased and the liquid level is moved towards the riser base to compensate for the difference in pressures.

The take-off and the injection points were seldom at similar height. Therefore, a choke was needed to stabilize the flow when the injection point was higher than the take-off point. For a normal u-tube scenario, the liquid would penetrate into the pipeline to settle at a point beyond that of the take-off point and thereby block the flow of gas through the bypass. By using a choke, an additional pressure loss is introduced to oppose the pressure difference between the two heights together with the frictional losses through the bypass. In some cases stabilized flow was achieved even though the injection point was higher than the take-off point. This behavior was found at higher gas flow rates and could be explained by the higher pressure loss through the bypass line, which in itself is sufficient to stabilize the flow. The other extreme is when the take-off point is higher than the injection point. This type of setup is found to be undesirable, because achieving stabilized flow has been difficult because the proximity of the riser base, resulting in dual

gas penetration, one from the riser base and the other from the bypass injection point. For certain cases the stabilized flow has been achieved with difficulty.

The dual penetration of gas into the riser was also observed during start-up, and existed for a very short time. The pressure and flow rate fluctuations were not as severe as in the severe slugging cycle, because gas is already flowing through the bypass before gas reaches the riser base through the pipeline. The instability during startup is present because the liquid level in the riser does not arrive at the surface at startup. The pressure equalization does not occur until the liquid has reached the riser top, and the stabilized conditions are achieved.

Severe slugging elimination using the self-lifting technique has been achieved for all inclination angles investigated. However, observations have showed that as the angle increased, the stable flow is easier to achieve. For the -1° downward angle, stabilized conditions have been achieved fairly easily, but it was also observed that the relative movement of the liquid length in the pipeline was easily affected by small pressure perturbations. The gas fingers towards the riser base and can create instabilities in the system if it reaches the riser base. However, during the experiments there were no observed cases where the stabilized flow could not be achieved. As the angle increases, a better separation of the phases occurs and thus a clear interface is observed. This is found to be desirable because the flow is stabilized more easily. Flowing at a higher angle showed a more chaotic flow behavior compared to the lower angles. This chaotic behavior did not affect the system as much as the "fingering" effect for the low angle of – 1° downwards, and did not create any instabilities during stabilized conditions using the bypass to stabilize the flow.

Chapter 5 MODELING

Two models are developed to simulate severe slugging and elimination using an external by-pass. The models are a transient model that can simulate both severe slugging occurrence and elimination using an external bypass, and a steady state model for optimizing the design of the by-pass system injection and take-off points.

5.1 Transient Model

The preliminary model is adapted to investigate the feasibility of the novel approach to eliminate severe slugging.

5.1.1 The Physical Model

The previously described prediction model based on Sarica and Shoham[27] approach is modified to account for the real gas law as opposed to the ideal gas law. Therefore, equation 7 is expressed as:

$$\rho_g = \rho_{sep} + \left\{ z_n - z - \int_z^{z_n} \alpha_r dz \right\} \frac{\rho_L g M}{ZRT} \tag{28}$$

5.1.2 Model Performance

The modified transient model can predict the severe slugging region, as well as, simulate the elimination of severe slugging using an external by-pass. In the following

section the model is evaluated against a wide range of data for severe slugging identification, pressure fluctuations and elimination.

5.1.2.1 Severe Slugging Region Prediction

Figures 5-1, 5-2 and 5-3 show the model prediction for severe slugging identification compared with the Bøe[5] prediction model and the experimental data acquired. From these figures, it can be seen that the model performs very well compared to the model of Bøe[5]. Similar to the data, the model also identifies that as the gas flow rate is increased, there is no clear boundary from severe slugging to stable operations, but in fact, it is a region where the oscillations become smaller and smaller until they reach, what could be said, to be stable. This region is referred to as a transition region. Point A represents the first time a continuous stream of gas comes into the riser, but in variable amounts, so that it will behave as if it is severe slugging.
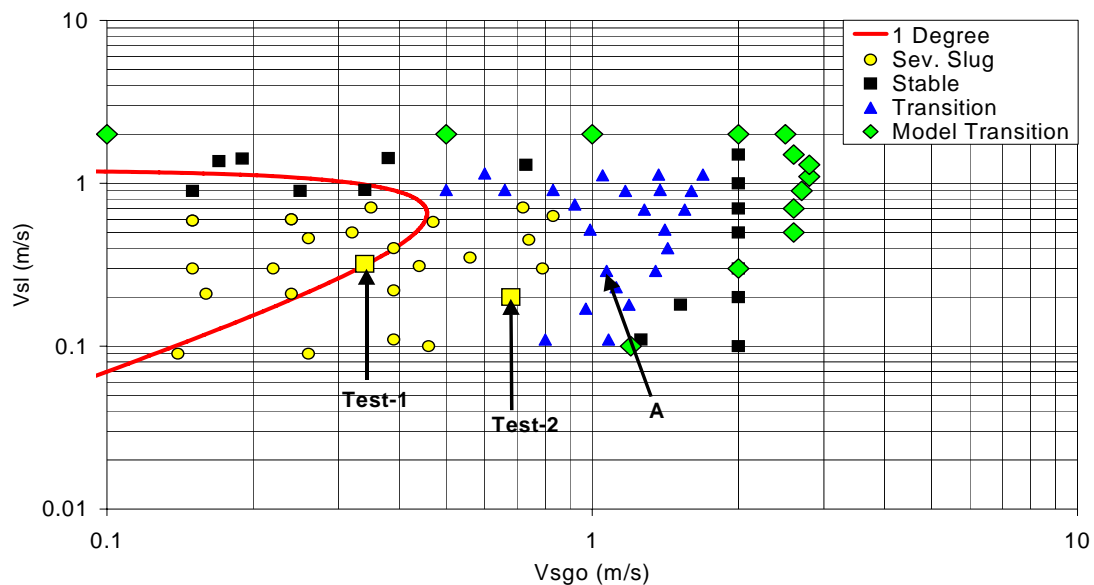
Figure 5–1: Severe slugging envelop for the large-scale facility, -1°
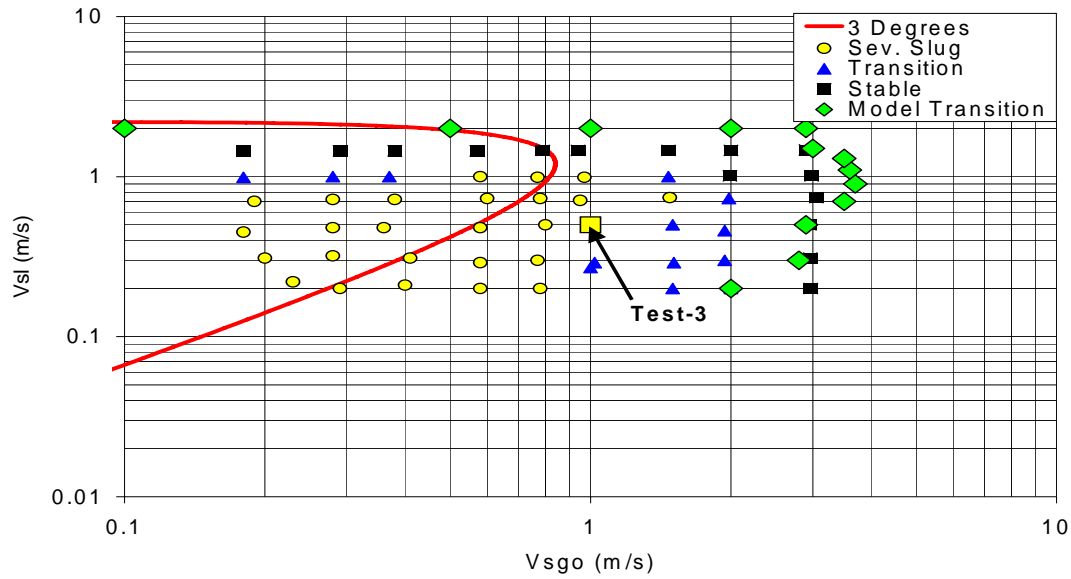
Figure 5–2: Severe slugging envelop for the large-scale facility, -3°
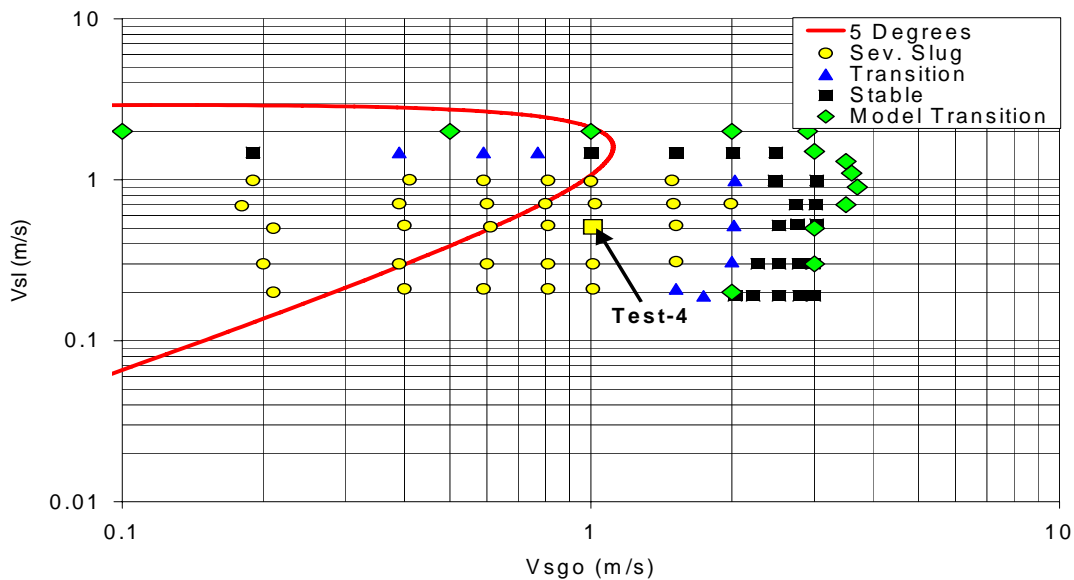
Figure 5–3: Severe slugging envelop for the large-scale facility, -5°

5.1.2.2 Severe Slugging Pressure Behavior Prediction

In the following section, the results of the model predictions compared to the experimental data for severe slugging cycle are shown for Tests 1-4. Figure 5-4 for Test-

1 shows that the model and experimental data are in good agreement on the minimum and maximum pressure in the pipeline during a severe slugging cycle. However, the model shows a severe slugging frequency that is slightly higher than that of the experimental data.
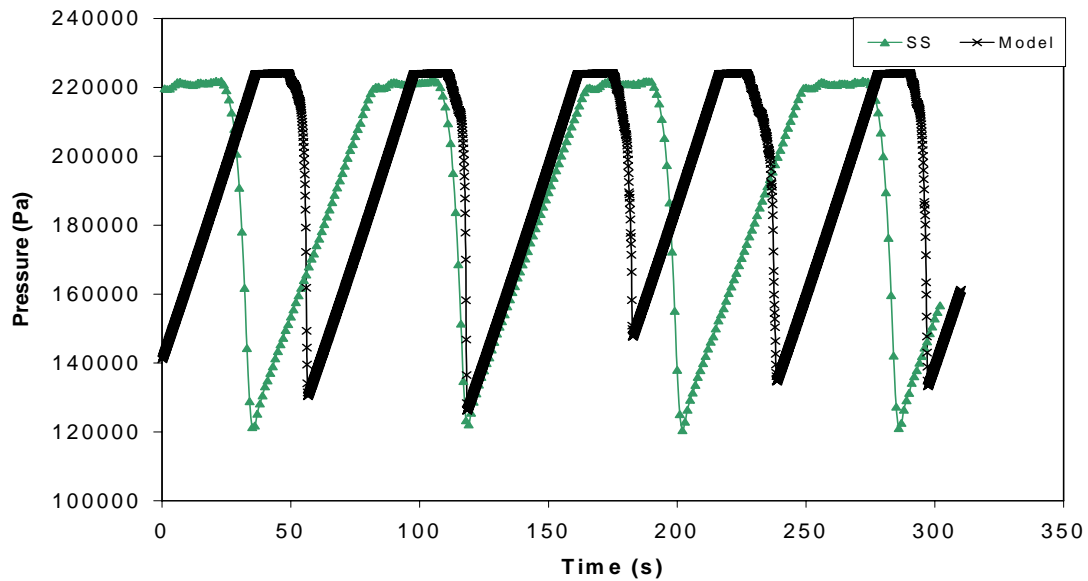
Figure 5–4: Pipeline pressure behavior for severe slugging (SS) cycle ($v_{SL} = 0.32$ m/s, $v_{Sg} = 0.35$ m/s, -1°)

The result for Test-2 are shown in Figure 5-5. For this case, the pressure difference between maximum and minimum pipeline pressure for the model compared to the experimental data does not agree very well. The explanation for this is that this point is very close to the experimental transition region, where gas continuously enters the riser. It is concluded that this region seems to occur earlier for the model compared to that of the experimental data.
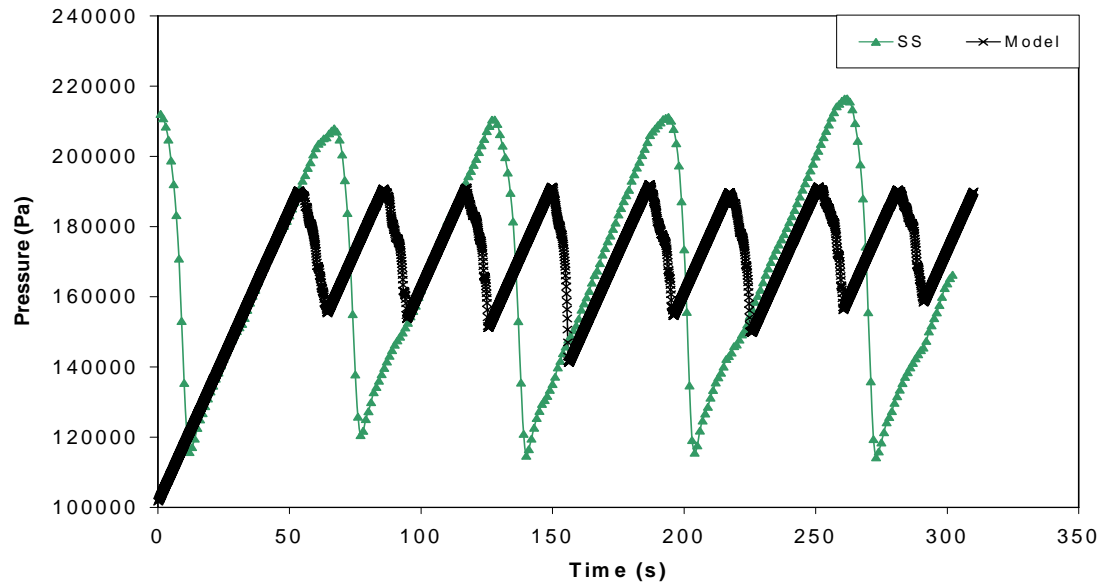
Figure 5–5: Pipeline pressure behavior for severe slugging (SS) cycle (v_{SL} = 0.20 m/s, v_{Sg} = 0.68 m/s, -1°)

Test-3 from Figure 5-6 shows similar behavior as Test-1 in that the model and the experimental data seem to agree well on the minimum and maximum pipeline pressure occurring during a severe slugging cycle. Again, the model shows a severe slugging frequency that is higher than that of the experimental data.
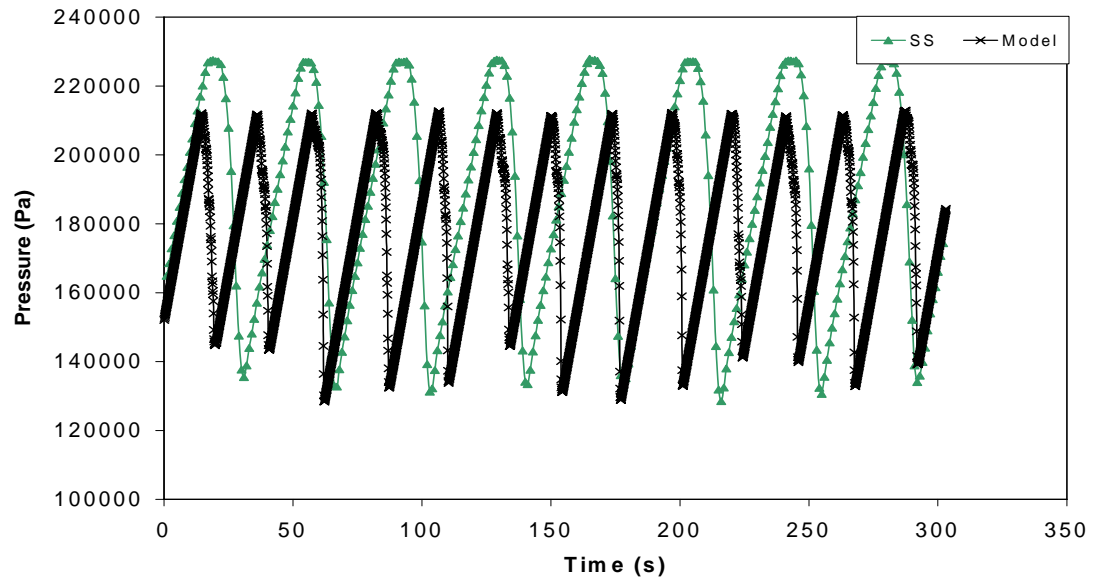
Figure 5–6: Pipeline pressure behavior for severe slugging (SS) cycle (v_{SL} = 0.50 m/s, v_{Sg} = 1.00 m/s, -3°)

Figure 5-7 shows similar behavior as Test-1 and Test-3. The maximum and minimum pressures in the pipeline for the model agree well with that of the experimental data, but the severe slugging frequency for the model is higher than that of the experiments.
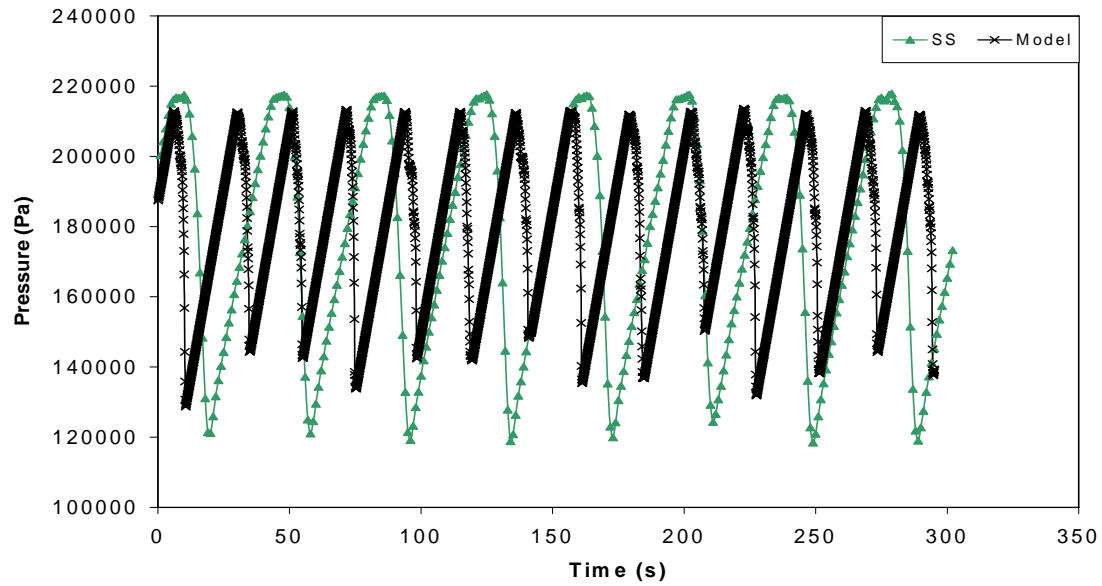
Figure 5–7: Pipeline pressure behavior for severe slugging (SS) cycle (v_{SL} = 0.51 m/s, v_{Sg} = 1.01 m/s, -5°)

5.1.2.3 Severe Slugging Elimination

The previously described test cases, Test-1, Test-2, Test-3, Test-4 and an additional test, Test-5 were used to evaluate the model using the by-pass to eliminate severe slugging.

Figures 5-8 and 5-9 show that the model predictions are very close to the experimental data. The model does not consider the distance to the take-off assuming that the gas can be taken-off without the concern of liquid blockage of the take-off. The experimental data shows only the stabilized pressure vs. time in the pipeline and not the expected transients occurring during start-up, that is why the experimental data shows a straight line throughout the experiment. In this case, the liquid penetration length in the pipeline is estimated to be 18.62 m and 17.61 m for stable operations, respectively. Those penetration lengths will exceed all of the take-off points and thereby blocking

them, and resulting in unstable operations. Therefore, a small pressure loss is induced using a ball valve as a choke for the experimental run to move the liquid penetration length to a level between the take-off point and the riser base to stabilize the flow.
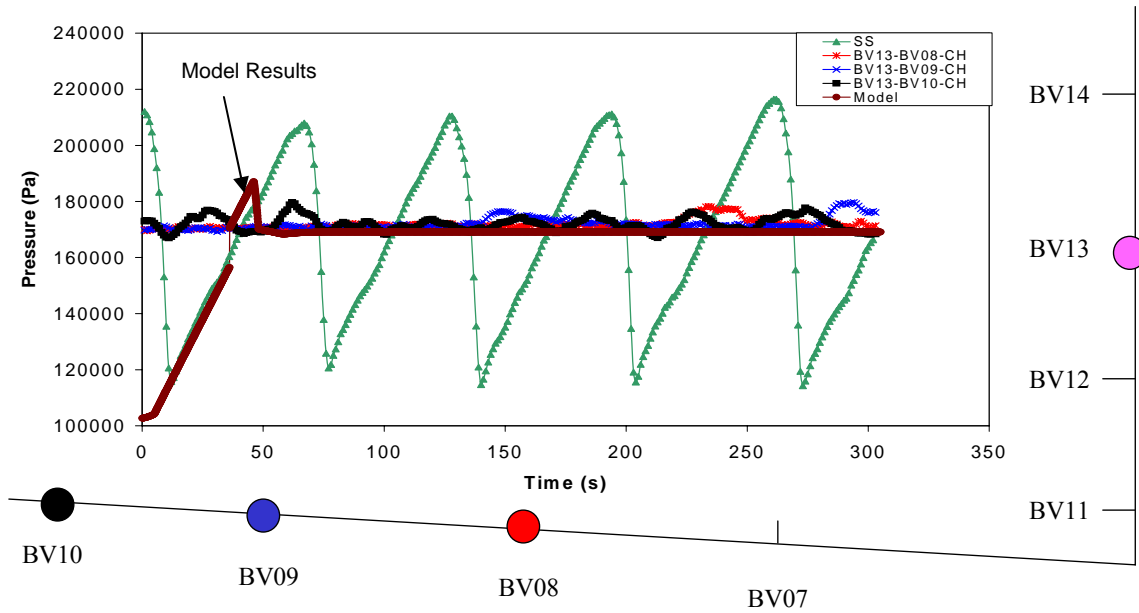
Figure 5–8: Elimination test for Test-1 using partially choked BV13-BV08 (v_{SL} = 0.32 m/s, v_{Sg} = 0.35 m/s, -1°)
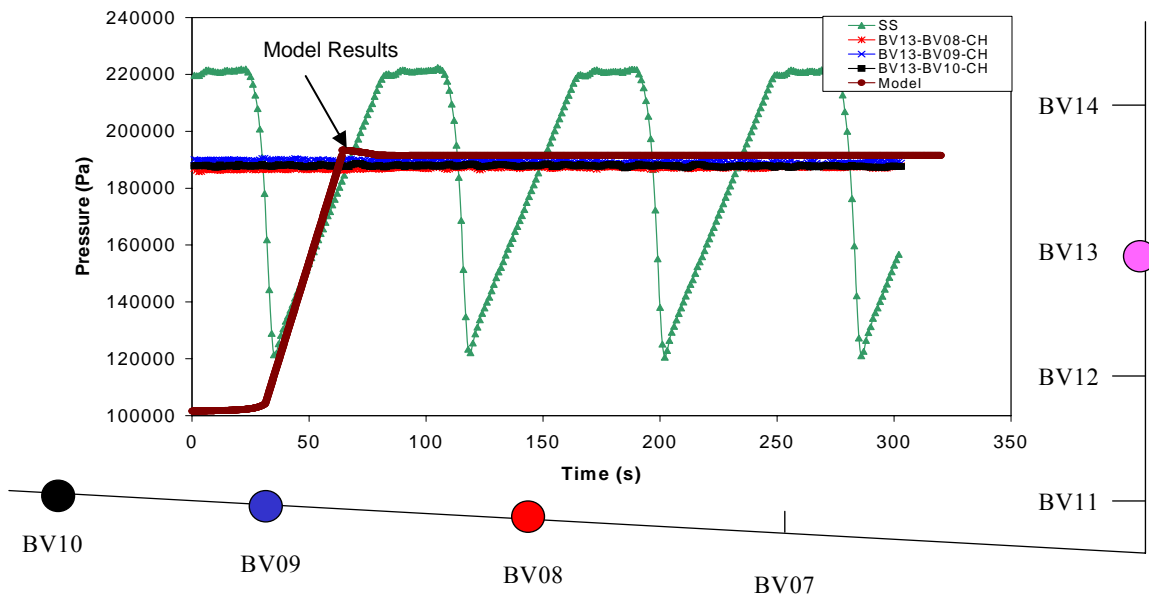
Figure 5–9: Elimination test for Test-2 using partially choked BV13-BV08 (v_{SL} = 0.20 m/s, v_{Sg} = 0.68 m/s, -1°)

Similar to Test-1 and Test-2, Figure 5-10 shows that the quality of the match between the experimental data and model is very good. As in the previous cases, a small choke setting is needed to ensure that the liquid does not penetrate to a point beyond the take-off point in the pipeline. In this case the mechanism is not the same as the previous case because the estimated liquid penetration length of 10.51 m does not exceed that of all the take-off points. It is observed that as opposed to blocking the take-off points, the liquid will flow back into the bypass injection point on the riser and thereby block the gas from flowing into the riser. This is due to a small pressure loss occurring over the bypass line that cannot sustain the required pressure at the injection point to ensure stable operations. The model under predicts the experimental data because it predicts the behavior regardless of liquid penetration length in the pipeline. Therefore, the difference is mainly due to the level of choking needed to stabilize the flow.
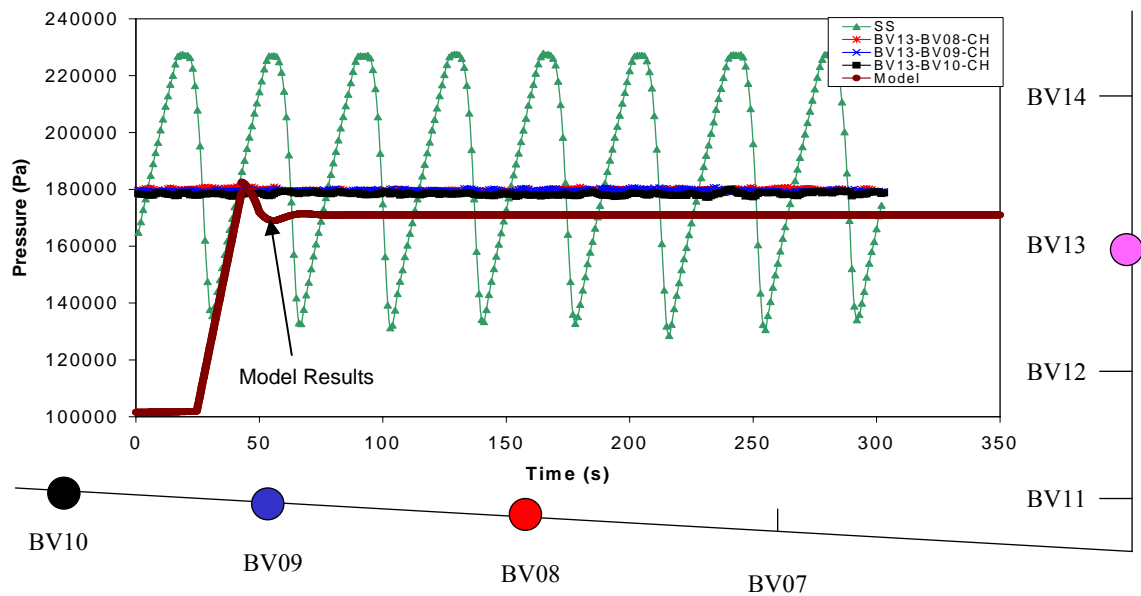
Figure 5–10: Elimination test for Test-3 using partially choked BV13-BV09 (v_{SL} = 0.50 m/s, v_{Sg} = 1.00 m/s, -3°)

Figure 5-11 shows similar results as the previous case, the model predicts the stabilized pipeline pressure very well.
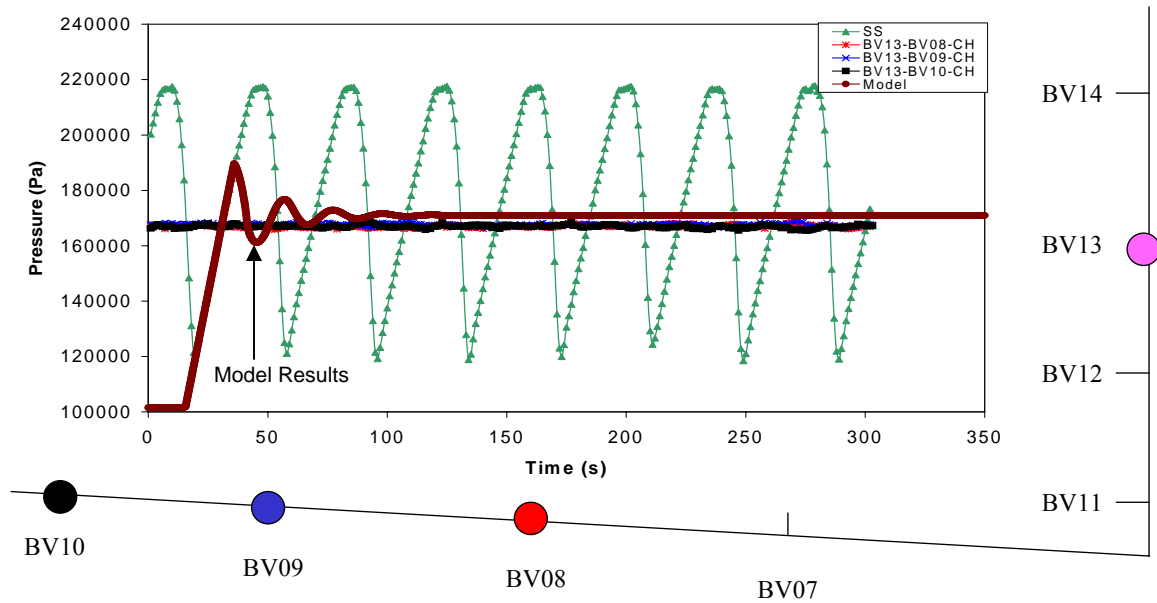
Figure 5–11: Elimination test for Test-4 using partially choked BV13-BV08 (v_{SL} = 0.51 m/s, v_{Sg} = 1.01 m/s, -5°)

Figure 5-12 shows a case where choking is not needed at the take-off point to stabilize the flow. As can be seen from Figure 5-12, the pressure match between the model and the experimental data is very good.
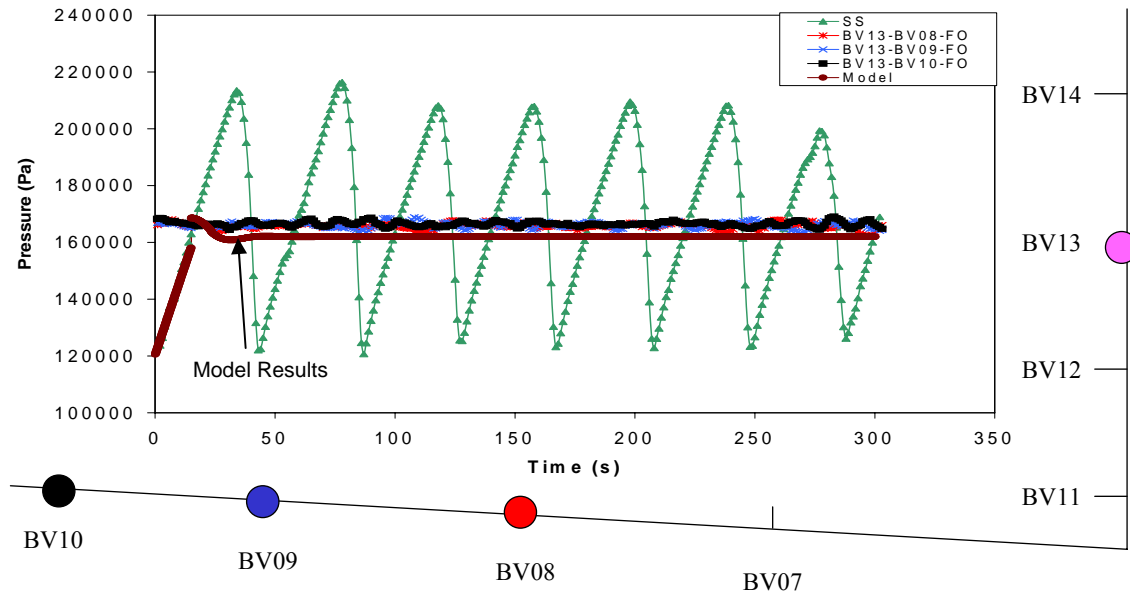
Figure 5–12: Elimination test for Test-5 using fully open BV13-BV08 (v_{SL} = 0.30 m/s, v_{Sg} = 1.01 m/s, -5°)

5.2 Steady State Model

The objectives of the steady state modeling study for the prevention of severe slugging in deep water pipeline/riser systems were two-fold: (i) to predict the conditions under which the severe slugging will be eliminated by bypassing gas to the base of the riser, and (ii) to develop design criteria and methodology for field application.

5.2.1 The Physical Model

Figure 5-13 shows a schematic of the system under consideration; gas and liquid enter the base of the riser by way of a downward sloping pipeline (at an angle θ to the horizontal) with diameter, d_p. It is assumed that the length of this downward sloping pipeline section is sufficient to ensure that two-phase flow close to the riser base is fully

stratified. Under normal (severe slugging) operation, gas and oil would proceed downward to the base of the riser, accumulate, and after sufficient pressure is built up in the gas "bubble", the mixture would be expelled to the surface through the riser with diameter d_r. In the proposed self-lifting system, however, high-pressure gas is removed from the pipeline at a distance L_{Bypass} from the riser base (point A, Figure 5-13), and re-injected into the riser at a height y_i from the base, (point B, Figure 5-13). Above the re-injection point, the two phases are lifted to the surface separator. In the pipeline section, it is assumed that the nose of the gas bubble (from the inlet 2-phase region) extends to a distance $L_{B,p}$ beyond the gas take-off point, and that gas only flows through the bypass, and liquid only flows around the base of the riser. (For successful operation of the severe slugging prevention system, it is obvious that $L_{B,p} \leq L_{Bypass}$).
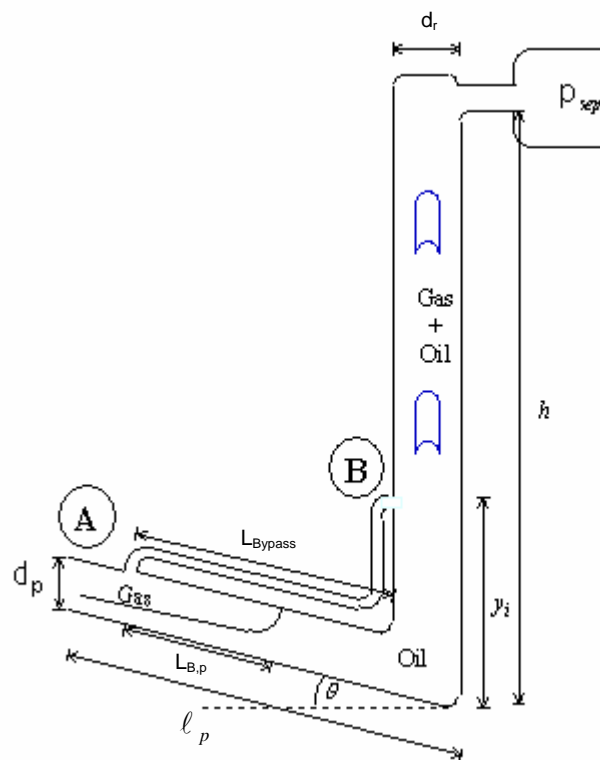
Figure 5–13: Schematic of pipeline/riser system

5.2.1.1 Criterion for Continuous Flow – Simplified Model

As a first approach to modeling the flow system, it is assumed that frictional pressure drops are negligible. Further, it is assumed that in the section of pipeline/riser/separator system under consideration, pressure and temperature variations are small enough that gas and liquid PVT and flow properties (e.g., densities, holdups, etc.) can be considered as approximately constant. Finally the gravitational pressure drops in the gas bypass is ignored.

In this first simplified model, there is no pressure drop between points A and B, regardless of whether the liquid or gas legs are considered. In particular, considering the hydrostatic balance on the liquid leg,

$$\rho_L g \left(L_{Bypass} - L_{B,p} \right) \sin(\theta) = \rho_L g \left(y_i - d_p \right) \qquad (29)$$

or

$$y_i = \left(L_{Bypass} - L_{B,p} \right) \sin(\theta) + d_p \qquad (30)$$

Clearly, under this assumption, the maximum height of the gas injection point is obtained when $L_{B,p} = 0$. In practice, there will be some pressure drop in the gas leg, so the optimal placement of the injection point would be determined by solving

$$\Delta p_g = \rho_L g \left(y_i - d_p - \left(L_{Bypass} - L_{B,p} \right) \sin(\theta) \right) \qquad (31)$$

for y_i.

Having fixed the positions of the take-off and injection points, a simple pressure balance shows that continuous flow would occur if the injection pressure at point B is sufficient to overcome the pressure losses in the remainder of the riser. That is

$$p_{sep} + \rho_L g \left(h - y_i \right) H_L = p_g - \Delta p_g \qquad (32)$$

Here H_L is the average liquid holdup in the riser, and the gas is assumed to have a negligible effect on the average fluid density in the riser. Moreover, it is assumed that the pressure losses in the gas bypass are negligible, (i.e., $\Delta p_g \approx 0$), and that gas pressure is described by the engineering equation of state, i.e.,

$$p_g\left(\ell_p - L_{B,p}\right)A_p\alpha = \frac{ZmRT}{M} \tag{33}$$

Where it is assumed that the liquid penetration length is located at the take-off point and A_p is the area of the pipeline, α is the gas void fraction in the inlet region, m is the mass of gas with molecular weight M in this volume, and T is the inlet temperature. Differentiating Eq. 32 with respect to time, using Eq. 33,

$$\frac{dp_{sep}}{dt} + \frac{g}{A_r}\frac{d\left(\rho_L(h - y_i)H_L A_r\right)}{dt} = \frac{ZRT}{M\left(\ell_p - L_{B,p}\right)A_p\alpha}W_G \tag{34}$$

where W_G is the mass flow rate of gas. Since $\dfrac{d\left(\rho_L(h - y_i)H_L A_r\right)}{dt}$ is the mass flow rate of liquid in the riser, W_L, Eq. 35, the condition under which flow will be continuous, can be written as

$$\frac{dp_{sep}}{dt} + \frac{g}{A_r}W_L = \frac{ZRT}{M\left(\ell_p - L_{B,p}\right)A_p\alpha} \tag{35}$$

So for continuous flow in the severe slugging prevention system, it is required that:

$$\frac{dp_{sep}}{dt} + \frac{g}{A_r}W_L \leq \frac{ZRT}{M\left(\ell_p - L_{Bypass}\right)A_p\alpha}W_g \tag{36}$$

So for continuous flow in the severe slugging prevention system, it is required that Equation 36 is analogous to the Bøe[5] criterion for predicting the severe slugging region in an unmodified pipeline/riser system.

In Fig. 5-14, the severe slugging region is plotted using both the original Bøe[5] criterion and the criterion given in Eq. 36. It is clearly seen that the severe slugging region has been reduced significantly with the use of the gas by-pass.
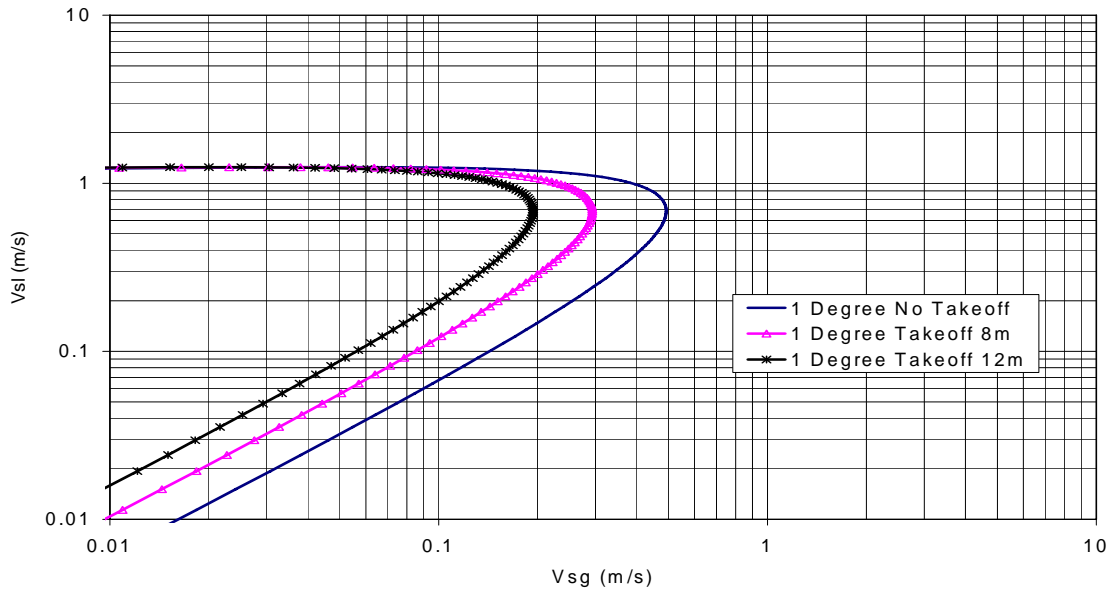
Figure 5–14: Criterion of Equation 36 for different take-off points

5.2.1.2 Criterion for Continuous Flow – Rigorous Model

In practice, there will be a pressure drop in the gas bypass leg (i.e., between A and B in Figure 5-13) that will determine the optimal location of the injection point (y_i). In this section, the rigorous equations for pressure drops in an operating gas bypass system are developed. As in the previous section, the system geometry is depicted in Figure 5-10.

Considering Figure 5-13, the gas bypass system will operate successfully as long as $0 \leq L_{B,p} \leq L_{Bypass}$. The minimum allowable pressure drop in the gas leg will occur when $L_{B,p} = 0$, and the hydrostatic pressure drop in the liquid leg is determined by the liquid

height difference, $y_i - d_p - L_{Bypass} \sin(\theta)$. If the pressure drop in the gas leg were to fall below this level, the nose of the gas bubble would recede to a point above the gas take-off point (A), and liquid would enter the gas bypass. At the opposite extreme, the maximum allowable pressure drop in the gas bypass occurs when $L_{B,p} = L_{Bypass}$; that is, when the hydrostatic pressure drop in the liquid leg is determined by the height difference $y_i - d_p$. If the pressure drop in the gas line were to exceed this, the gas bubble would circulate around the bottom of the riser and aerate the liquid. Under this mode of operation, gas would enter the riser via the path of minimum resistance. A successfully operating system would exhibit a bypass pressure drop between the minimum and maximum allowable pressure drops described above.

Since pressure drops across the liquid and gas bypass legs must be equal for steady flow, we will focus only on the liquid leg. The maximum allowable pressure drop (with a fully-penetrating bubble) assumes the form:

$$\Delta p_{L,max} = \rho_L g \left(y_i - d_p\right) + \frac{2 f_{L,R} \rho_L}{d_R} \left(\frac{Q_o}{A_r}\right)^2 \left(y_i - d_p\right) + \Delta p_{elbow} \qquad (37)$$

Similarly, the minimum allowable pressure drop (with a fully penetrating bubble – i.e., gas bubble extending to the base of the riser), is given by

$$\Delta p_{L,min} = \rho_L g \left(y_i - d_p - L_{Bypass} \sin(\theta)\right) + \frac{2 f_{L,p} \rho_L}{d_p} \left(\frac{Q_o}{A_p}\right)^2 x +$$
$$\frac{2 f_{L,R} \rho_L}{d_r} \left(\frac{Q_o}{A_r}\right)^2 \left(y_i - d_p\right) + \Delta p_{elbow} \qquad (38)$$

As noted previously, successful operation of the bypass requires that the pressure drop across the gas bypass falls between the values predicted by Eqs. 37 and 38. A derivation

of the pressure drop in a pipeline where there is a stationary penetrating bubble is shown in Appendix C.

5.2.2 Model Performance

In this section the steady state model is compared to the experimental data. The steady state model gives the bound between the minimum and maximum pressure losses needed through the bypass to ensure that the flow is stable. Figure 5-15 shows the differential between maximum and minimum pressure losses through the bypass versus inclination angle for the BV13-BV10 case. From Figure 5-15 it can be seen that the pressure span will increase with pipeline inclination angle holding the take-off and injection point constant. When the inclination angle goes to zero (horizontal), there will be no pressure span available. This is consistent since severe slugging is not expected to occur for a horizontal pipeline. In Appendix D the results from the model are shown together with the experimental data. The minimum and maximum pressure losses reported from the model are reported together with the actual pressure losses through the bypass. The experimental pressure loss through the bypass should fall inside the bound of the minimum and maximum pressure losses to ensure stable flow as reported by the model.
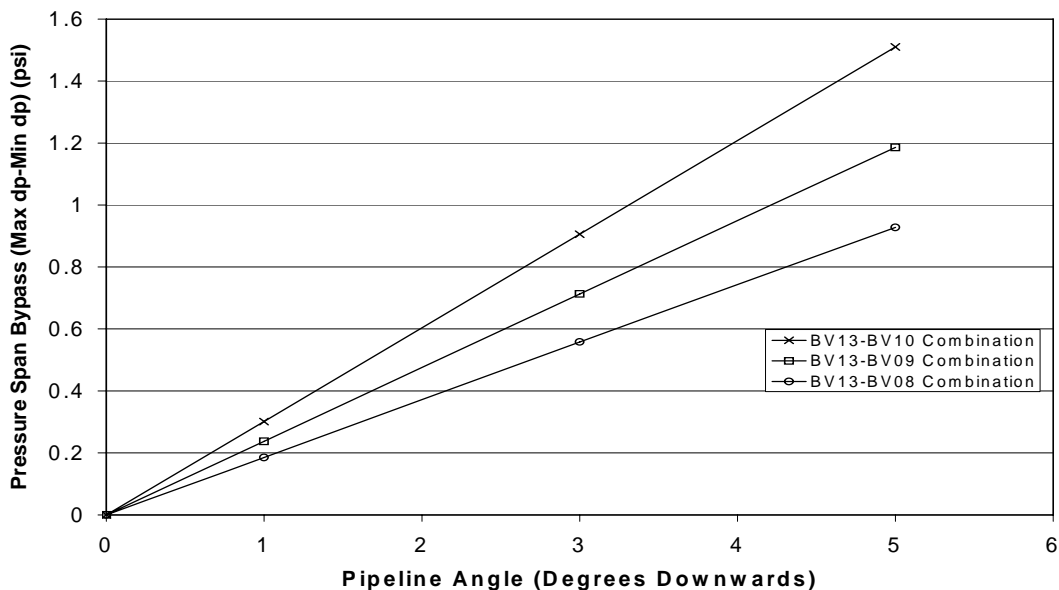
Figure 5–15: Pressure versus pipeline angle for BV13-BV10 case

For the -1° case, 92 of the reported experimental points falls within that region, while 25 falls outside. All of the cases reported outside the region fall very close to one of the boundaries, indicating that the liquid penetration length is either close to the riser base or to the take-off point. For the -3° case 151 cases fall within the region between minimum and maximum pressure losses needed to ensure stable flow, while only 5 cases fall outside this region. Again, all of the points falling outside of the region are very close to either the minimum or maximum pressure loss points to ensure stable flow. For the last angle of −5°, all of the 162 experimental points fall inside the region predicted by the model to ensure stable flow. Therefore, it can be concluded that the model gives accurate predictions of the pressure bound needed to ensure stable operations using the bypass option.

Chapter 6 SUMMARY AND CONCLUSIONS

This last chapter presents a summary of the study and the specific conclusions that can be drawn from the experimental and modeling studies performed. It also discusses limitations of the current models and possible suggestions for improvements in future studies.

6.1 Summary

A novel approach has been tested and verified to remedy severe slugging in pipeline-riser systems, by transferring the pipeline gas (in-situ gas) to the riser at a point above the riser base. This transfer process will reduce both the hydrostatic head in the riser and the pressure in the pipeline, consequently attenuating severe slugging occurrence. This approach can be considered as self-gas lifting (i.e., no additional gas injection is required from the platform).

An extensive experimental analysis has been conducted to investigate the characteristics of the proposed severe slugging attenuation method. The experimental results have revealed the physical mechanisms of the proposed method. Experimental observations have shown that it is ideal to place the injection point at the same level or slightly higher than the take-off point for optimum performance. An uncertainty analysis was performed to ensure the consistency of pressure transducers, temperature probes, mass flow meters and propagation of superficial liquid and gas velocities.

A modified transient model and a steady state model are used to model the flow behavior of severe slugging and elimination. The transient model can predict the severe slugging region, the pipeline pressure fluctuations during a severe slugging cycle, and the pipeline pressure for the elimination case. The steady state model can be used for optimizing the injection and take-off points for the bypass in conjunction with the transient model. Overall both models show results that are in good agreement with the experimental data. The proposed method has been shown to be insensitive to variations in both gas and liquid flow rates for a wide range of operating conditions. Overall, the proposed method has been proven to be very effective for severe slugging attenuation in a pipeline-riser system.

6.2 Conclusions

From the experimental and modeling studies performed during the course of this research, the following conclusions are drawn.

1. A novel approach to eliminate severe slugging has been tested and verified using a small-scale facility, and further investigated using a large-scale facility.

2. Experimental observations showed that severe slugging can exist well outside the region predicted by existing prediction models.

3. From the experimental studies, it was observed that a small choking is needed to stabilize the flow when the injection point is at a higher level than the take-off point. The pressure loss through the choke is very small compared to that of the pipeline pressure.

4.   Two different mechanisms govern the choking of the take-off point. If the liquid penetration length in the pipeline exceeds that of the take-off point, an additional pressure loss through a choke at the take-off point is needed to move the liquid penetration length to a point between the riser base and take-off point. The other mechanism is due to liquid coming into the injection point because there is not enough pressure loss through the bypass to keep a constant pressure at the injection point.

5. Experiments show that the elimination method is not sensitive to changes in both liquid and gas flow rates.

6. A constant choke setting for different flow rates is able to eliminate a substantial part of the severe slugging envelope. This region will shrink as the take-off point is moved closer to the riser base and increase as it is moved farther away from the riser base. This is due to having more differential pressure span to work with for this case.

7. A transient model was modified to predict the pipeline pressure for the novel elimination technique.

8. The transient model predicts the severe slugging region, the pipeline pressure during a severe slugging, and the pipeline pressure for the novel elimination technique very well compared to the experimental data.

9. A steady state model was developed as a design tool for optimizing the injection and take-off points. This model is in very good agreement with the experimental data.

6.3 Recommendations

Some suggestions are presented that can further improve the experimental part as well as the modeling efforts in future studies. A variable choke controlled by a PC based system would improve the overall experimental facility. Such a device could more easily be used to stabilize the flow. The bypass system can be designed so that hoses do not have to be changed when switching from one injection port to another one. Flow rate measurements are important, not only at the inlet of the pipe, but also at the outlet or the separator. Such a device could give a better indication of the flow rate variations during a severe slugging cycle.

Modeling is an integral part of this study. Although they are assumed to be negligible, the pressure losses in the pipeline or riser during severe slugging or stable operations can be incorporated for completeness of the transient model. Also, it would be of great benefit to incorporate the scenario of blockage of the take-off point if at all possible.

Considering the interest in the industry for severe slugging attention, the following suggestions for future work are presented.

1. Large scale studies of the self-lifting concept.
2. Study of self-lifting for lazy-s shaped risers.
3. Investigation of self-lifting for hilly terrain pipeline and riser system.
4. Down hole separation and re-injection.
5. Further studies of self-lifting with different bypass diameters and various choking and valve configuration.

6. Three-phase flow severe slugging prediction and elimination studies.

BIBLIOGRAPHY

1. Almeida, A. R., and Gonçalves M. A. L.: "Venturi for severe slugging elimination", presented at the 9th International Conference Multiphase '99 – Paper #53, 1999.

2. Barbuto, F. A.: "Method of Eliminating Severe Slug in Multi-Phase Flow Subsea Lines," Application for UK Patent, #2 282 399, 1995.

3. Barbuto, F. A., and Caetano, E. F.: "On the Occurrence of Severe Slugging Phenomenon in Fargo-1 Platform, Campos Basin, Offshore Brazil," *5th BHRG International Conference Proceedings*, 491-504, Cannes, France 1991.

4. Bendiksen et al.: "The Dynamic Two-Fluid Model OLGA: Theory and Application," *SPE Production Engineering*, 171-180, May 1991.

5. Bøe, A.: "Severe Slugging Characteristics; Part 1: Flow Regime for Severe Slugging; Part 2: Point Model Simulation Study," presented at Selected Topics in Two-Phase Flow, Trondheim, Norway, March 1981.

6. Courbot, A.: "Prevention of Severe Slugging in the Dunbar 16" Multiphase Pipeline," OTC 8196, 1996 Offshore Technology Conference, 445-452, 1996.

7. Corteville et al.: "An Experimental Study of Severe Slugging in Multiphase Production Lines," *7th BHRG International Conference Proceedings*, 105-121, Cannes, France, 1995.

8. Dieck, R. H.: "Measurements Uncertainty Methods and Application," 2nd Ed. Instrument Society of America, USA, 1997.

9. Fabre, J., et al.: "Severe Slugging in Pipeline/Riser Systems," SPE 16846, Presented at 1987 SPE ATCE, Dallas, TX, Sept. 1987.

10. Farghaly, M. A.: "Study of Severe Slugging in Real Offshore Pipeline Riser-Pipe System," SPE 15726, Presented at SPE Middle East Oil Technology Conference, Manama, Bahrain March 1987.

11. Hall, A. R. W., and Butcher, G. R.: "Transient Simulation of Two-Phase Hydrocarbon Flows in Pipelines," Paper I4, European Two-Phase Flow Group Meeting, June 6-10 1993, Hanover.

12. Hassanein, T., and Fairhurst, P.: "Challenges in The Mechanical and Hydraulic Aspects of Riser Design for Deep Water Developments," 1998 IBC UK Conf. Ltd. Offshore Pipeline Technology Conference, Oslo, Norway, 1998.

13. Henriot, V. et al.: "Simulation of Process to Control Severe Slugging: Application to the Dunbar Pipeline," SPE 56461, presented at 1999 SPE Annual ATCE, 3-6 October, Houston, TX.

14. Hill, T. J.: "Riser-Base Gas Injection into the S.E. Forties Line," Proceedings, 4th International Conference, 133-148, BHRA 1989.

15. Hill, T. J.: "Gas Injection at Riser Base Solves Slugging, Flow Problems," *Oil and Gas J.*, 88-92 February 26, 1990.

16. Hollenberg et al.: "A Method to Suppress Severe Slugging in Flow-Line Riser Systems," 7th BHRG International Conference Proceedings, **88-103**, Cannes, France, 1995.

17. Jansen, F. E.: "Elimination of Severe Slugging in a Pipeline-Riser System," MS. Thesis, U. of Tulsa, 1990.

18. Johal, K. S. et al.: "An Alternative Economic Method to Riser-Base Gas Lift for Deep Water Subsea Oil/Gas Field Developments," SPE 38541, presented at 1997 Offshore Europe Conference, 487-492, Aberdeen, Scotland 9-12 September 1997.

19. Juprasert, S.: "Two-Phase Flow in an Inclined Pipeline Riser-Pipe System," MS. Thesis, U. of Tulsa, 1976.

20. Kaasa, Ø.: "A Subsea Slug Catcher to Prevent Severe Slugging," 6th Underwater Technology International Conference, Bergen, Norway, 1990.

21. Kashou, S. F.: "Severe Slugging in S-Shaped or Catenary Risers: OLGA Prediction and Experimental Verification," IBC Tech. Serv., Advances in Multiphase Tech. INT. Conference, 1996.

22.   Larsen et al.: "PeTra: A Novel Computer Code for Simulation of Slug Flow," SPE 38841, presented at the 1997 SPE ATCE, San Antonio, TX Oct. 5-8, 1997.

23.   McGuinness, M., and Cooke, D.: "Partial Stabilization at St. Joseph," 3rd International Offshore and Polar Engineering Conference, 235-241, June 6-11, Singapore 1993.

24.   Montgomery, J. A., and Yeung, H. C.: "The Stability of Fluid Production from a Flexible Riser," ETCE2000/PROD-10072 presented at ETCE/OAME2000 Joint Conference, New Orleans, LA, February 14-17, 2000.

25.   Philbin, M., and Black, P. S.: "Analysis of Severe Slugging in Satellite Field Development Using a Transient Multiphase Flow Simulator," IBC Multiphase Operations Offshore, London, UK, 1991.

26.   Pots, B. F. M., et al.: "Severe Slug Flow in Offshore Flow-Line/Riser Systems," SPE 13723, presented at SPE Middle East Oil Technology Conference, Manama, Bahrain, March 1985.

27.   Sarica, C. and Shoham, O.: "A Simplified Transient Model for Pipeline-Riser Systems," *Chemical Engineering Science*, 46, No: **9**, pp. 2167-2179, 1991.

28.   Sarica, C. and Tengesdal, J. Ø.: "A New Technique to Eliminate Severe Slugging in Pipeline/Riser Systems," SPE 63185, Presented at the 2000 SPE ATCE, Dallas, TX, October 1-4, 2000.

29.   Schmidt, Z.: "Experimental Study of Gas-Liquid Flow in a Pipeline-Riser Pipe System," MS. Thesis, U. of Tulsa 1976.

30.   Schmidt, Z.: "Experimental Study of Two-Phase Slug Flow in a Pipeline-Riser Pipe System," Ph.D. Dissertation, U. of Tulsa 1977.

31.   Schmidt, Z. et al.: "Choking Can Eliminate Severe Pipeline Slugging," *Oil and Gas J.* **12**, 230-8, 1979.

32.   Schmidt, Z. et al.: "Severe Slugging in Offshore Pipeline-Riser Pipe System," *SPEJ*, 27-38, 1985.

33.   Song S., and Kouba, G. (2000-a): "Characterization of Multiphase Flow in Ultra-Deep Subsea Pipeline/Riser System," ETCE2000/PROD-10052, ETCE/OAME2000 Joint Conference, New Orleans, LA, Feb. 14-17, 2000.

34.   Song S., and Kouba, G. (2000-b): "Fluids Transport Optimization Using Seabed Separation," ETCE2000/PROD-10051, ETCE/OAME2000 Joint Conference, New Orleans, LA, Feb. 14-17, 2000.

35.   Taitel, Y.: "Stability of Severe Slugging," *Int. J. Multiphase Flow.* **2**, 203-217, 1986.

36.   Taitel, Y. and Dukler, A. E.: "A Model for Predicting Flow Regime Transition in Horizontal and Near Horizontal Gas-Liquid Flow," *AIChE Journal*, 22, No. 1, pp. 47-55 (1976).

37.   Taitel, Y. et al.: "Severe Slugging in a Pipeline-Riser System, Experiments and Modeling," *Int. J. Multiphase Flow*. 1, 57-68, 1990.

38.   Tin, V.: "Severe Slugging in Flexible Risers," *5th BHRG International Conference Proceedings*, 507-525, Cannes, France 1991.

39.   Tin, V. and Sarshar, M. M.: "An Investigation of Severe Slugging Characteristics in Flexible Risers," *6th BHRG International Conference Proceedings*, 205-228, Cannes, France, 1993.

40.   Vierkandt, S.: "Severe Slugging in a Pipeline-Riser System, Experiments and Modeling," MS. Thesis, U. of Tulsa, 1988.

41.   Wyllie, M. W. J., and Brackenridge, A.: "A Retrofit Solution to Reduce Slugging Effects in Multiphase Subsea Pipelines − The Internal Riser Insert System (IRIS)," 1994 Subsea International Conference, 1994.

42.   Wyllie, M. W. J.: " Apparatus for Inserting into a Conduit," UK Patent Application GB 2 280 460, 1995.

43.   Yocum, B.T.: "Offshore Riser Slug Flow Avoidance, Mathematical Model for Design and Optimization," SPE 4312, presented at SPE European Meeting, London, April 1973.

44.   Zuber, N and Findlay, J. A.: "Average volumetric concentration in two-phase flow systems," *J. Heat Transfer*, Ser. **87**, 453-458, 1965.

45.   Xu, Z. G.: "Solutions to Slugging Problems Using Multiphase Simulations," 3rd IBC Multiphase Metering Int. Conference March 1997.

.

Appendix A Uncertainty Analysis Results

Table A-1: Summary of Instrument Uncertainty (Random, Systematic and Overall)

Instrument	Range	Random Uncertainty (Engr. Units)	Systematic Uncertainty (Engr. Units)	Degrees of Freedom (df)	Overall Uncertainty (UASME) (Engr. Units)
PT1 (psi)	0-80	0.0153	0.2683	Infinity	0.3125
PT2 (psi)	0-80	0.0146	0.2683	Infinity	0.3125
PT3 (psi)	0-100	0.0849	0.2638	Infinity	0.3068
DPT1 (psi)	0-12.5	0.0035	0.0419	Infinity	0.0489
DPT2 (psi)	0-12.5	0.0084	0.0419	Infinity	0.0504
DPT3 (psi)	0-20	0.0119	0.0670	Infinity	0.0803
DPT4 (psi)	0-32	0.0146	0.1073	Infinity	0.1277
DPT5 (psi)	0-12.5	0.0065	0.0419	Infinity	0.0500
DPT6 (psi)	0-32	0.0136	0.1073	Infinity	0.1277
DPT7 (psi)	0-2	0.0010	0.0067	Infinity	0.0080
DPT8 (psi)	0-20	0.0027	0.0670	Infinity	0.0780
TT1 (°F)	32-180	0.3393	0.0434	Infinity	0.3970
TT2 (°F)	32-180	0.0254	0.0434	Infinity	0.0527
TT3 (°F)	32-180	0.1979	0.0434	Infinity	0.2342
CMF025 (lb/min)	0.04-40	0.0013	0.0076	Infinity	0.0125
DS150 (lb/min)	28-2800	0.0022	0.0513	Infinity	0.0597
θ	0-9 ft	-	0.0500	-	0.0500

Table A-2: Uncertainty propagation results for -1° angle

Run #	Standard Conditions		V_{SL} Uncertainty	V_{Sg} Uncertainty
1 Degree	V_{SL} (m/s)	V_{Sg} (m/s)	(m/s)	(m/s)
1	0.09	0.14	0.0001164	0.0102435
2	0.09	0.26	0.0001164	0.0116272
3	0.1	0.46	0.0001171	0.0128254
4	0.11	0.39	0.0001183	0.0127388

Run #	Standard Conditions		V$_{SL}$ Uncertainty	V$_{Sg}$ Uncertainty
1 Degree	V$_{SL}$ (m/s)	V$_{Sg}$ (m/s)	(m/s)	(m/s)
5	0.2	0.68	0.0001204	0.0126079
6	0.21	0.16	0.0001219	0.0094922
7	0.21	0.27	0.0001209	0.0100581
8	0.22	0.39	0.0001231	0.0108235
9	0.3	0.16	0.0001264	0.0094633
10	0.3	0.24	0.0001267	0.0095926
11	0.3	0.79	0.0001274	0.0128768
12	0.31	0.45	0.0001271	0.0107260
13	0.32	0.34	0.0001291	0.0102925
14	0.35	0.57	0.0001329	0.0112071
15	0.4	0.38	0.0001366	0.0104319
16	0.45	0.76	0.0001411	0.0112241
17	0.46	0.26	0.0001417	0.0098514
18	0.5	0.30	0.0001465	0.0094021
19	0.58	0.47	0.0001547	0.0096012
20	0.59	0.15	0.0001569	0.0092309
21	0.6	0.24	0.0001565	0.0095525
22	0.63	0.83	0.0001636	0.0116109
23	0.71	0.35	0.0001703	0.0092410
24	0.71	0.72	0.0001702	0.0103567
25	0.11	0.80	0.0001153	0.0139428
26	0.11	1.07	0.0001157	0.0166677
27	0.11	1.26	0.0001160	0.0190056
28	0.17	0.98	0.0001193	0.0160214
29	0.18	1.19	0.0001193	0.0183045
30	0.18	1.52	0.0001194	0.0221876
31	0.23	1.12	0.0001237	0.0173038
32	0.29	1.07	0.0001260	0.0146581
33	0.29	1.35	0.0001264	0.0177197
34	0.4	1.42	0.0001364	0.0187358
35	0.52	0.99	0.0001498	0.0130668
36	0.52	1.41	0.0001504	0.0168134
37	0.69	1.29	0.0001693	0.0132490
38	0.69	1.54	0.0001692	0.0151028

Run #	Standard Conditions		V$_{SL}$ Uncertainty	V$_{Sg}$ Uncertainty
1 Degree	V$_{SL}$ (m/s)	V$_{Sg}$ (m/s)	(m/s)	(m/s)
39	0.74	0.92	0.0001781	0.0120190
40	0.9	0.15	0.0001961	0.0082041
41	0.9	0.24	0.0001972	0.0085337
42	0.9	1.16	0.0001992	0.0120186
43	0.9	1.60	0.0002001	0.0148320
44	0.91	0.34	0.0001979	0.0088612
45	0.91	0.50	0.0001987	0.0093662
46	0.91	0.66	0.0001989	0.0098981
47	0.91	0.83	0.0001993	0.0105227
48	0.91	1.38	0.0002001	0.0133505
49	1.12	1.04	0.0002334	0.0110380
50	1.13	1.37	0.0002343	0.0125212
51	1.13	1.68	0.0002353	0.0144736
52	1.15	0.60	0.0002381	0.0094864
53	1.3	0.73	0.0002656	0.0099429
54	1.37	0.16	0.0002734	0.0081125
55	1.42	0.19	0.0002860	0.0082535
56	1.43	0.38	0.0002871	0.0085945

Table A-3: Uncertainty propagation results for -3° angle

Run #	Standard Conditions		V$_{SL}$ Uncertainty	V$_{Sg}$ Uncertainty
3 Degree	V$_{SL}$ (m/s)	V$_{Sg}$ (m/s)	(m/s)	(m/s)
1	0.22	0.23	0.00686222	0.0089571
2	0.2	0.30	0.00692429	0.0101150
3	0.21	0.39	0.00696782	0.0105565
4	0.2	0.58	0.00681093	0.0104793
5	0.2	0.79	0.00683098	0.0122351
6	0.31	0.20	0.00683819	0.0086215
7	0.32	0.28	0.00683661	0.0089122
8	0.31	0.41	0.00682342	0.0089431
9	0.29	0.58	0.00684986	0.0102070
10	0.3	0.77	0.00690431	0.0113804
11	0.45	0.18	0.00678319	0.0077813

Run #	Standard Conditions		V$_{SL}$ Uncertainty	V$_{Sg}$ Uncertainty
3 Degree	V$_{SL}$ (m/s)	V$_{Sg}$ (m/s)	(m/s)	(m/s)
12	0.48	0.28	0.00678628	0.0080113
13	0.48	0.37	0.00681775	0.0083216
14	0.48	0.58	0.00690652	0.0096255
15	0.5	0.80	0.00686565	0.0101472
16	0.5	0.99	0.00685741	0.0110214
17	0.7	0.19	0.00691709	0.0083620
18	0.72	0.28	0.00695759	0.0086372
19	0.72	0.38	0.00689877	0.0087385
20	0.73	0.60	0.00689909	0.0093892
21	0.73	0.79	0.00693291	0.0101498
22	0.71	0.95	0.00689045	0.0104414
23	0.74	1.48	0.00695466	0.0136354
24	1	0.58	0.00683427	0.0086236
25	0.99	0.77	0.00681389	0.0089722
26	0.99	0.96	0.00687986	0.0099971
27	0.27	1.00	0.00699702	0.0144498
28	0.27	1.49	0.00699307	0.0192940
29	0.27	1.92	0.00699077	0.0241638
30	0.2	2.06	0.00694859	0.0281029
31	0.29	1.02	0.00683536	0.0127984
32	0.29	1.50	0.00683378	0.0168622
33	0.3	1.94	0.00683599	0.0211483
34	0.31	2.97	0.00694727	0.0353212
35	0.3	4.06	0.00683410	0.0462277
36	0.46	1.46	0.00692133	0.0148966
37	0.49	1.94	0.00692326	0.0192062
38	0.5	2.94	0.00694430	0.0314977
39	0.73	1.98	0.00690583	0.0170518
40	0.74	3.05	0.00691419	0.0284786
41	0.99	0.18	0.00683994	0.0078195
42	1	0.27	0.00683521	0.0079630
43	1	0.38	0.00683395	0.0081977
44	1	1.48	0.00693415	0.0131903
45	1.01	1.99	0.00694160	0.0171420

Run #	Standard Conditions		V_{SL} Uncertainty	V_{Sg} Uncertainty
3 Degree	V_{SL} (m/s)	V_{Sg} (m/s)	(m/s)	(m/s)
46	1.01	2.98	0.00693868	0.0233211
47	1.45	0.19	0.00692597	0.0079765
48	1.45	0.28	0.00693276	0.0081278
49	1.45	0.38	0.00693697	0.0083029
50	1.45	0.57	0.00694086	0.0087909
51	1.46	0.79	0.00693697	0.0093722
52	1.46	0.93	0.00693956	0.0098615
53	1.46	1.48	0.00694800	0.0118876
54	1.46	1.99	0.00694280	0.0144465
55	1.47	2.90	0.00692855	0.0189366

Table A-4: Uncertainty propagation results for -5° angle

Run #	Standard Conditions		V_{SL} Uncertainty	V_{Sg} Uncertainty
5 Degree	V_{SL} (m/s)	V_{Sg} (m/s)	(m/s)	(m/s)
1	0.2	0.22	0.0001137	0.0093034
2	0.21	0.41	0.0001145	0.0102543
3	0.21	0.60	0.0001140	0.0111037
4	0.21	0.81	0.0001144	0.0132659
5	0.21	1.00	0.0001146	0.0149787
6	0.3	0.20	0.0001137	0.0088966
7	0.3	0.39	0.0001146	0.0100646
8	0.3	0.60	0.0001152	0.0114691
9	0.3	0.81	0.0001155	0.0129289
10	0.3	1.02	0.0001138	0.0132756
11	0.31	1.52	0.0001136	0.0179840
12	0.5	0.20	0.0001155	0.0095165
13	0.51	0.61	0.0001145	0.0106640
14	0.51	1.02	0.0001136	0.0122217
15	0.52	0.39	0.0001145	0.0099611
16	0.52	0.81	0.0001148	0.0117542
17	0.52	1.54	0.0001152	0.0177003
18	0.69	0.19	0.0001127	0.0084464
19	0.71	0.39	0.0001142	0.0091185

Run #	Standard Conditions		V_{SL} Uncertainty	V_{Sg} Uncertainty
5 Degree	V_{SL} (m/s)	V_{Sg} (m/s)	(m/s)	(m/s)
20	0.71	0.60	0.0001145	0.0096620
21	0.71	0.80	0.0001142	0.0102766
22	0.71	1.03	0.0001150	0.0117948
23	0.71	1.49	0.0001146	0.0142017
24	0.72	1.98	0.0001149	0.0184468
25	0.98	1.00	0.0001131	0.0104216
26	0.99	0.20	0.0001146	0.0087764
27	0.99	0.60	0.0001144	0.0096348
28	0.99	0.83	0.0001142	0.0101914
29	0.99	1.50	0.0001133	0.0129615
30	1	0.41	0.0001143	0.0096764
31	0.1	1.53	0.0001148	0.0241547
32	0.1	2.00	0.0001148	0.0316807
33	0.1	2.51	0.0001148	0.0403642
36	0.19	2.03	0.0001143	0.0305012
37	0.19	2.22	0.0001143	0.0336050
38	0.19	2.52	0.0001144	0.0389818
39	0.19	2.78	0.0001144	0.0435658
40	0.19	2.98	0.0001144	0.0472818
41	0.21	1.52	0.0001138	0.0196627
42	0.3	2.28	0.0001146	0.0316724
43	0.3	2.52	0.0001146	0.0355563
44	0.3	2.78	0.0001145	0.0396766
45	0.3	2.98	0.0001145	0.0430618
46	0.31	2.00	0.0001138	0.0236085
47	0.52	2.02	0.0001142	0.0232554
48	0.52	2.52	0.0001143	0.0278325
49	0.53	2.76	0.0001143	0.0326131
50	0.53	3.02	0.0001144	0.0361270
51	0.7	2.74	0.0001148	0.0286713
52	0.7	3.02	0.0001148	0.0319885
53	0.99	2.03	0.0001133	0.0168529
54	0.99	2.46	0.0001150	0.0226818
55	0.99	3.03	0.0001149	0.0275121

Run #	Standard Conditions		V_{SL} Uncertainty	V_{Sg} Uncertainty
5 Degree	V_{SL} (m/s)	V_{Sg} (m/s)	(m/s)	(m/s)
56	1.47	1.00	0.0001151	0.0105197
57	1.47	1.52	0.0001151	0.0130394
58	1.47	2.02	0.0001151	0.0157838
59	1.48	0.19	0.0001149	0.0085941
60	1.48	0.39	0.0001150	0.0089234
61	1.48	0.58	0.0001150	0.0093512
62	1.48	0.77	0.0001152	0.0100196
63	1.48	2.48	0.0001152	0.0184349

Appendix B Repeatability Tests
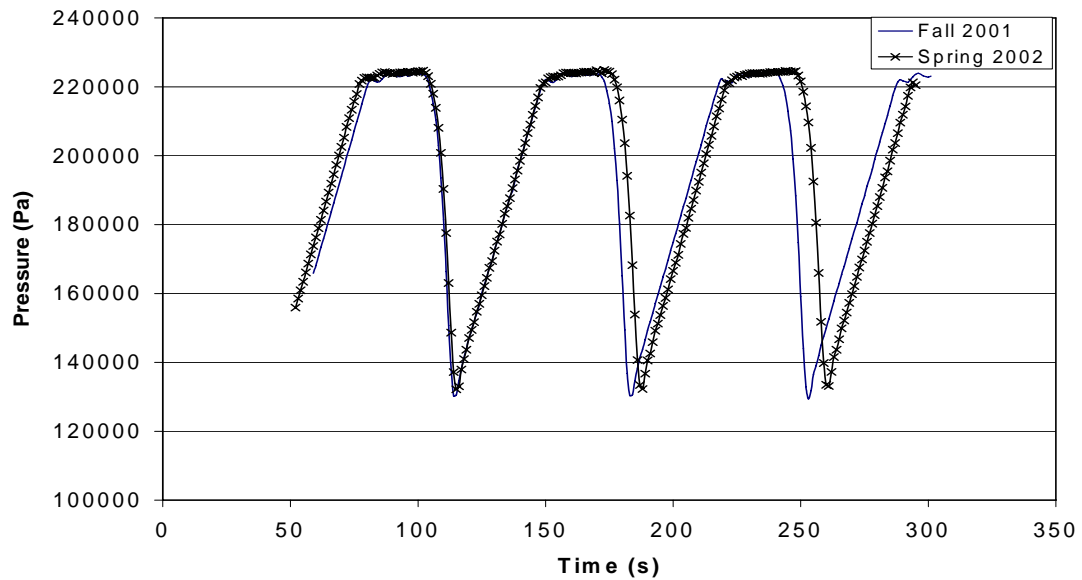
Figure B–1: Severe slugging repeatability test for v_{SL} = 0.40 m/s, and v_{Sg} = 0.39 m/s, -1°
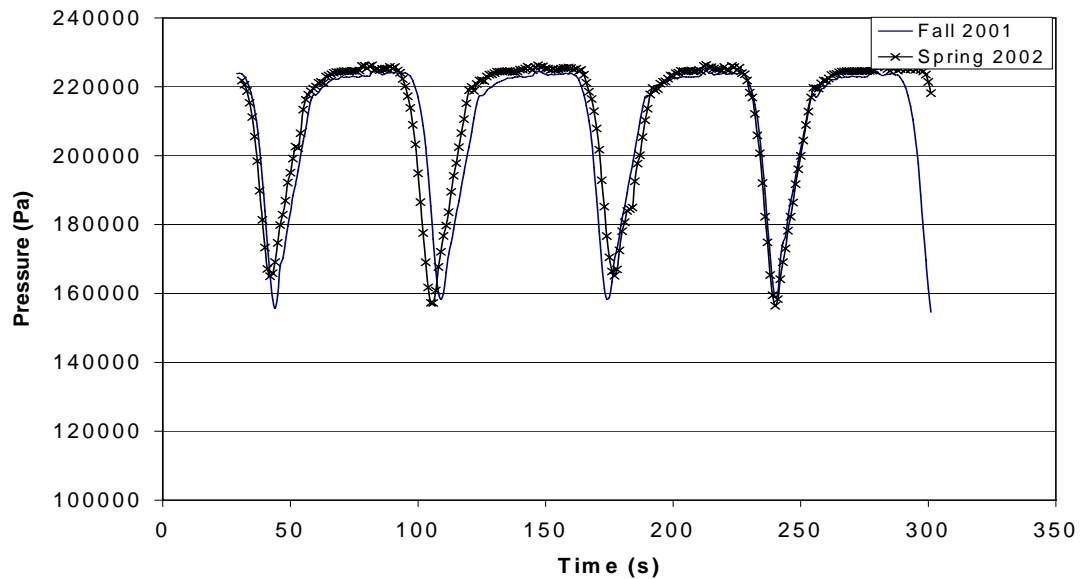
Figure B–2: Severe slugging repeatability test for v_{SL} = 0.60 m/s, and v_{Sg} = 0.24 m/s, -1°
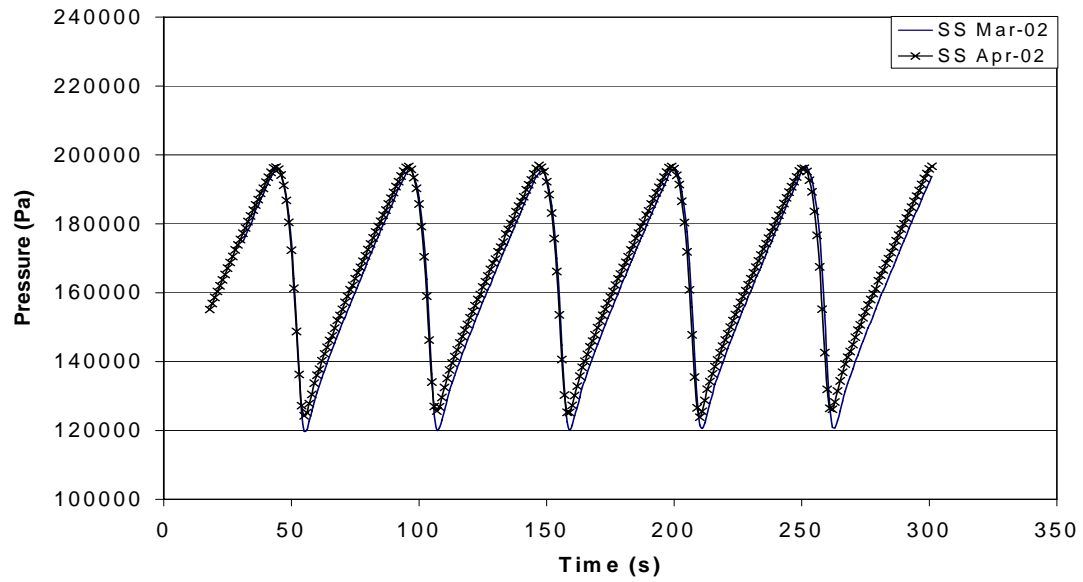
Figure B–3: Severe slugging repeatability test for v_{SL} = 0.20 m/s, and v_{Sg} = 0.80 m/s, -3°
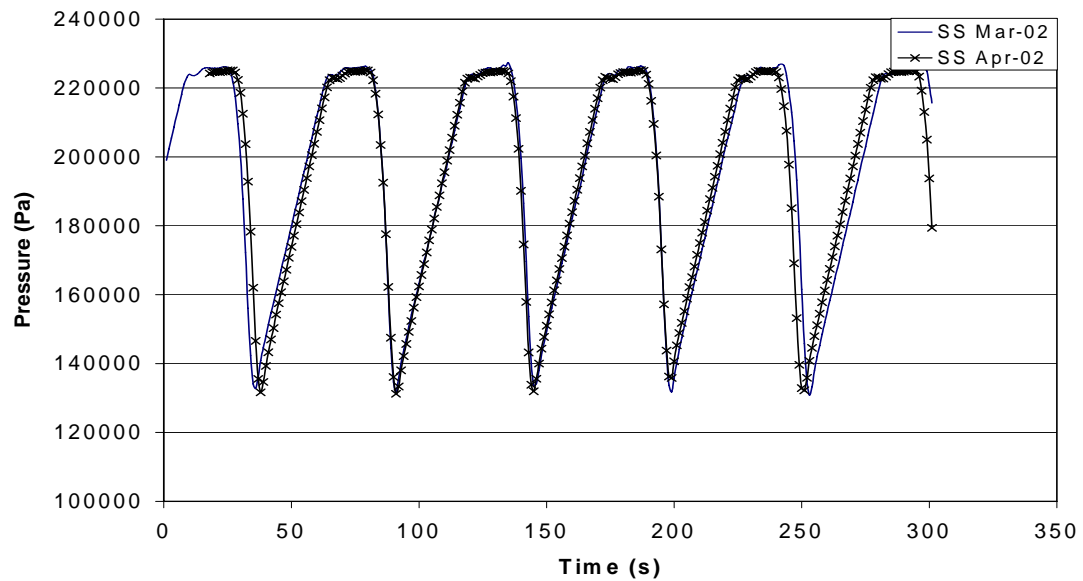
Figure B–4: Severe slugging repeatability test for v_{SL} = 0.50 m/s, and v_{Sg} = 0.60 m/s, -3°
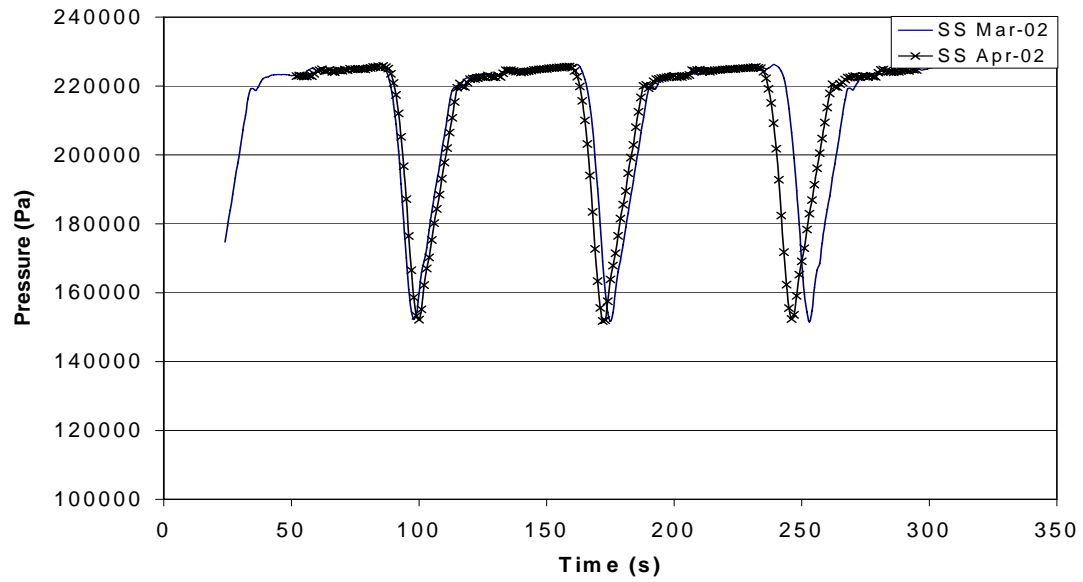
Figure B–5: Severe slugging repeatability test for v_{SL} = 0.70 m/s, and v_{Sg} = 0.30 m/s, -3°
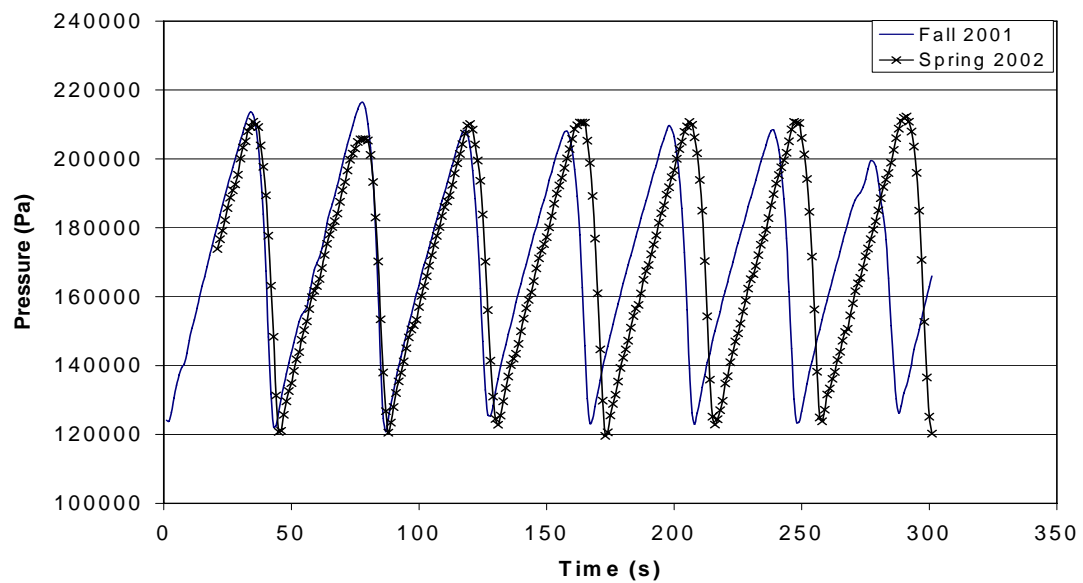
Figure B–6: Severe slugging repeatability test for v_{SL} = 0.30 m/s, and v_{Sg} = 1.01 m/s, -5°
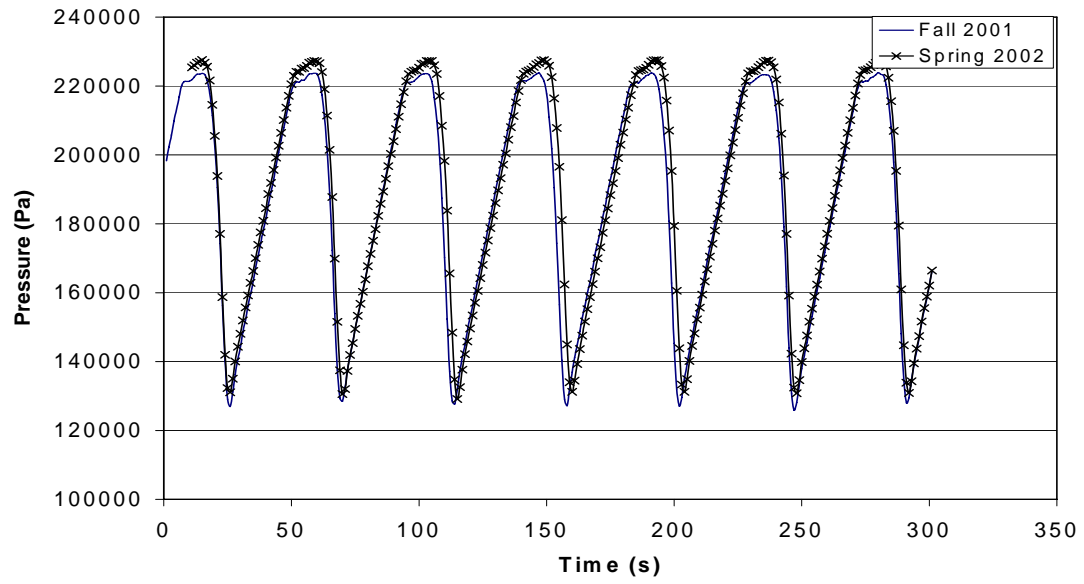
Figure B–7: Severe slugging repeatability test for $v_{SL} = 0.52$ m/s, and $v_{Sg} = 0.81$ m/s, -5°

Appendix C Pressure Drop in Penetrating Bubble

The pressure drop expression in a pipeline where there is a stationary penetrating bubble is derived in this appendix. The starting point is the combined momentum equation for stratified flow proposed by Taitel and Dukler[36]:

$$\tau_{Wg} \frac{S_g}{A_g} - \tau_{WL} \frac{S_L}{A_L} + \tau_i S_i \left(\frac{1}{A_L} + \frac{1}{A_g} \right) - (\rho_L - \rho_g)g \sin \theta = 0 \qquad (\text{C-1})$$

Since, the gas is not flowing, i.e., there are no shear stresses between flowing gas and the pipe wall or the gas-liquid interface, Eq. C-1 simplifies to

$$-\tau_{WL} \frac{S_L}{A_L} - (\rho_L - \rho_g)g \sin \theta = 0 \qquad (\text{C-2})$$

where

$$\tau_{WL} = f_L \frac{\rho_L v_L^2}{2} \qquad (\text{C-3})$$
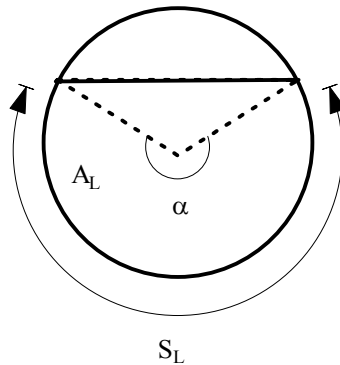
Figure C–1: Schematic of cross section of pipe with a penetrating bubble

Figure C-1 shows a schematic of a cross-section of a pipeline containing a penetrating gas bubble. Let α denote the angle subtended at the center of the pipe by the horizontal gas-liquid interface. From the geometry of the figure, we can write the following relationships:

$$S_L = \frac{d_p \alpha}{2} \qquad\qquad (\text{C-4})$$

$$A_L = \frac{d_p^2 (\alpha - \sin(\alpha))}{8} \qquad\qquad (\text{C-5})$$

$$H_L = \frac{(\alpha - \sin(\alpha))}{2\pi} \qquad\qquad (\text{C-6})$$

In terms of the system geometry, the combined momentum balance for the penetrating bubble can be written as

$$\frac{8 f_L \rho_L v_{SL}^2}{(\rho_L - \rho_g) d_p g \sin(\theta)} + \frac{(\alpha - \sin(\alpha))^3}{\pi^2 \alpha} = 0 \qquad\qquad (\text{C-7})$$

Equation C-7 can be solved for the angle α using Newton-Rhapson iteration. The derivative of Eq. C-7 with respect to α is given by

$$\frac{dM}{d\alpha} = \frac{(\alpha - \sin(\alpha))^2 (2\alpha + \sin(\varepsilon) - 3\alpha \cos(\alpha))}{\pi^2 \alpha^2} \qquad\qquad (\text{C-8})$$

Upon solution of Eq. C-7 for α, the system parameters can be calculated using Eqs. C-4 to C-6, and the pressure drop in the penetrating bubble section is determined from

$$-A_L \left.\frac{dp}{dx}\right)_L - \tau_{WL} S_L - \rho_L A_L g \sin\theta = 0 \qquad\qquad (\text{C-9})$$

Appendix D Steady State Model Results

Table D-1: Steady state model and experimental results

v_{SL} (m/s)	v_{Sg} (m/s)	Angle -	Takeoff Point	Injection Point	Max Δp psi	Min Δp psi	Actual Δp psi
0.09	0.26	1	10	13	0.836	0.535	0.68
0.09	0.26	1	9	13	0.836	0.599	0.67
0.09	0.26	1	8	13	0.836	0.651	0.75
0.09	0.26	1	10	12	0.418	0.116	0.08
0.09	0.26	1	9	12	0.418	0.181	0.27
0.09	0.26	1	8	12	0.418	0.233	0.22
0.11	0.39	1	10	13	0.828	0.528	0.71
0.11	0.39	1	9	13	0.828	0.592	0.64
0.11	0.39	1	8	13	0.828	0.644	0.57
0.11	0.39	1	10	12	0.413	0.113	0.13
0.11	0.39	1	9	12	0.413	0.177	0.19
0.11	0.39	1	8	12	0.413	0.229	0.27
0.2	0.68	1	10	13	0.828	0.528	0.39
0.2	0.68	1	9	13	0.828	0.592	0.53
0.2	0.68	1	8	13	0.828	0.644	0.61
0.2	0.68	1	9	12	0.413	0.177	0.22
0.2	0.68	1	8	12	0.413	0.229	0.23
0.21	0.16	1	10	13	0.828	0.528	0.45
0.21	0.16	1	9	13	0.828	0.592	0.61
0.21	0.16	1	8	13	0.828	0.644	0.68
0.21	0.16	1	10	12	0.413	0.113	0.14
0.21	0.16	1	9	12	0.413	0.177	0.22
0.21	0.16	1	8	12	0.413	0.229	0.18
0.21	0.24	1	10	13	0.828	0.528	0.56
0.21	0.24	1	9	13	0.828	0.592	0.56
0.21	0.24	1	8	13	0.828	0.644	0.58
0.21	0.24	1	10	12	0.413	0.113	0.09
0.21	0.24	1	9	12	0.413	0.177	0.21
0.21	0.24	1	8	12	0.413	0.229	0.24
0.22	0.39	1	10	13	0.828	0.528	0.52
0.22	0.39	1	9	13	0.828	0.592	0.55
0.22	0.39	1	8	13	0.828	0.644	0.61
0.22	0.39	1	10	12	0.413	0.113	0.08

v_{SL} (m/s)	v_{Sg} (m/s)	Angle -	Takeoff Point	Injection Point	Max Δp psi	Min Δp psi	Actual Δp psi
0.22	0.39	1	9	12	0.413	0.177	0.19
0.22	0.39	1	8	12	0.413	0.229	0.28
0.3	0.15	1	10	13	0.828	0.528	0.64
0.3	0.15	1	10	12	0.413	0.113	0.09
0.3	0.15	1	9	12	0.413	0.177	0.18
0.3	0.15	1	8	12	0.413	0.229	0.14
0.3	0.22	1	10	13	0.828	0.528	0.49
0.3	0.22	1	9	13	0.828	0.592	0.61
0.3	0.22	1	8	13	0.828	0.644	0.61
0.3	0.22	1	10	12	0.413	0.113	0.19
0.3	0.22	1	9	12	0.413	0.177	0.14
0.3	0.22	1	8	12	0.413	0.229	0.22
0.3	0.79	1	10	13	0.828	0.528	0.59
0.3	0.79	1	9	13	0.828	0.592	0.76
0.3	0.79	1	8	13	0.828	0.644	0.74
0.3	0.79	1	10	12	0.413	0.113	0.20
0.3	0.79	1	9	12	0.413	0.177	0.26
0.3	0.79	1	8	12	0.413	0.229	0.31
0.31	0.44	1	10	13	0.828	0.528	0.68
0.31	0.44	1	9	13	0.828	0.592	0.74
0.31	0.44	1	8	13	0.828	0.644	0.82
0.31	0.44	1	10	12	0.413	0.113	0.17
0.31	0.44	1	9	12	0.413	0.177	0.29
0.31	0.44	1	8	12	0.413	0.229	0.30
0.32	0.34	1	10	13	0.828	0.528	0.51
0.32	0.34	1	9	13	0.828	0.592	0.59
0.32	0.34	1	8	13	0.828	0.644	0.52
0.32	0.34	1	10	12	0.413	0.113	0.13
0.32	0.34	1	9	12	0.413	0.177	0.15
0.32	0.34	1	8	12	0.413	0.229	0.24
0.4	0.39	1	10	13	0.828	0.528	0.62
0.4	0.39	1	9	13	0.828	0.592	0.68
0.4	0.39	1	8	13	0.828	0.644	0.74
0.4	0.39	1	10	12	0.413	0.113	0.17
0.4	0.39	1	9	12	0.413	0.177	0.26
0.4	0.39	1	8	12	0.413	0.229	0.33
0.45	0.74	1	10	13	0.828	0.528	0.60
0.45	0.74	1	9	13	0.828	0.592	0.60
0.45	0.74	1	8	13	0.828	0.644	0.67
0.45	0.74	1	9	12	0.413	0.177	0.19
0.45	0.74	1	8	12	0.413	0.229	0.23
0.46	0.26	1	10	13	0.828	0.528	0.71

v_{SL} (m/s)	v_{Sg} (m/s)	Angle -	Takeoff Point	Injection Point	Max Δp psi	Min Δp psi	Actual Δp psi
0.46	0.26	1	9	13	0.828	0.592	0.63
0.46	0.26	1	8	13	0.828	0.644	0.82
0.46	0.26	1	10	12	0.413	0.113	0.21
0.46	0.26	1	9	12	0.413	0.177	0.31
0.46	0.26	1	8	12	0.413	0.229	0.27
0.5	0.32	1	10	13	0.828	0.528	0.53
0.5	0.32	1	9	13	0.828	0.592	0.78
0.5	0.32	1	8	13	0.828	0.644	0.60
0.5	0.32	1	10	12	0.413	0.113	0.13
0.5	0.32	1	9	12	0.413	0.177	0.25
0.5	0.32	1	8	12	0.413	0.229	0.24
0.58	0.47	1	10	13	0.828	0.528	0.71
0.58	0.47	1	9	13	0.828	0.592	0.75
0.58	0.47	1	10	12	0.413	0.113	0.22
0.58	0.47	1	9	12	0.413	0.177	0.22
0.58	0.47	1	8	12	0.413	0.229	0.29
0.59	0.15	1	10	13	0.828	0.528	0.68
0.59	0.15	1	9	13	0.828	0.592	0.53
0.59	0.15	1	8	13	0.828	0.644	0.73
0.59	0.15	1	10	12	0.413	0.113	0.24
0.59	0.15	1	9	12	0.413	0.177	0.21
0.59	0.15	1	8	12	0.413	0.229	0.20
0.6	0.24	1	10	13	0.828	0.528	0.55
0.6	0.24	1	9	13	0.828	0.592	0.77
0.6	0.24	1	8	13	0.828	0.644	0.82
0.6	0.24	1	10	12	0.413	0.113	0.29
0.6	0.24	1	9	12	0.413	0.177	0.24
0.6	0.24	1	8	12	0.413	0.229	0.32
0.63	0.83	1	10	13	0.828	0.528	0.71
0.63	0.83	1	9	13	0.828	0.592	0.69
0.63	0.83	1	8	13	0.828	0.644	0.74
0.63	0.83	1	10	12	0.413	0.113	0.20
0.63	0.83	1	9	12	0.413	0.177	0.23
0.63	0.83	1	8	12	0.413	0.229	0.35
0.71	0.72	1	10	13	0.828	0.528	0.68
0.71	0.72	1	9	13	0.828	0.592	0.77
0.71	0.72	1	8	13	0.828	0.644	0.80
0.71	0.72	1	10	12	0.413	0.113	0.32
0.71	0.72	1	9	12	0.413	0.177	0.35
0.71	0.72	1	8	12	0.413	0.229	0.40
0.2	0.29	3	10	14	1.345	0.438	1.18
0.2	0.29	3	9	14	1.345	0.632	0.81

v_{SL} (m/s)	v_{Sg} (m/s)	Angle -	Takeoff Point	Injection Point	Max Δp psi	Min Δp psi	Actual Δp psi
0.2	0.29	3	8	14	1.345	0.787	0.88
0.2	0.29	3	10	13	0.835	-0.071	0.52
0.2	0.29	3	9	13	0.835	0.122	0.48
0.2	0.29	3	8	13	0.835	0.277	0.41
0.2	0.58	3	10	14	1.345	0.438	0.78
0.2	0.58	3	9	14	1.345	0.632	0.92
0.2	0.58	3	8	14	1.345	0.787	0.87
0.2	0.58	3	10	13	0.835	-0.071	0.62
0.2	0.58	3	9	13	0.835	0.122	0.52
0.2	0.58	3	8	13	0.835	0.277	0.42
0.2	0.78	3	10	14	1.345	0.438	0.60
0.2	0.78	3	9	14	1.345	0.632	0.75
0.2	0.78	3	8	14	1.345	0.787	0.96
0.2	0.78	3	10	13	0.835	-0.071	0.34
0.2	0.78	3	9	13	0.835	0.122	0.37
0.2	0.78	3	8	13	0.835	0.277	0.40
0.21	0.4	3	10	14	1.345	0.438	0.85
0.21	0.4	3	9	14	1.345	0.632	0.85
0.21	0.4	3	8	14	1.345	0.787	0.79
0.21	0.4	3	10	13	0.835	-0.071	0.36
0.21	0.4	3	9	13	0.835	0.122	0.46
0.21	0.4	3	8	13	0.835	0.277	0.37
0.22	0.23	3	10	14	1.345	0.438	0.97
0.22	0.23	3	9	14	1.345	0.632	0.80
0.22	0.23	3	8	14	1.345	0.787	0.70
0.22	0.23	3	10	13	0.835	-0.071	0.37
0.22	0.23	3	9	13	0.835	0.122	0.32
0.22	0.23	3	8	13	0.835	0.277	0.35
0.29	0.58	3	10	14	1.345	0.438	0.98
0.29	0.58	3	9	14	1.345	0.632	1.20
0.29	0.58	3	8	14	1.345	0.787	0.98
0.29	0.58	3	10	13	0.835	-0.071	0.68
0.29	0.58	3	9	13	0.835	0.122	0.63
0.29	0.58	3	8	13	0.835	0.277	0.51
0.3	0.77	3	10	14	1.345	0.438	0.66
0.3	0.77	3	9	14	1.345	0.632	1.06
0.3	0.77	3	8	14	1.345	0.787	1.16
0.3	0.77	3	10	13	0.835	-0.071	0.49
0.3	0.77	3	9	13	0.835	0.122	0.58
0.3	0.77	3	8	13	0.835	0.277	0.56
0.31	0.2	3	10	14	1.345	0.438	0.90
0.31	0.2	3	9	14	1.345	0.632	1.04

v_{SL} (m/s)	v_{Sg} (m/s)	Angle -	Takeoff Point	Injection Point	Max Δp psi	Min Δp psi	Actual Δp psi
0.31	0.2	3	8	14	1.345	0.787	1.03
0.31	0.2	3	10	13	0.835	-0.071	0.64
0.31	0.2	3	9	13	0.835	0.122	0.67
0.31	0.2	3	8	13	0.835	0.277	0.39
0.31	0.41	3	10	14	1.345	0.438	1.27
0.31	0.41	3	9	14	1.345	0.632	1.06
0.31	0.41	3	8	14	1.345	0.787	0.98
0.31	0.41	3	10	13	0.835	-0.071	0.68
0.31	0.41	3	9	13	0.835	0.122	0.68
0.31	0.41	3	8	13	0.835	0.277	0.46
0.32	0.28	3	10	14	1.345	0.438	1.06
0.32	0.28	3	9	14	1.345	0.632	1.22
0.32	0.28	3	8	14	1.345	0.787	0.94
0.32	0.28	3	10	13	0.835	-0.071	0.52
0.32	0.28	3	9	13	0.835	0.122	0.59
0.32	0.28	3	8	13	0.835	0.277	0.64
0.45	0.18	3	10	14	1.345	0.438	1.04
0.45	0.18	3	9	14	1.345	0.632	1.00
0.45	0.18	3	8	14	1.345	0.787	1.09
0.45	0.18	3	10	13	0.835	-0.071	0.48
0.45	0.18	3	9	13	0.835	0.122	0.62
0.45	0.18	3	8	13	0.835	0.277	0.72
0.48	0.28	3	10	14	1.345	0.438	1.21
0.48	0.28	3	9	14	1.345	0.632	0.95
0.48	0.28	3	8	14	1.345	0.787	1.05
0.48	0.28	3	10	13	0.835	-0.071	0.76
0.48	0.28	3	9	13	0.835	0.122	0.57
0.48	0.28	3	8	13	0.835	0.277	0.57
0.48	0.36	3	10	14	1.345	0.438	0.94
0.48	0.36	3	9	14	1.345	0.632	1.36
0.48	0.36	3	8	14	1.345	0.787	0.97
0.48	0.36	3	10	13	0.835	-0.071	0.59
0.48	0.36	3	9	13	0.835	0.122	0.77
0.48	0.36	3	8	13	0.835	0.277	0.67
0.48	0.58	3	10	14	1.345	0.438	1.13
0.48	0.58	3	9	14	1.345	0.632	1.15
0.48	0.58	3	8	14	1.345	0.787	1.16
0.48	0.58	3	10	13	0.835	-0.071	0.36
0.48	0.58	3	9	13	0.835	0.122	0.53
0.48	0.58	3	8	13	0.835	0.277	0.38
0.5	0.8	3	10	14	1.345	0.438	1.01
0.5	0.8	3	9	14	1.345	0.632	1.22

v_{SL} (m/s)	v_{Sg} (m/s)	Angle -	Takeoff Point	Injection Point	Max Δp psi	Min Δp psi	Actual Δp psi
0.5	0.8	3	8	14	1.345	0.787	1.02
0.5	0.8	3	10	13	0.835	-0.071	0.80
0.5	0.8	3	9	13	0.835	0.122	0.65
0.5	0.8	3	8	13	0.835	0.277	0.68
0.5	1	3	10	14	1.345	0.438	1.07
0.5	1	3	9	14	1.345	0.632	1.01
0.5	1	3	8	14	1.345	0.787	1.09
0.5	1	3	10	13	0.835	-0.071	0.45
0.5	1	3	9	13	0.835	0.122	0.61
0.5	1	3	8	13	0.835	0.277	0.50
0.7	0.19	3	10	14	1.345	0.438	0.98
0.7	0.19	3	9	14	1.345	0.632	1.07
0.7	0.19	3	8	14	1.345	0.787	0.99
0.7	0.19	3	10	13	0.835	-0.071	0.53
0.7	0.19	3	9	13	0.835	0.122	0.69
0.7	0.19	3	8	13	0.835	0.277	0.49
0.71	0.95	3	10	14	1.345	0.438	1.20
0.71	0.95	3	9	14	1.345	0.632	1.18
0.71	0.95	3	8	14	1.345	0.787	1.06
0.71	0.95	3	10	13	0.835	-0.071	0.61
0.71	0.95	3	9	13	0.835	0.122	0.67
0.71	0.95	3	8	13	0.835	0.277	0.69
0.72	0.28	3	10	14	1.345	0.438	1.22
0.72	0.28	3	9	14	1.345	0.632	1.03
0.72	0.28	3	8	14	1.345	0.787	0.97
0.72	0.28	3	10	13	0.835	-0.071	0.95
0.72	0.28	3	9	13	0.835	0.122	0.77
0.72	0.28	3	8	13	0.835	0.277	0.7
0.72	0.38	3	10	14	1.345	0.438	1.11
0.72	0.38	3	9	14	1.345	0.632	1.22
0.72	0.38	3	8	14	1.345	0.787	1.00
0.72	0.38	3	10	13	0.835	-0.071	0.71
0.72	0.38	3	9	13	0.835	0.122	0.74
0.72	0.38	3	8	13	0.835	0.277	0.59
0.73	0.6	3	10	14	1.345	0.438	1.20
0.73	0.6	3	9	14	1.345	0.632	1.11
0.73	0.6	3	8	14	1.345	0.787	0.94
0.73	0.6	3	10	13	0.835	-0.071	0.72
0.73	0.6	3	9	13	0.835	0.122	0.76
0.73	0.6	3	8	13	0.835	0.277	0.46
0.73	0.78	3	10	14	1.345	0.438	1.06
0.73	0.78	3	9	14	1.345	0.632	1.21

v_{SL} (m/s)	v_{Sg} (m/s)	Angle -	Takeoff Point	Injection Point	Max Δp psi	Min Δp psi	Actual Δp psi
0.73	0.78	3	8	14	1.345	0.787	1.08
0.73	0.78	3	10	13	0.835	-0.071	0.57
0.73	0.78	3	9	13	0.835	0.122	0.65
0.73	0.78	3	8	13	0.835	0.277	0.54
0.74	1.48	3	10	14	1.345	0.438	1.26
0.74	1.48	3	9	14	1.345	0.632	1.32
0.74	1.48	3	8	14	1.345	0.787	1.15
0.74	1.48	3	10	13	0.835	-0.071	0.72
0.74	1.48	3	9	13	0.835	0.122	0.73
0.74	1.48	3	8	13	0.835	0.277	0.70
0.99	0.77	3	10	14	1.345	0.438	1.23
0.99	0.77	3	9	14	1.345	0.632	1.24
0.99	0.77	3	8	14	1.345	0.787	1.07
0.99	0.77	3	10	13	0.835	-0.071	0.90
0.99	0.77	3	9	13	0.835	0.122	0.96
0.99	0.77	3	8	13	0.835	0.277	0.75
0.99	0.97	3	10	14	1.345	0.438	1.27
0.99	0.97	3	9	14	1.345	0.632	1.19
0.99	0.97	3	8	14	1.345	0.787	1.25
0.99	0.97	3	10	13	0.835	-0.071	0.67
0.99	0.97	3	9	13	0.835	0.122	0.80
0.99	0.97	3	8	13	0.835	0.277	0.71
1	0.58	3	10	14	1.345	0.438	1.09
1	0.58	3	9	14	1.345	0.632	1.26
1	0.58	3	8	14	1.345	0.787	1.17
1	0.58	3	10	13	0.835	-0.071	0.69
1	0.58	3	9	13	0.835	0.122	0.87
1	0.58	3	8	13	0.835	0.277	0.78
0.2	0.21	5	10	14	1.345	-0.164	0.73
0.2	0.21	5	9	14	1.345	0.158	0.68
0.2	0.21	5	8	14	1.345	0.416	0.59
0.2	0.21	5	10	13	0.835	-0.675	0.58
0.2	0.21	5	9	13	0.835	-0.351	0.35
0.2	0.21	5	8	13	0.835	-0.093	0.23
0.21	0.4	5	10	14	1.345	-0.164	0.39
0.21	0.4	5	9	14	1.345	0.158	0.90
0.21	0.4	5	8	14	1.345	0.416	0.82
0.21	0.4	5	10	13	0.835	-0.675	0.24
0.21	0.4	5	9	13	0.835	-0.351	0.22
0.21	0.4	5	8	13	0.835	-0.093	0.39
0.21	0.59	5	9	14	1.345	0.158	0.81
0.21	0.59	5	8	14	1.345	0.416	0.83

v_{SL} (m/s)	v_{Sg} (m/s)	Angle -	Takeoff Point	Injection Point	Max Δp psi	Min Δp psi	Actual Δp psi
0.21	0.59	5	10	13	0.835	-0.675	0.17
0.21	0.59	5	9	13	0.835	-0.351	0.27
0.21	0.59	5	8	13	0.835	-0.093	0.38
0.21	0.81	5	10	14	1.345	-0.164	0.36
0.21	0.81	5	9	14	1.345	0.158	0.74
0.21	0.81	5	8	14	1.345	0.416	1.04
0.21	1.01	5	10	14	0.835	-0.164	0.28
0.21	1.01	5	9	14	0.835	0.158	0.43
0.21	1.01	5	8	14	0.835	0.416	0.76
0.3	0.2	5	10	14	1.345	-0.164	0.66
0.3	0.2	5	9	14	1.345	0.158	0.95
0.3	0.2	5	8	14	1.345	0.416	0.78
0.3	0.2	5	10	13	0.835	-0.675	0.22
0.3	0.2	5	9	13	0.835	-0.351	0.25
0.3	0.2	5	8	13	0.835	-0.093	0.35
0.3	0.39	5	10	14	1.345	-0.164	0.46
0.3	0.39	5	9	14	1.345	0.158	1.21
0.3	0.39	5	8	14	1.345	0.416	0.79
0.3	0.39	5	10	13	0.835	-0.675	0.24
0.3	0.39	5	9	13	0.835	-0.351	0.25
0.3	0.39	5	8	13	0.835	-0.093	0.29
0.3	0.6	5	10	14	1.345	-0.164	0.36
0.3	0.6	5	9	14	1.345	0.158	0.65
0.3	0.6	5	8	14	1.345	0.416	0.62
0.3	0.6	5	10	13	0.835	-0.675	0.08
0.3	0.6	5	9	13	0.835	-0.351	0.24
0.3	0.6	5	8	13	0.835	-0.093	0.22
0.3	0.81	5	10	14	1.345	-0.164	0.43
0.3	0.81	5	9	14	1.345	0.158	0.46
0.3	0.81	5	8	14	1.345	0.416	0.46
0.3	0.81	5	10	13	0.835	-0.675	0.15
0.3	0.81	5	9	13	0.835	-0.351	0.26
0.3	0.81	5	8	13	0.835	-0.093	0.25
0.3	1.01	5	10	14	1.345	-0.164	0.32
0.3	1.01	5	9	14	1.345	0.158	0.49
0.3	1.01	5	8	14	1.345	0.416	0.61
0.31	1.52	5	9	14	1.345	0.158	0.98
0.31	1.52	5	8	14	1.345	0.416	0.78
0.5	0.21	5	10	14	1.345	-0.164	0.37
0.5	0.21	5	9	14	1.345	0.158	0.59
0.5	0.21	5	8	14	1.345	0.416	0.87
0.5	0.21	5	10	13	0.835	-0.675	0.15

v_{SL} (m/s)	v_{Sg} (m/s)	Angle -	Takeoff Point	Injection Point	Max Δp psi	Min Δp psi	Actual Δp psi
0.5	0.21	5	9	13	0.835	-0.351	0.12
0.5	0.21	5	8	13	0.835	-0.093	0.05
0.5	0.21	5	9	12	0.416	-0.769	0.24
0.5	0.21	5	8	12	0.416	-0.511	0.09
0.51	0.61	5	10	14	1.345	-0.164	0.42
0.51	0.61	5	9	14	1.345	0.158	0.77
0.51	0.61	5	8	14	1.345	0.416	0.77
0.51	0.61	5	10	13	0.835	-0.675	0.03
0.51	0.61	5	9	13	0.835	-0.351	0.25
0.51	0.61	5	8	13	0.835	-0.093	0.31
0.51	1.01	5	10	14	1.345	-0.164	0.50
0.51	1.01	5	9	14	1.345	0.158	0.51
0.51	1.01	5	8	14	1.345	0.416	0.60
0.51	1.01	5	10	13	0.835	-0.675	-0.09
0.51	1.01	5	9	13	0.835	-0.351	-0.02
0.51	1.01	5	8	13	0.835	-0.093	-0.06
0.52	0.4	5	10	14	1.345	-0.164	1.00
0.52	0.4	5	9	14	1.345	0.158	1.11
0.52	0.4	5	8	14	1.345	0.416	0.85
0.52	0.4	5	10	13	0.835	-0.675	0.22
0.52	0.4	5	9	13	0.835	-0.351	0.19
0.52	0.4	5	8	13	0.835	-0.093	0.15
0.52	0.81	5	10	14	1.345	-0.164	0.78
0.52	0.81	5	9	14	1.345	0.158	0.62
0.52	0.81	5	8	14	1.345	0.416	0.42
0.52	0.81	5	10	13	0.835	-0.675	0.06
0.52	0.81	5	9	13	0.835	-0.351	0.40
0.52	0.81	5	8	13	0.835	-0.093	0.25
0.52	1.52	5	9	14	1.345	0.158	0.24
0.52	1.52	5	8	13	0.835	-0.1	-0.08
0.69	0.18	5	10	14	1.345	-0.164	0.90
0.69	0.18	5	9	14	1.345	0.158	0.86
0.69	0.18	5	8	14	1.345	0.416	0.80
0.69	0.18	5	10	13	0.835	-0.675	0.33
0.69	0.18	5	9	13	0.835	-0.351	0.72
0.69	0.18	5	8	13	0.835	-0.093	0.53
0.71	0.39	5	10	14	1.345	-0.164	0.84
0.71	0.39	5	9	14	1.345	0.158	0.90
0.71	0.39	5	8	14	1.345	0.416	1.05
0.71	0.39	5	10	13	0.835	-0.675	0.22
0.71	0.39	5	9	13	0.835	-0.351	0.52
0.71	0.39	5	8	13	0.835	-0.093	0.36

v_{SL} (m/s)	v_{Sg} (m/s)	Angle -	Takeoff Point	Injection Point	Max Δp psi	Min Δp psi	Actual Δp psi
0.71	0.6	5	10	14	1.345	-0.164	0.62
0.71	0.6	5	9	14	1.345	0.158	1.21
0.71	0.6	5	8	14	1.345	0.416	0.89
0.71	0.6	5	10	13	0.835	-0.675	0.48
0.71	0.6	5	9	13	0.835	-0.351	0.39
0.71	0.6	5	8	13	0.835	-0.093	0.46
0.71	0.8	5	10	14	1.345	-0.164	0.58
0.71	0.8	5	9	14	1.345	0.158	0.88
0.71	0.8	5	8	14	1.345	0.416	0.91
0.71	0.8	5	10	13	0.835	-0.675	0.21
0.71	0.8	5	9	13	0.835	-0.351	0.29
0.71	0.8	5	8	13	0.835	-0.093	0.55
0.71	1.02	5	10	14	1.345	-0.164	0.68
0.71	1.02	5	9	14	1.345	0.158	0.75
0.71	1.02	5	8	14	1.345	0.416	0.84
0.71	1.02	5	10	13	0.835	-0.675	0.35
0.71	1.02	5	9	13	0.835	-0.351	0.36
0.71	1.02	5	8	13	0.835	-0.093	0.48
0.71	1.5	5	10	14	1.345	-0.164	0.88
0.71	1.5	5	9	14	1.345	0.158	0.87
0.71	1.5	5	8	14	1.345	0.416	1.01
0.72	1.99	5	8	14	1.345	0.416	0.94
0.98	1	5	10	14	1.345	-0.164	0.94
0.98	1	5	9	14	1.345	0.158	1.13
0.98	1	5	8	14	1.345	0.416	1.08
0.98	1	5	10	13	0.835	-0.675	0.44
0.98	1	5	9	13	0.835	-0.351	0.59
0.98	1	5	8	13	0.835	-0.093	0.58
0.99	0.19	5	10	14	1.345	-0.164	0.75
0.99	0.19	5	9	14	1.345	0.158	1.18
0.99	0.19	5	8	14	1.345	0.416	1.00
0.99	0.19	5	10	13	0.835	-0.675	0.52
0.99	0.19	5	9	13	0.835	-0.351	0.34
0.99	0.19	5	8	13	0.835	-0.093	0.45
0.99	0.19	5	10	12	0.416	-1.09	0.11
0.99	0.19	5	9	12	0.416	-0.769	0.17
0.99	0.19	5	8	12	0.416	-0.511	0.22
0.99	0.59	5	10	14	1.345	-0.164	0.81
0.99	0.59	5	9	14	1.345	0.158	1.07
0.99	0.59	5	8	14	1.345	0.416	1.09
0.99	0.59	5	10	13	0.835	-0.675	0.50
0.99	0.59	5	9	13	0.835	-0.351	0.64

v$_{SL}$ (m/s)	v$_{Sg}$ (m/s)	Angle -	Takeoff Point	Injection Point	Max Δp psi	Min Δp psi	Actual Δp psi
0.99	0.59	5	8	13	0.835	-0.093	0.64
0.99	0.81	5	10	14	1.345	-0.164	0.74
0.99	0.81	5	9	14	1.345	0.158	1.19
0.99	0.81	5	8	14	1.345	0.416	1.14
0.99	0.81	5	10	13	0.835	-0.675	0.52
0.99	0.81	5	9	13	0.835	-0.351	0.68
0.99	0.81	5	8	13	0.835	-0.093	0.68
0.99	1.49	5	10	14	1.345	-0.164	0.84
0.99	1.49	5	9	14	1.345	0.158	0.99
0.99	1.49	5	8	14	1.345	0.416	0.99
0.99	1.49	5	10	13	0.835	-0.675	0.55
0.99	1.49	5	9	13	0.835	-0.351	0.69
0.99	1.49	5	8	13	0.835	-0.093	0.56
1	0.41	5	10	14	1.345	-0.164	1.10
1	0.41	5	9	14	1.345	0.158	1.04
1	0.41	5	8	14	1.345	0.416	1.05
1	0.41	5	10	13	0.835	-0.675	0.61
1	0.41	5	9	13	0.835	-0.351	0.59
1	0.41	5	8	13	0.835	-0.093	0.47
1	0.41	5	10	12	0.416	-1.09	0.14
1	0.41	5	9	12	0.416	-0.769	0.23
1	0.41	5	8	12	0.416	-0.511	0.16